SYNTHESIS OF FUNCTIONALIZED PORPHYRINS FOR APPLICATION AS SOFT MATERIALS

Mr. Dumrongsak Aryuwananon

A Dissertation Submitted in Partial Fulfillment of the Requirements

for the Degree of Doctor of Philosophy in Chemistry

Department of Chemistry

FACULTY OF SCIENCE

Chulalongkorn University

Academic Year 2022

การสังเคราะห์พอร์ไฟรินที่มีหมู่ฟังก์ชันเพื่อการประยุกต์เป็นวัสดุอ่อน

นายดำรงศักดิ์ อายุวนานนท์

วิทยานิพนธ์นี้เป็นส่วนหนึ่งของการศึกษาตามหลักสูตรปริญญาวิทยาศาสตรดุษฎีบัณฑิต
สาขาวิชาเคมี ภาควิชาเคมี
คณะวิทยาศาสตร์ จุฬาลงกรณ์มหาวิทยาลัย
ปีการศึกษา 2565

Thesis Title	SYNTHESIS OF FUNCTIONALIZED PORPHYRINS FOR APPLICATION AS SOFT MATERIALS
By	Mr. Dumrongsak Aryuwananon
Field of Study	Chemistry
Thesis Advisor	Professor BUNCHA PULPOKA, Doctorat

Accepted by the FACULTY OF SCIENCE, Chulalongkorn University in Partial Fulfillment of the Requirement for the Doctor of Philosophy

.... Dean of the FACULTY OF SCIENCE

(Professor POLKIT SANGVANICH, Ph.D.)

DISSERTATION COMMITTEE

.... Chairman

(Professor VUDHICHAI PARASUK, Ph.D.)

.... Thesis Advisor

(Professor BUNCHA PULPOKA, Doctorat)

.... Examiner

(Professor PATCHANITA THAMYONGKIT, Ph.D.)

.... Examiner

(Professor THAWATCHAI TUNTULANI, Ph.D.)

.... External Examiner

(Assistant Professor Suttinun Phongtamrug, Ph.D.)

ดำรงศักดิ์ อายุวนานนท์ : การสังเคราะห์พอร์ไฟรินที่มีหมู่ฟังก์ชันเพื่อการประยุกต์เป็น
วัสดุอ่อน. (SYNTHESIS OF FUNCTIONALIZED PORPHYRINS FOR APPLICATION
AS SOFT MATERIALS) อ.ที่ปรึกษาหลัก : ศ. ดร.บัญชา พูลโภคา

อนุกรมของพอร์ไฟรินที่มีหมู่ฟังก์ชันได้รับการออกแบบและสังเคราะห์ขึ้นด้วยปฏิกิริยา
เคมีอินทรีย์ โดยเปลี่ยนหมู่แทนที่ตำแหน่งพารา- ที่อยู่บนตำแหน่งมีโซของวงพอร์ไฟรินเป็นอีเทอร์
เอสเทอร์และยูเรีย ด้วยอัลคิลสายโซ่ยาว 3 ขนาดที่แตกต่างกัน (3-5, 7-9, 11) และปฏิกิริยาการ
เติมโลหะของอนุพันธ์พอร์ไฟริน ด้วยโลหะบางชนิดในกลุ่ม 3d เพื่อให้มีคุณสมบัติลิควิดคริสตัลและ
การเติมลิแกนด์แนวแกนเพื่อเพิ่มสมบัติสปินคลอส-โอเวอร์ของสารเชิงซ้อนพอร์ไฟรินที่มีหมู่ฟังก์ชัน
อนุพันธ์พอร์ไฟรินแต่ละอนุกรมประกอบด้วย 3 ความยาวของสายโซ่ที่แตกต่างกัน (3-5, 7-9, 11)
รวมทั้งสารเชิงซ้อนโคบอลต์(II) (3-5a, 7-9a) นิกเกิล(II) (3-5b, 7-9b) และเหล็ก(III) (3-5c, 7-9c)
ได้รับการพิสูจน์เอกลักษณ์ด้วยวิธีการทางสเปคโทรสโคปีซึ่งประกอบด้วย นิวเคลียร์แมกเนติกเร
โซแนนซ์ อินฟราเรด ยูวี-วิซิเบิลและแมสสเปคโทรสโคป สารประกอบเป้าหมายได้นำไปศึกษา
พฤติกรรมทางสัณฐานมีโซ และพฤติกรรมทางแม่เหล็ก โดยวิธีการวัดปริมาณความร้อนด้วยการ
สแกนแบบดิฟเฟอเรนเชียล และเครื่องซุปเบอร์คอนดักติงควอนตรัมอินเตอร์เฟอเรนซ์ ตามลำดับ
สารเชิงซ้อนพอร์ไฟรินส่วนใหญ่แสดงสมบัติลิควิดคริสตัล ได้แก่ สารเชิงซ้อนโคบอลต์(II) สาร
เชิงซ้อนนิกเกิล(II) และสารเชิงซ้อนเหล็ก(III) (4-5c, 7-9a,b,c) แต่สารประกอบเชิงซ้อนพอร์ไฟรินที่
มีลิแกนด์แนวแกน (7-9a-อิมิดาโซล, 5c-อิมิดาโซล) เป็นสารประกอบเชิงซ้อนที่แสดงสมบัติเป็น
วัสดุพาราแมกเนติก

จุฬาลงกรณ์มหาวิทยาลัย
CHULALONGKORN UNIVERSITY

สาขาวิชา   เคมี   ลายมือชื่อนิสิต ....
ปีการศึกษา   2565   ลายมือชื่อ อ.ที่ปรึกษาหลัก ....

5972815223 : MAJOR CHEMISTRY

KEYWORD: Porphyrin, Synthesis, functional, soft materials

Dumrongsak Aryuwananon : SYNTHESIS OF FUNCTIONALIZED PORPHYRINS FOR APPLICATION AS SOFT MATERIALS. Advisor: Prof. BUNCHA PULPOKA, Doctorat

The series of functionalized porphyrins was designed and synthesized by varying *para*-substituents on *meso*-position of porphyrin ring as ether, ester, and urea with three different long alkyl chains (3-5, 7-9, 11). Afterwards, metalation of porphyrin derivatives by some 3d metals to serve as soft materials, liquid crystal, and axial ligands were introduced to provide spin-crossover property.

Each series of functionalized porphyrin derivatives with three different chain lengths (3-5, 7-9, 11) and their Co(II) (3-5a,7-9a), Ni(II) (3-5b,7-9b), and Fe (III) (3-5c,7-9c) complexes were characterized by spectroscopic techniques consisting of NMR, IR, UV-visible and MS. The desired compounds were studied their mesomorphic and magnetic behaviors by DSC and SQUID, respectively.

Most metalloporphyrins such as Ni(II), Co(II) and Fe(III) complexes (4-5c, 7-9a,b,c) exhibited liquid crystalline property whereas some axial-ligand complexes (7-9a-imidazole, 5c-imidazole) behaved as paramagnetic soft materials.

Field of Study:	Chemistry	Student's Signature	....
Academic Year:	2022	Advisor's Signature	....

ACKNOWLEDGEMENTS

TABLE OF CONTENTS

LIST OF TABLES

จุฬาลงกรณ์มหาวิทยาลัย

CHULALONGKORN UNIVERSITY

LIST OF FIGURES

CHAPTER 1

INTRODUCTION

Soft materials are advance materials which can change their forms depend on external stimuli; temperature, force and chemicals[1]. Most of soft materials compose of dynamic parts and rigid parts. The originated forms reversibly intermolecular non-covalent bonds which provides soft property of the materials while the latter constructs stronger interactions such as coordination bonding, ionic interaction or dipole interaction which responsible for switchable functions such as thermochromism[2], mechanochromism[3], spin-crossover[4, 5]. Soft materials are express various unique properties and functionalities that originated form flexibilities associated with their structures. The specific property, controlling of soft metal complexes, can be accomplished by adding long alkyl chains (C_nH_{2n+1}) onto the periphery of the rigid structures. Long chain alkyl substituted complexes were anticipated to exhibit new properties associated with flexible and soft structures by synergistic effects between the alkyl-chain structural dynamics and the electron dynamic occurring at metal centers[5, 6].

Porphyrin liquid crystals are membered discotic mesogens and are of considerable interest for optoelectronics, display and data storage devices[7-11]. Porphyrins possess all the necessary properties including synthetic versatility, thermal stability, and a number of special photochemical properties. Combination of a rigid macrocycle with flexible long-chain aliphatic substituents facilitates self-assembling of discotic molecules into a supramolecular ensemble owing to plane-plane interactions[10, 12]. The size of long-chain aliphatic substituents plays a considerable

role in the mesomorphic properties of such compounds and in the formation of certain mesophases[9]. The supramolecular interactions enable these discotic liquid crystals to form columnar phase which can be applied for smart materials; organic field effect transistors (OFETs), organic photovoltaic solar cells, organic light emitting diodes (OLEDs), sensors, *etc*[13, 14]. The first liquid crystalline porphyrin was reported in 1980[15]. Since then, numerous efforts were paid for the development of these discotic liquid crystalline porphyrins and related metalloporphyrins[11-14, 16].

Spin-crossover (SCO) is a general spin-state switching phenomenon between a high-spin (HS) and low-spin (LS) electronic configurations in a transition metal center. The SCO phenomenon is widely recognized as an example of molecular bistability. The SCO compounds most widely studied are six-coordinate first-row transition metal complexes with d^4-d^7 configurations[17]. Furthermore, The spin states of some complexes are exhibited high spin (HS; S=5/2), moderate spin (MS; S=3/2) and low spin (LS; S=1/2)[18] which depend on axial ligand nature, substituents and shape of moiety[19]. In 2017, Ide and co-workers studied the spin-crossover on six-coordinate iron(III) porphyrin complexes with pyridine-N oxide derivatives[20], and following year (2018) they reported the nickel (II) pyrrocorphin derivatives reacted with pyridine moieties to provide magnetic properties in wild range temperatures[21].

Nevertheless, no research has been reported the spin-crossover on porphyrin liquid crystalline with long alkyl chains and porphyrin metallomesogens though they are highly interested. Combination of softness with spin-crossover properties in long chains functionalized porphyrins has extreme challenge to design, synthesize and demonstrate their properties in order to realize the desire materials.

This research presents the design and synthesis of new metalloporphyrin liquid crystals with long-chain functionality on porphyrin macrocycles and their transition metal complexes. All structures of synthetic compounds were characterized by spectroscopic analysis and studied their liquid crystalline and magnetic properties. It is wished to explore the new smart materials which may perform advanced utilizations in the future.

OBJECTIVES

The purpose of this research project was design and synthesis of new series of functionalized porphyrins; including the ether, ester and urea functionalities, and their transition metal complexes to serve as soft materials. Then, the mesomorphic behaviors and the spin-crossover properties of the synthetic complexes were investigated.

จุฬาลงกรณ์มหาวิทยาลัย
CHULALONGKORN UNIVERSITY

CHAPTER 2

LITERATURE REVIEW

2.1 Synthesis of symmetrical porphyrins

Adler and co-worker[22] (1967) reported the simplified synthesis of *meso*-tetraphenylporphin (TPP), which resulted from mechanistic studied on preparation of porphyrins. The general condition for porphyrins synthesis uses propionic acid as a solvent under reflux and atmospheric oxygen for condensation of pyrrole and benzaldehyde and then oxidation to TPP. The crude mixture was treated with methanol to remove undesired product and water to wash acid in the crude solid, the resulting was filtrated and dried to receive the porphyrin crystal in around 20% yield.

Bettelheim and co-workers[23] (1987) reported the synthesis and electrochemical polymerization of amino-, pyrrole-, and hydroxy-substituted tetraphenylporphyrins and theirs nickel and cobalt complexes. The porphyrin electro-oxidative polymerization of *meso*-substituted phenylporphyrin films showed reductive electrochemical and electronic spectroscopic properties similar to oxidations of monomer solutions from thin polymeric coating electrodes in acetonitrile and dichloromethane. Among cobalt complexes of porphyrin derivatives, only the film of cobalt tetrakis(*o*-aminophenyl) porphyrin revealed a split cobalt (III/II) wave in aqueous acid and base which acted as good oxygen reduction catalysts.

Luguya and colleagues[24] (2004) published the regioselective nitration of the phenyl groups of *meso*-tetraphenylporphyrins by sodium nitrite in trifluoroacetic acid. The results showed nitrated products with $NaNO_2$ in TFA at *para*-position in 80-90% yield. Furthermore, the reduction of nitrophenyl groups on porphyrin ring to aminophenylporphyrins by $SnCl_2$/HCl. The *tri*-carboranylporphyrin could be prepared by reaction of *tri*-aminoporphyrin with formyl-*o*-carborane and then reduced by $NaBH_4$.

Cretu and team synthesized *meso*-tetra(3-hydroxyphenyl) porphyrin, *via* Alder's method, in propionic anhydride and propionic acid as solvent and studied its spectroscopic properties. The porphyrin product was precipitated by hexane and purified by silica gel column chromatography. The ^{1}H-NMR, FT-IR, fluorescence, and UV-visible spectroscopies were employed to elucidate the structure of target compound and investigate the photophysical properties in various solvents and acid media. The desired product can be new opto-electronic materials which can apply in PDT therapy, solar energy conversion and catalysis.

Liu[25] (2003) reported the synthesis and characterization of *meso*-tetrakis(4-*n*-alkanoyloxyphenyl) porphyrins and theirs zinc complexes (Fig. 2.1) as liquid crystalline models. They investigated liquid crystalline behavior by differential scanning calorimetry (DSC). The results showed that the series of long alkyl chain ester substituted porphyrins and theirs zinc complexes exhibited low transition temperatures and wide mesophase ranges.
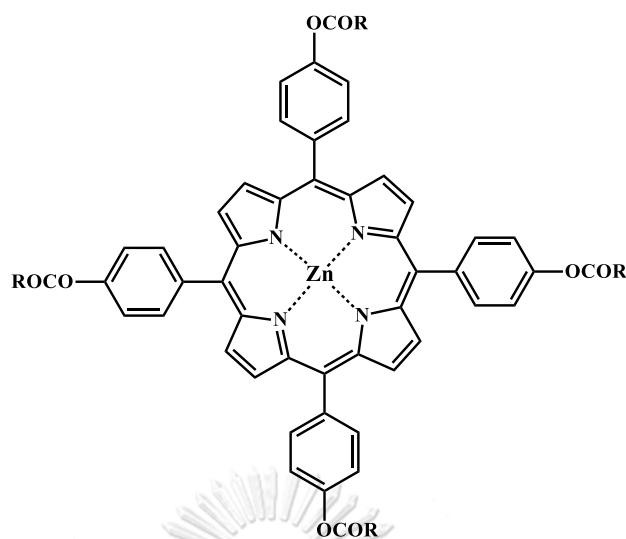
Fig. 2.1 Structure of *meso*-tetrakis(4-*n*-alkanoyloxyphenyl) porphyrin Zn complex

Liu and Shi[12] (2007) synthesized *meso*-tetrakis(4-*n*-alkanoyloxyphenyl) porphyrins and theirs cobalt and nickel metals complexes and studied liquid crystalline properties shown in Fig. 2.2. Among twelve compounds, nine complexes were explored to exhibit liquid crystal properties and showed a hexagonal columnar discotic columnar (Col$_h$) phase. All of synthesized compounds were confirmed their structures by ^{1}H-NMR, IR, UV, MS measurements, and elemental analysis (EA). These liquid crystal (LC) compounds were investigated by cyclic voltammetry, luminescence, and surface photovoltage spectroscopy.
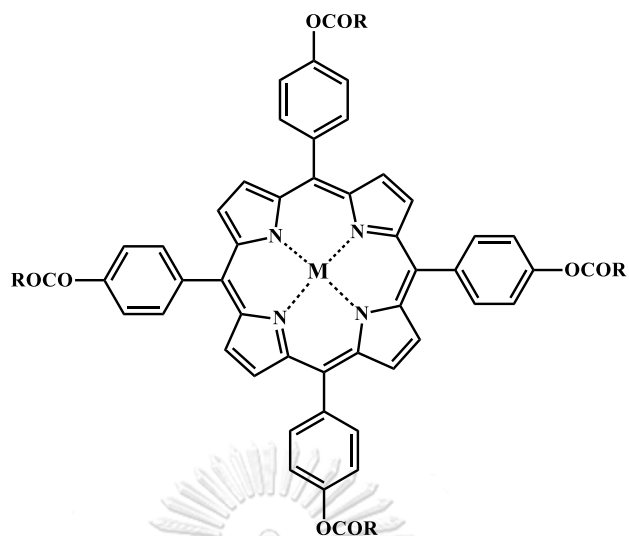
Fig. 2.2 *meso*-Tetrakis(4-*n*-alkanoyloxyphenyl) porphyrin metal complexes

(M=Co and Ni).

Liu[26] (2012) studied liquid crystalline properties of novel magnesium complexes of *meso-tetrakis*(4-*n*-alkoxyphenyl) porphyrins (Fig. 2.3). Molecular characterizations of all synthesized compounds were determined by ^{1}H-NMR, IR, UV-vis, MS, and elemental analysis (EA). Differential scanning calorimetry (DSC) and polarizing microscope (PM) were used to investigate the liquid crystalline behaviors of all the Mg complexes. Six of nine compounds were found to exhibit liquid crystal property.
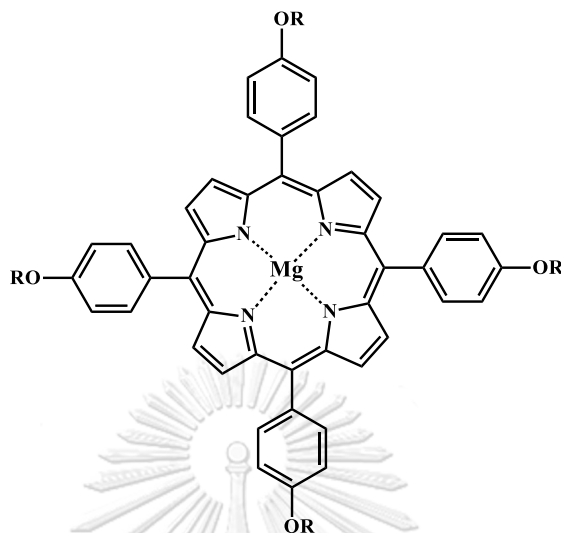
Fig. 2.3 *meso-Tetrakis*(4-*n*-alkoxyphenyl) porphyrin magnesium complexes.

Sun and team[16] (2011) synthesized a novel series of substituted tetraphenylporphyrin iron chloride complexes by one-pot mixed solvent method and two-step method. IR, FIR, UV-vis spectroscopies, and elemental analysis were used to determine the molecular structure of all iron complexes. The results showed that the one-pot mixed solvent method was better than two-step method in terms of yields, reaction time and convenient workup of reaction mixtures. The best condition was the reaction in mixed solvent, propionic acid, glacial acetic acid and *m*-nitrotoluene under reflux for 2 h which provided the highest yields (28-40%).

Sun and co-workers[27] (2007) reported novel amide porphyrin derivatives, and their metal complexes. The new porphyrin was designed and synthesized *via* amination of 4-aminophenyl groups at *meso-* position of porphyrin macrocycle. Transition metals [Mn, Fe, Co, Ni, Cu, Zn] were used to prepare the amide porphyrin complexes (Fig. 2.4), and they were characterized by elemental analysis, UV-vis, IR,

^{1}H-NMR, molar conductivity, DSC, POM, cyclic voltammetry, luminescence, and surface photovoltage spectroscopies. The porphyrin ligand showed liquid crystalline behavior and exhibited a high phase transition temperature and broad mesophase temperature. The results of photovoltaic properties and charge transfer process of all compounds revealed that all the complexes were p-type semiconductors.
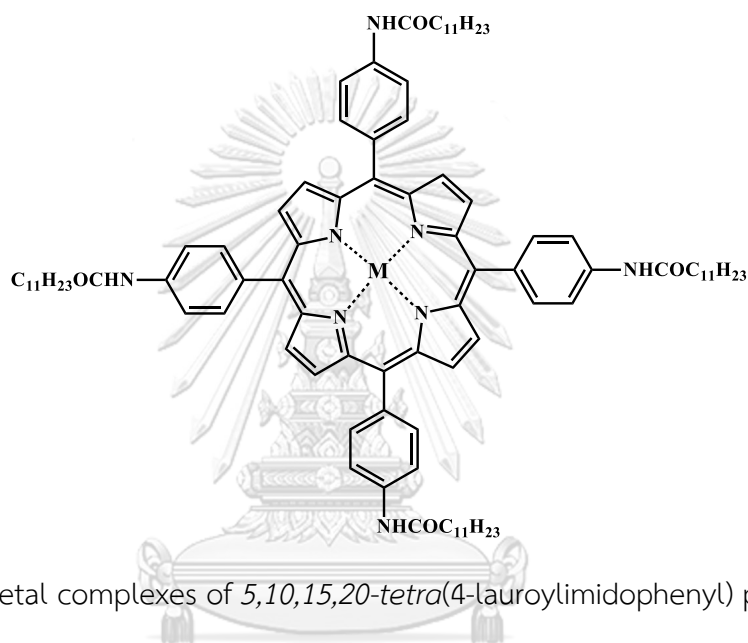
Fig. 2.4 Metal complexes of *5,10,15,20-tetra*(4-lauroylimidophenyl) porphyrins.

Sun *et al.*[28] (2008) studied electrochemical and spectroscopic properties of a series of *meso-tetra*(*p*-alkylamidophenyl) porphyrin LCs and their Mn complexes by UV-visible, FT-IR, Raman, fluorescence spectroscopies, thermal analysis, and cyclic voltammetry. All results indicated that the properties of porphyrin compounds were depended on the length of side chains. The DSC study of porphyrins and Mn complex showed continuous process of decomposition.

Fedulova and co-workers[11] (2008) synthesized and investigated mesomorphism of 4-substituted tetraphenylporphyrin derivatives and their complexes. The complexes were characterized by NMR, FT-IR, UV-visible

spectroscopies, and elemental analysis. Mesomorphic property was investigated by optical polarization microscopy and thermotropic mesomorphism was studied by optical thermo-polarization microscope. Some complex showed good thermotropic mesogen property in a wide range temperature.

Bragina and collages reported a series of new lipophilic and amphiphilic tetraphenylporphyrins and their metal complexes. The mesogenic properties were investigated by optical polarization microscopy and differential scanning calorimetry. Zinc and cobalt complexes were obtained in 90-95% yields from porphyrin ligands. The phase transition temperature results of all compounds indicated that discotic symmetrical long chain *meso*-aryl-substituted porphyrins exhibited thermotropic and lyotropic behavior in non-polar solvents, some of them were glassing mesogens. Zinc (II) and Co (II) ions were incorporated with porphyrin derivatives to increase the number of mesogenic compounds and to change mesogenic properties in comparison with porphyrin ligands.

Rumyantseva *et al.*[29] (2013) reported the improved method to synthesize tetrakis(4-hydroxyphenyl) porphyrins. The method was developed from Alder-Longo method by using three solvents mixture; propionic acid, acetic acid, and nitrobenzene (2:1:1). The porphyrin purification was carried out by ethyl acetate extraction with 56% yield.

Zhang and colleges[30] (2017) synthesized porphyrin derivatives as liquid crystalline and applied for photovoltaic device. All porphyrins with four *meso*-substituted amide groups and their zinc complexes, were investigated by TG, DSC, POM, XRD, AFM. The photoelectric property was examined by using the porphyrin

derivatives as donor materials and 3,4,9,10-perylenetetracarboxylic dianhydride (PTCDA) as the acceptor materials. The results found that photoelectric conversion efficiency (PCEs) improved after metal atom coordination, compared with the porphyrin ligands.

2.1.1 Ester series

Li and co-workers[31] (2008) reported the novel ester functionalized porphyrin and their metal complexes as liquid crystal. ^{1}H-NMR, FT-IR spectroscopies and elemental analysis were employed to confirm the molecular structures of all compounds. Mesomorphic studies using DSC, POM, and X-ray diffraction spectroscopy showed that all compounds exhibited thermotropic mesophases over a wide temperature range and low liquid crystalline transition temperatures.

Li and colleges[32] (2008) studied organic photovoltaic properties of new light-harvesting liquid crystalline porphyrin series. The chemical structures of all compounds were identified by ^{1}H-NMR, FT-IR spectroscopies, and elemental analysis. The synchrotron X-ray diffraction was used to confirm the homeotropic alignment, which molecular arrangement could be provided the most efficient pathway of hole conduction along the columnar axis, and the light-harvesting molecules were arranged with the largest area to the incident light. The results indicated that the new and efficient ways to develop organic photovoltaics by homeotropically aligned liquid crystal thin film.

Tsuchida *et al.*[33] (1990) reported the synthesis, characterization and oxygenation of bis-fenced porphyrins and their iron (II) and cobalt (II) complexes. The

iron (II) ester-functionalized porphyrin complex formed dioxygen adduct which was stable and reversible in toluene at ambient temperature. The half-life for irreversible oxygenation was longer than 24 hours. The steric groups on phenyl rings of porphyrin decreased the binding constants for ligands and for dioxygen. The binding characteristics of the ligand was clarified by Mössbauer and IR spectroscopic measurements. The kinetic results of oxygenation suggested that the low oxygen affinity was brought about primarily by high rate of ligand dissociation.

Fedulova and co-workers[34] (2007) synthesized the lipophilic tetraphenylporphyrins with long chain fatty acid ester functionalized at *para*-position of the phenyl rings to design supramolecular lipid ensembles in nanoscale. The preparation methods of porphyrins were conducted in two ways: with use dipyrrometane and monopyrrole condensations. The synthesis of symmetrical porphyrins by dipyrrometane condensation provided a range of 55-75% yields and was followed by oxidation with DDQ in range of 38-54% yields.

2.1.2 Ether series

Formirovsky and co-workers[35] (2012) reported the new amphiphilic alkoxyarylporphyrins with long-chain substituent functionalities and their complexes. Their liquid crystal properties were studied by POM in two modes: heating and cooling. The results revealed that manifestation of LC properties was affected by the length of aliphatic moiety, the nature of terminal polar groups, and the presence of a complex-forming metal.

Zheng and colleges[36] (2013) studied the liquid crystalline properties of the new di-substituted arylporphyrin and their transition metal complexes. They reported the synthesis, chemical characterization by ^{1}H-NMR, FT-IR spectroscopies and elemental analysis and the liquid crystalline behavior by DSC, XRD and POM. The results indicated that there was an increase in the liquid crystalline phase with increasing chain length.

2.1.3 Urea series

Luguya and colleges[24] (2004) studied the synthetic method and reaction of *meso*-(*p*-nitrophenyl) porphyrins. They reported the regioselective nitration of phenyl groups of *meso*-tetraphenylporphyrin by using $NaNO_2$ and TFA. The degree of reaction was controlled by the equivalent of $NaNO_2$ and the reaction time. The aminophenylporphyrin could be reduced from nitrophenylporphyrin under standard $SnCl_2$/HCl condition. Reaction of aminoporphyrin with carboranyl aldehyde and then reduction by $NaBH_4$ gave an amine linkage between porphyrin and carborane moiety. All compounds were confirmed by ^{1}H-NMR, FT-IR and MALDI-TOF mass spectroscopies and elemental analysis.

Karimipour *et al.* synthesized urea-amino functionalized porphyrins and studied their antibacterial and antifungal activities. All compounds were characterized by ^{1}H-NMR, FTIR, UV-vis spectroscopic techniques and elemental analysis. The biological activities of synthetic compounds *in vitro* were investigated by agar-disc diffusion method against some gram (-), (+) bacteria and some fungi. The

results concluded that Co and Mn porphyrin complexes showed that they had higher against antibacterial and anti-fungal inhibitory activities than porphyrin ligands.

Alliband and co-workers[37] (2013) reported the synthesis and characterization of new picket porphyrin receptors to bind phosphatidylglycerol which acted as the anionic phospholipid found in bacterial membranes. The urea-picket porphyrins were designed to bind with the phosphate anion and glycerol hydroxyl residues of lipid. All compounds were prepared and characterized by HRMS and ^{1}H-NMR spectroscopy. The results concluded that the receptor-lipid stoichiometry of binding to the receptor's pickets was allowed for all the lipid and receptor functional groups to fully align, 1:1 complex formation. The complementary binding pockets, urea picket porphyrins, suggested any kinds of stable pickets with nearly placed binding units of the lipid.

Tamaru *et al.*[38] (2002) studied a urea porphyrin-based gelator assembly reinforced by peripheral groups and chirally twisted from chiral urea additives. The new urea porphyrin was synthesized and investigated to aggregate into 1D-direction as organo-gel phase in organic solvents; anisole and diethyl ether. The spectroscopic results and electron-micrographic observation indicated that the π-π stacking interaction among macrocyclic moieties and hydrogen-bonding interaction among urea moieties were synergistically operated for stable 1D aggregation for gel formation.

2.2 Synthesis of metalloporphyrins

Adler et al.[39] (1970) prepared metalloporphyrins from metalation of porphyrin ligand with metal salts. This complexation depended on thermodynamic stability of the complex, and the rates of reaction were generally slowed. The investigated procedure consisted of the porphyrin and divalent metal salt to react in refluxing dimethylformamide (DMF), which the advantages of DMF as a reaction medium stemmed relatively large liquid range and high boiling point. At low temperature, the metalloporphyrin often allowed precipitated or crystallized out of the reaction medium to collect the product by filtration or extraction. The improved method had afforded high yields after further purification (more than 90 % based on the ligand).

2.3 Synthesis of terpyridine derivatives

Lee *et al.*[40] (2013) reported the synthesis and characterization of tris-alkoxylphenylterpyridine Co (II) complexes to investigate the mesomorphic and magnetic properties. The tri-alkoxy-substituted benzaldehyde was used to prepare terpyridine derivatives *via* aldol condensation reaction by 2-acetyl pyridine and ammonia solution. Cobalt (II) tetrafluoroborate hexahydrate coordinated with alkoxyphenylterpyridine ligands to get the target complexes. All complexes were characterized by spectroscopic techniques; NMR, FT-IR, and X-ray diffraction method, and studied mesophase and magnetic behaviors. Long alkyl chains Co (II) complex (Fig. 2.5) was exhibited a gradual spin state between low spin and high spin in 327-338 K, triggered by the synchronicity of spin-crossover and mesophase transition.
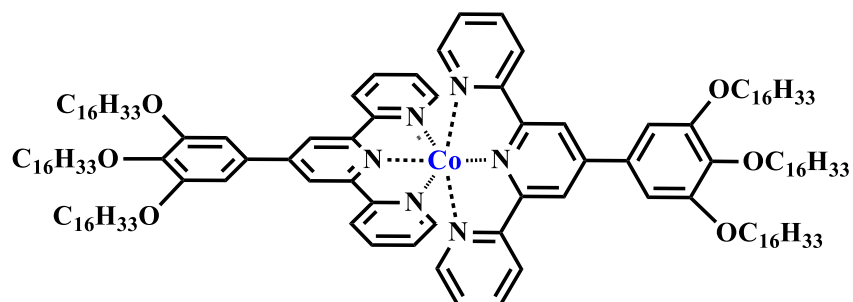
Fig. 2.5 Structure of *tris*-hexadodecoxyphenylterpyridine Co (II) complex.

Jouaiti[41] (2021) reported the one-pot synthesis of terpyridinebenzaldehyde derivatives at room temperature. Starting from diethoxymethylbenzaldehyde isomers reacted with acetylpyridine in a presence of KOH in ethanol and ammonia solution, then deprotection by acid catalysis, in high yield.

Cho and co-workers[42] (2007) prepared the *tetrakis*-(terpyridinylphenyl) porphyrin and ruthenium (II) complexes and studied photovoltaic properties and self-assembly behaviors. The target porphyrin was synthesized by Adler method of 4-formylphenylterpyridine and pyrrole in refluxing propionic acid and was isolated in 3% yield. The Ru (II)-terpyridyl and Zn-porphyrin complex was shown photovoltaic properties and exhibited normal direction self-assembly on nanowire.

Dixon *et al.*[43] (2001) studied the photoinduced electron transfer process of porphyric dyads and triads of Ir (III) *bis*-terpyridine complexes. Their photophysical properties have been determined by steady-state and time-resolved methods. The results concluded that the Zn and Au triads porphyrin complexes can be transfer electron on ground-state charge-transfer interactions.

Odobel *et al.*[44] (1993) studied the photoinduced electron transfer process of Rh (III) *bis*-terpyridine Zn porphyrin complexes. The desired porphyrin was prepared by Adler procedure, which isolated product in 7% yield. The Rh (III) terpyridine complexation was carried out using $RhCl_3,3H_2O$ in refluxing ethanol, then coupled with Zn-terpyridinyl porphyrin to afford the target compound. Luminescence studies shown that the Rh (III)-terpyridinyl porphyrin Zn complex (I) (Fig. 2.6) allowed electron transfer between Zn (II) and Rh (III) complex.
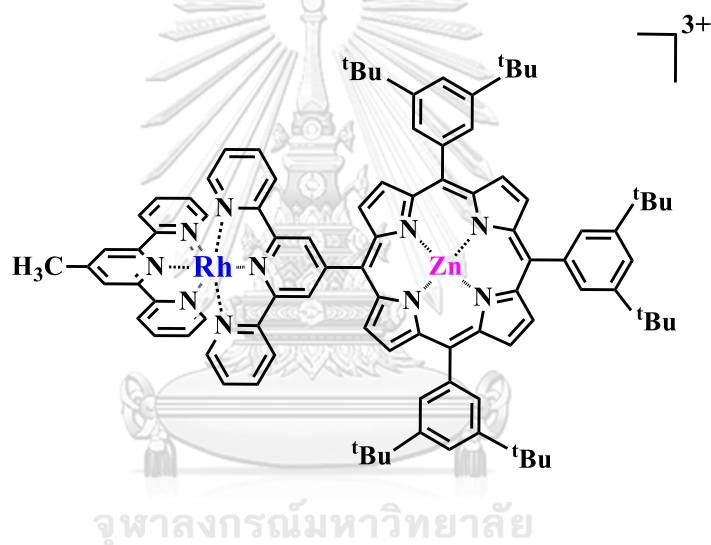

Fig. 2.6 Structure of Rh (III)-terpyridinyl porphyrin Zn complex (I).

CHAPTER 3

MATERIALS AND METHODS

3.1 Materials

Pyrrole, 4-hydroxybenzaldehyde, 4-nitrobenzaldehyde, 4-*n*-octyloxybenzaldehyde, 4-formylphenyl boronic acid, dodecanoic acid, hexadecanoic acid, octadecanoic acid, 1-bromododecane, 1-bromooctadecane, *n*-octadecyl isocyanate, 2,2-dimethyl propane-1,3-diol, trifluoroacetic acid (TFA) and anhydrous tetrahydrofuran (THF) were purchased from TCI Japan. Propionic acid, acetic acid, potassium carbonate, iron (II) chloride, tin (II) chloride, *N,N*-dimethylformamide (DMF) and nitrobenzene were purchased from Merck and used without further purification. Pyrrole was purified by distillation before used.

Column chromatography was performed on a glass column by silica gel 60 (Merck, 0.063-0.200 mm). Thin layer chromatography (TLC) was carried out on Merck TLC silica gel 60 F_{254} supported on aluminium plates (20x20 cm).

3.2 Instrumentation

Nuclear magnetic resonance (^{1}H-NMR and ^{13}C-NMR) measurements were recorded on JEOL 500 MHz NMR at Chulalongkorn University, Bangkok, Thailand in deuterated solvents ($CDCl_3$, acetone-D_6, DMSO-D_6) using the solvent residual proton signals as the internal standard.

Matrix-assisted laser desorption and ionization time-of-flight mass spectrometry (MALDI-TOF MS) were performed on a Bruker Autoflex III Smartbean mass spectrometer and Direct analysis in real time (DART) mass spectrometry was achieved on JEOL AccuTOF™ mass spectrometer at Chulalongkorn University, Bangkok, Thailand.

Elemental analysis (C, H, N) was carried out on THERMO (FLASH 2000) at Scientific and Technological Research Equipment Centre Chulalongkorn University, Bangkok, Thailand.

FT-IR spectra were taken on a Nicolet iS50 FTIR spectrometer at Chulalongkorn University, Bangkok, Thailand, number of scans = 32.

UV-vis spectra were collected on a Cary UV-vis spectrophotometer at Chulalongkorn University, Bangkok, Thailand using dichloromethane (DCM) as solvent, scan from 200 to 800 nm.

Differential scanning calorimetry (DSC) thermal analysis was carried out on a NETZSCH DSC 204 F1 Phoenix calorimeter at Scientific and Technological Research Equipment Centre Chulalongkorn University, Bangkok, Thailand.

Magnetic susceptibilities of samples were analyzed on a Quantum Design MPMS-5S magnetometer (SQUID) at Kumamoto University, Kumamoto, Japan.
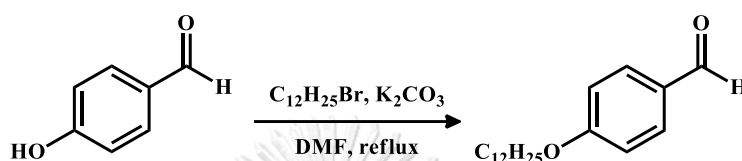
3.3 Methods

3.3.1 Preparation of *meso*-tetra(4-alkyloxyphenyl)porphyrin derivatives

I. Synthesis of 4-*n*-alkyloxybenzaldehydes (1-2)

4-n-Dodecyloxybenzaldehyde (1)

4-Hydroxybenzaldehyde 4.00 g (32.75 mmol) and anhydrous potassium carbonate (5.0 g, 36.18 mmol) were dissolved in 25 mL of dry *N,N*-dimethylformamide, stirred and heated at reflux. 1-Bromododecane 9.00 g (1.1 eq, 36.18 mmol) was added into the mixture and heating was continued until reaction completion. The reaction mixture dissolved with water and extracted with ethyl acetate in three times, then the organic layer was washed with water, dried over anhydrous Na_2SO_4, and the solvents were removed *in vacuo*. The product was purified by column chromatography on G60 silica gel to obtain the colorless oil; Yield 94 %, R_f = 0.36 (Hexane: EtOAc, 19:1).

[1]**H-NMR** (500 MHz, $CDCl_3$, δ (ppm)): 9.78 (s, 1H, C*H*O), 7.73 (d, *J* = 8.8 Hz, 2H), 6.90 (d, *J* = 8.7 Hz, 2H), 3.94 (t, *J* = 6.6 Hz, 2H), 1.75-1.69 (m, 2H), 1.41-1.18 (m, 18H), 0.80 (t, *J* = 7.0 Hz, 3H).

[13]**C-NMR** (500 MHz, $CDCl_3$, δ (ppm)): 190.75, 164.32, 132.00, 129.81, 114.78, 68.46, 31.99, 29.73, 29.71, 29.66, 29.63, 29.42, 29.12, 26.03, 25.88, 22.76, 14.18.

MALDI-TOF (m/z): calcd. for $C_{19}H_{30}O_2$ = 290.22, found = 290.435.

4-n-Octadecyloxybenzaldehyde (2)
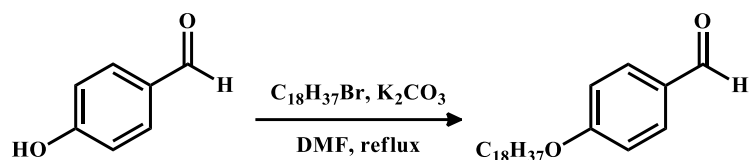
4-*n*-Octadecyloxybenzaldehyde **(2)** was synthesized by the same procedure as the synthesis of compound **(1)** by using 2.00 g (16.38 mmol) of 4-hydroxybenzaldehyde 2.50 g (18.09 mmol) of anhydrous potassium carbonate and 1-bromooctadecane 6.00 g (1.1 eq, 18.02 mmol) dissolved in 20 mL of dry *N,N*-dimethylformamide. The product was crystallized by mixture of DCM and methanol to obtain the white solid; Yield 98 %, R_f = 0.48 (Hexane: EtOAc, 19:1).

^{1}**H-NMR** (500 MHz, CDCl$_3$, δ (ppm)): 9.87 (s, 1H, C*H*O), 7.82 (d, *J* = 8.5 Hz, 2H), 6.99 (d, *J* = 8.7 Hz, 2H), 4.03 (t, *J* = 6.6 Hz, 2H), 1.82-1.78 (m, 2H), 1.49-1.25 (m, 30H), 0.88 (t, *J* = 6.9 Hz, 3H).

^{13}**C-NMR** (500 MHz, CDCl$_3$, δ (ppm)): 190.92, 164.36, 132.07, 129.80, 114.82, 68.51, 32.01, 29.78, 29.66, 29.63, 29.44, 29.42, 29.13, 26.04, 22.77, 14.20.

MALDI-TOF (*m/z*): calcd. for C$_{25}$H$_{42}$O$_2$ = 374.32, found = 375.185 [M+H$^+$].

II. Synthesis of *meso-tetra*(4-alkyloxyphenyl) porphyrins (3-5)
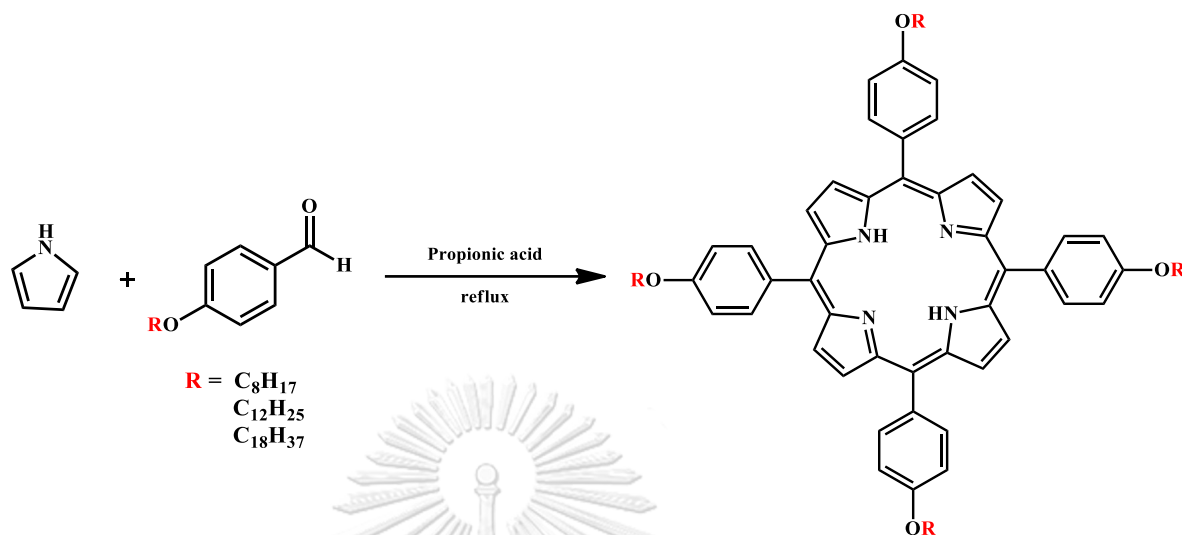
General procedure

4-*n*-Alkyloxybenzaldehyde was dissolved in propionic acid. The solution was heated to reflux under continuous stirring for 30 min. Pyrrole (1 eq.) was slowly added into the heated solution by addition funnel and the heating was continued further until reaction completion (6 -24 h) monitored by TLC. After the reaction mixture was cooled down to room temperature, methanol was added into the reaction mixture. The product was filtrated and washed with methanol to give dark-purple solid. The crude product was purified by column chromatography and recrystallized to afford the porphyrin crystals.

5,10,15,20-*Tetra*(4-*n*-octyloxyphenyl) porphyrin (3): 332 mg, yield 28%, R_f = 0.30 (7:3, Hexane: DCM), the purple crystals.

^{1}H-NMR (500 MHz, CDCl$_3$, δ (ppm)): 8.88 (s, 8H, β-H), 8.11 (d, J = 8.4 Hz, 8H), 7.26 (d, J = 8.6 Hz, 8H), 4.22 (t, J = 6.5 Hz, 8H), 2.01-1.95 (m, 8H), 1.62-1.37 (m, 40H), 0.95 (t, J = 6.8 Hz, 12H), -2.72 (s, 2H).

^{13}**C-NMR** (500 MHz, CDCl$_3$, δ (ppm)): 159.04, 135.69, 134.54, 119.90, 112.78, 68.42, 32.00, 29.61, 29.45, 26.35, 22.77, 14.27.

MALDI-TOF (m/z): calcd. for C$_{76}$H$_{94}$N$_4$O$_4$ = 1126.73, found = 1126.258 [M$^+$].

EA: calcd. for C$_{76}$H$_{94}$N$_4$O$_4$: C, 80.95; H, 8.40; N, 4.97. found: C, 81.09; H, 8.28; N, 5.01.

FT-IR, ν_{max} (cm^{-1}): 3316.55, 2922.39, 2849.59, 1604.78, 1507.15, 1464.07, 1238.76, 1173.36, 964.37, 837.14, 802.63, 789.37, 738.84.

UV-vis, λ_{max} (nm): 423, 519, 557, 594, 652.

5,10,15,20-*Tetra*(4-*n*-dodecyloxyphenyl) porphyrin (4): 279 mg, yield 34%, R$_f$ = 0.30 (8:2, Hexane: DCM), the purple crystals.

^{1}**H-NMR** (500 MHz, CDCl$_3$, δ (ppm)): 8.87 (s, 8H, β-H), 8.10 (d, J = 8.4 Hz, 8H), 7.26 (d, J = 8.5 Hz, 8H), 4.23 (t, J = 6.5 Hz, 8H), 2.00-1.94 (m, 8H), 1.62-1.32 (m, 72H), 0.91 (t, J = 6.9 Hz, 12H), -2.73 (s, 2H).

^{13}**C-NMR** (500 MHz, CDCl$_3$, δ (ppm)): 159.04, 135.69, 134.53, 119.91, 112.78, 68.41, 32.06, 29.83, 29.78, 29.64, 29.61, 29.50, 26.34, 22.82, 14.25.

MALDI-TOF (m/z): calcd. for C$_{92}$H$_{126}$N$_4$O$_4$ = 1350.98, found = 1350.679 [M$^+$].

EA: calcd. for C$_{92}$H$_{126}$N$_4$O$_4$: C, 81.73; H, 9.39; N, 4.14. found: C, 81.63; H, 9.41; N, 4.21.

FT-IR, ν_{max} (cm^{-1}): 3314.47, 2918.72, 2848.86, 1604.46, 1507.01, 1463.23, 1239.43, 1172.88, 965.66, 840.35, 801.69, 789.32, 738.52.

UV-vis, λ_{max} (nm): 423, 520, 557, 596, 652.

5,10,15,20-*Tetra*(4-*n*-octadecyloxyphenyl) porphyrin (5): 234 mg, yield 32%, R_f = 0.40 (9:1, Hexane: DCM), the purple crystals.

^{1}H-NMR (500 MHz, CDCl$_3$, δ (ppm)): 8.86 (s, 8H, β-H), 8.10 (d, J = 8.3 Hz, 8H), 7.26 (d, J = 8.5 Hz, 8H), 4.23 (t, J = 6.5 Hz, 8H), 2.01-1.95 (m, 8H), 1.65-1.26 (m, 112H), 0.88 (t, J = 6.8 Hz, 12H), -2.75 (s, 2H).

^{13}C-NMR (500 MHz, CDCl$_3$, δ (ppm)): 159.05, 135.70, 134.55, 119.93, 112.79, 68.41, 32.06, 29.86, 29.81, 29.68, 29.51, 26.37, 22.82, 14.25.

MALDI-TOF (m/z): calcd. for C$_{116}$H$_{174}$N$_4$O$_4$ = 1687.35, found = 1687.930 [M$^+$].

EA: calcd. for C$_{116}$H$_{174}$N$_4$O$_4$: C, 82.51; H, 10.39; N, 3.32. found: C, 82.44; H, 10.60; N, 3.38.

FT-IR, ν_{max} (cm^{-1}): 3315.22, 2916.66, 2849.01, 1605.43, 1508.08, 1463.85, 1240.33, 1173.74, 966.20, 840.00, 802.38, 790.34, 738.72, 718.70, 630.92.

UV-vis, λ_{max} (nm): 422, 519, 556, 595, 652.

III. Metalation of *meso-tetra*(4-alkyloxyphenyl) porphyrin metal complexes (3-5, a-c)
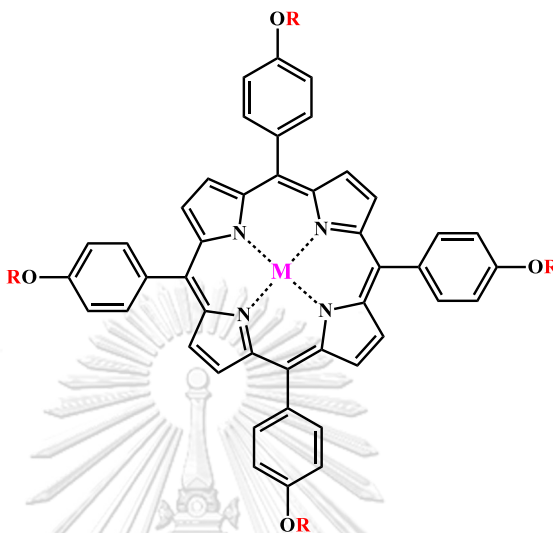
General procedure

The Porphyrin (1 mmol) was dissolved in 20 mL of dry dimethylformamide (DMF) and heated under nitrogen atmosphere. Metal ion (10 mmol) was dissolved in 2.0 mL of dry DMF, added into the solution, and reflux until reaction completed (2-24 h.) observed by TLC. The reaction mixture was dissolved with water and extracted with dichloromethane. The organic layer was washed with water twice, dried over anhydrous Na_2SO_4 and concentrated *in vacuo*. The crude product was purified by column chromatography on G60 silica gel and/or recrystallized by mixture of DCM and MeOH to provide the porphyrin metal complexes.

Cobalt (II) complexes (3-5, a)

5,10,15,20-*Tetra*(4-octyloxyphenyl) porphyrin Co (II) (3a): 98 mg, yield 89 %, R_f = 0.27 (8:2, Hexane: DCM), the red crystals.

MALDI-TOF (m/z): calcd. for $C_{76}H_{92}CoN_4O_4$ = 1183.62, found = 1184.385 [M$^+$].

FT-IR, ν_{max} (cm^{-1}): 2922.49, 2849.53, 1605.29, 1506.66, 1456.11, 1350.42, 1280.46, 1241.50, 1173.78, 999.93, 802.68, 717.16.

UV-vis, λ_{max} (nm): 416, 531.

5,10,15,20-*Tetra*(4-dodecyloxyphenyl) porphyrin Co (II) (4a): 65 mg, yield 90 %, R_f = 0.22 (9:1, Hexane: DCM), the red crystals.

MALDI-TOF (m/z): calcd. for $C_{92}H_{124}CoN_4O_4$ = 1407.90, found =1407.935 [M$^+$].

UV-vis, λ_{max} (nm): 416, 531.

5,10,15,20-*Tetra*(4-octadecyloxyphenyl) porphyrin Co (II) (5a): 80 mg, yield 84 %, R_f = 0.35 (9:1, Hexane: DCM), the red crystals.

MALDI-TOF (m/z): calcd. for $C_{116}H_{172}CoN_4O_4$ = 1744.27, found =1745.990 [M+H$^+$].

UV-vis, λ_{max} (nm): 415, 531.

Nickel (II) complexes (3-5, b)

5,10,15,20-*Tetra*(4-octyloxyphenyl) porphyrin Ni (II) (3b): 97 mg, yield 94 %, R_f = 0.35 (8:2, Hexane: DCM), the red crystals.

^{1}H-NMR (500 MHz, CDCl$_3$, δ (ppm)): 8.76 (s, 8H, β-H), 7.89 (d, J = 8.50 Hz, 8H), 7.19 (d, J = 8.50 Hz, 8H), 4.19 (t, J = 6.57 Hz, 8H), 1.97-1.93 (m, 8H), 1.63-1.33 (m, 40H), 0.92 (t, J = 6.87 Hz, 12H).

MALDI-TOF (m/z): calcd. for $C_{76}H_{92}NiN_4O_4$ = 1182.65, found =1182.393 [M$^+$].

UV-Vis, λ_{max} (nm): 420, 529.

5,10,15,20-*Tetra*(4-dodecyloxyphenyl) porphyrin Ni (II) (4b): 95 mg, yield 91%, R_f = 0.30 (9:1, Hexane: DCM), the red crystals.

^{1}H-NMR (500 MHz, CDCl$_3$, δ (ppm)): 8.76 (s, 8H, β-H), 7.89 (d, J = 8.25 Hz, 8H), 7.19 (d, J = 9.05 Hz, 8H), 4.19 (t, J = 6.55 Hz, 8H), 1.98-1.93 (m, 8H), 1.64-1.29 (m, 72H), 0.89 (t, J = 7.0 Hz, 12H).

MALDI-TOF (m/z): calcd. for $C_{92}H_{124}NiN_4O_4$ = 1406.9, found =1408.001 [M+H$^+$].

UV-Vis, λ_{max} (nm): 421, 528.

5,10,15,20-*Tetra*(4-octadecyloxyphenyl) porphyrin Ni (II) (5b): 111 mg, yield 88%, R_f = 0.45 (9:1, Hexane: DCM), the red crystals.

¹H-NMR (500 MHz, CDCl₃, **δ** (ppm)): 8.76 (s, 8H, **β**-H), 7.89 (d, *J* = 8.75 Hz, 8H), 7.19 (d, *J* = 8.25 Hz, 8H), 4.19 (t, *J* = 6.55 Hz, 8H), 1.98-1.93 (m, 8H), 1.64-1.26 (m, 112H), 0.87 (t, *J* = 7.0 Hz, 12H).

MALDI-TOF (m/z): calcd. for $C_{116}H_{172}NiN_4O_4$ = 1743.27, found =1744.486 [M+H⁺].

UV-vis, λ$_{max}$ (nm): 420, 529.

Iron (III) complexes (3-5, c)

5,10,15,20-*Tetra*(4-octyloxyphenyl) porphyrin Fe (III) (3c): 95 mg, yield 68 %, the purple crystals.

MALDI-TOF (m/z): calcd. for $C_{76}H_{92}FeN_4O_4$ = 1180.65, found =1180.727 [M⁺].

UV-vis, λ$_{max}$ (nm): 416, 573.

5,10,15,20-*Tetra*(4-dodecyloxyphenyl) porphyrin Fe (III) (4c): 95 mg, yield 62 %, the purple crystals.

MALDI-TOF (m/z): calcd. for $C_{92}H_{124}FeN_4O_4$ = 1404.90, found =1406.244 [M+H⁺].

UV-vis, λ$_{max}$ (nm): 416, 573.

5,10,15,20-*Tetra*(4-octadecyloxyphenyl) porphyrin Fe (III) (5c): 111 mg, yield 69 %, the purple crystals.

MALDI-TOF (m/z): calcd. for $C_{116}H_{172}FeN_4O_4$ = 1741.27, found =1742.661 [M+H$^+$].

UV-vis, λ_{max} (nm): 415, 574.

3.3.2 Preparation of *meso-tetra*(4-alkylcarbonyloxyphenyl)porphyrin derivatives

I. Synthesis of meso-tetra(4-hydroxyphenyl) porphyrin (6)
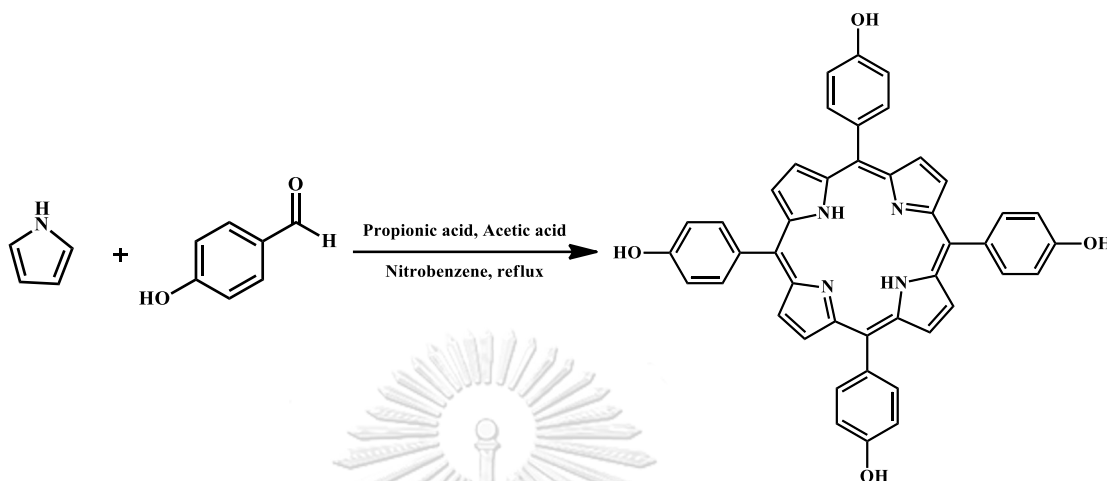
4-Hydroxybenzaldehyde (1.83 g, 15 mmol) dissolved in propionic acid, acetic acid nitrobenzene (5:12:8 mL) then stirred and reflux for 30 min. Pyrrole (1.0 mL, 15 mmol) was added into the solution and refluxed until complete reaction monitored by TLC. After the reaction mixture cooled down to room temperature, the crude product was filtered off to give dark blue solid. It was purified by column chromatography G60 silica gel; R_f = 0.25 (1:1, Hexane: EtOAc) and recrystallized in mixture of acetone and hexane to afford the blue crystals; 648 mg, yield 27%.

^{1}H-NMR (500 MHz, Acetone-D$_6$, δ (ppm)): 8.97 (s, 4H, ArO*H*), 8.90 (s, 8H, β-*H*), 8.04 (d, *J* = 8.4 Hz, 8H), 7.27 (d, *J* = 8.4 Hz, 8H), -2.71 (s, 2H).

^{13}C-NMR (500 MHz, Acetone-D$_6$, δ (ppm)): 205.53, 157.60, 135.63, 133.21, 120.18, 113.87.

MALDI-TOF (m/z): calcd. for C$_{44}$H$_{30}$N$_4$O$_4$ = 678.23, found = 678.540 [M$^+$].

FT-IR, ν_{max} (cm^{-1}): 3495.07, 3389.42, 1604.26, 1504.73, 1470.72, 1255.42, 1192.13, 1170.58, 965.38, 840.67, 795.05, 728.16.

II. Synthesis of *meso*-tetra(4-alkylcarbonyloxyphenyl) porphyrins (7-9)
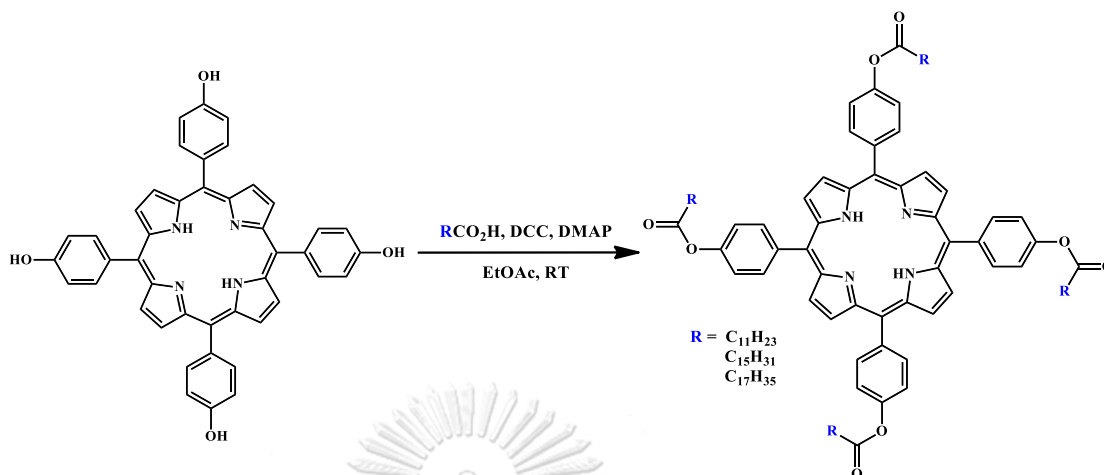
General procedure

Saturated fatty acid (10 mmol) and *N,N'*-dicyclohexylcarbodiimide (DCC) (10.1 mmol) were dissolved in 25 mL of EtOAc and stirred for 10 min, then *N,N*-dimethylaminopyridine (DMAP) (0.1 mmol) was added. After 30 min, the solution of *tetra*(4-hydroxy) phenylporphyrin (1 mmol) in 5 mL of EtOAc was added into the reaction mixture and stirred at room temperature until reaction completed (48-72 h.) monitored by TLC. The dicyclohexylurea was removed from reaction mixture by filtration, then washed with water and brine. The organic phase was dried by anhydrous Na$_2$SO$_4$, and the solvents were removed by rotary evaporator under vacuum. The desired product was purified by column chromatography and recrystallization.

5,10,15,20-*Tetra*(4-dodecylcarbonyloxyphenyl) porphyrin (7): 332 mg, yield 83%, R_f = 0.25 (19:1, Hexane: EtOAc), the purple crystals.

^{1}H-NMR (500 MHz, CDCl$_3$, **δ** (ppm)): 8.89 (s, 8H, **β**-H), 8.22 (d, *J* = 8.4 Hz, 8H), 7.50 (d, *J* = 8.5 Hz, 8H), 2.75 (t, *J* = 7.5 Hz, 8H), 1.94-1.91 (m, 8H), 1.55-1.31 (m, 64H), 0.90 (t, *J* = 6.9 Hz, 12H), -2.82 (s, 2H).

^{13}C-NMR (500 MHz, CDCl$_3$, **δ** (ppm)): 172.42, 150.82, 139.61, 135.40, 120.01, 119.36, 34.74, 32.04, 29.76, 29.47, 25.19, 22.81, 14.16.

MALDI-TOF (m/z): calcd. for $C_{92}H_{118}N_4O_8$ = 1406.89, found = 1407.988 [M+H$^+$].

EA: calcd. for $C_{92}H_{118}N_4O_8$: C, 78.48; H, 8.45; N, 3.98. found: C, 78.57; H, 9.31; N, 3.82.

FT-IR, ν$_{max}$ (cm^{-1}): 3315.64, 2920.77, 2850.93, 1758.02, 1500.53, 1468.08, 1197.88, 1163.19, 1130.46, 1109.60, 966.79, 798.66, 730.60.

UV-vis, λ$_{max}$ (nm): 419, 514, 550, 588, 645.

5,10,15,20-*Tetra*(4-hexadecylcarbonyloxyphenyl) porphyrin (8): 279 mg, yield 89%, R_f = 0.30 (19:1, Hexane: EtOAc), the red-purple crystals.

^{1}H-NMR (500 MHz, CDCl$_3$, **δ** (ppm)): 8.88 (s, 8H, **β**-H), 8.21 (d, *J* = 8.4 Hz, 8H), 7.50 (d, *J* = 8.5 Hz, 8H), 2.75 (t, *J* = 7.5 Hz, 8H), 1.94-1.91 (m, 8H), 1.55-1.27 (m, 96H), 0.87 (t, *J* = 6.9 Hz, 12H), -2.82 (s, 2H).

¹³**C-NMR** (500 MHz, CDCl₃, **δ** (ppm)): 172.60, 150.81, 139.54, 135.39, 120.00, 119.35, 34.73, 32.02, 29.81, 29.76, 29.64, 29.46, 29.33, 25.18, 22.78, 14.22.

MALDI-TOF (m/z): calcd. for $C_{108}H_{150}N_4O_8$ = 1631.15, found = 1632.236 [M+H⁺].

EA: calcd. for $C_{108}H_{150}N_4O_8$: C, 79.46; H, 9.26; N, 3.43. found: C, 79.57; H, 9.31; N, 3.32.

FT-IR, **ν**_{max} (cm⁻¹): 3315.94, 2917.19, 2849.27, 1758.52, 1498.83, 1467.49, 1198.34, 1164.56, 1135.85, 1109.60, 966.67, 794.53, 719.23.

UV-vis, λ_{max} (nm): 419, 516, 550, 589, 645.

5,10,15,20-*Tetra*(4-octadecylcarbonyloxyphenyl) porphyrin (9): 234 mg, yield 78%, R_f = 0.40 (19:1, Hexane: EtOAc), the red-purple crystals.

¹**H-NMR** (500 MHz, CDCl₃, **δ** (ppm)): 8.88 (s, 8H, **β**-H), 8.21 (d, *J* = 8.3 Hz, 8H), 7.50 (d, *J* = 8.3 Hz, 8H), 2.75 (t, *J* = 7.5 Hz, 8H), 1.94-1.91 (m, 8H), 1.55-1.25 (m, 112H), 0.87 (t, *J* = 6.9 Hz, 12H), -2.83 (s, 2H).

¹³**C-NMR** (500 MHz, CDCl₃, **δ** (ppm)): 172.60, 150.81, 139.54, 135.39, 120.00, 119.35, 34.73, 32.01, 29.81, 29.76, 29.64, 29.46, 29.34, 25.19, 22.78, 14.21.

MALDI-TOF (m/z): calcd. for $C_{116}H_{166}N_4O_8$ = 1743.27, found = 1745.065. [M+H⁺]

EA: calcd. for $C_{116}H_{166}N_4O_8$: C, 79.86; H, 9.59; N, 3.21. found: C, 78.53; H, 9.57; N, 3.16.

FT-IR, ν_{max} (cm^{-1}): 3316.32, 2917.16, 2849.45, 1758.92, 1499.25, 1467.45, 1199.06, 1164.61, 1136.00, 966.93, 796.17, 719.17.

UV-vis, λ_{max} (nm): 419, 514, 548, 590, 646.

III. Metalation of *meso-tetra*(4-alkylcarbonyloxyphenyl) porphyrin metal complexes (7-9, a-c)
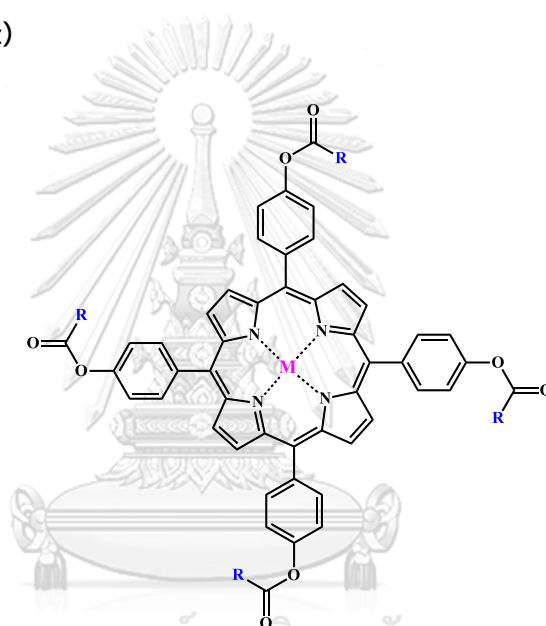
General procedure

The Porphyrin (1 mmol) was dissolved in dry tetrahydrofuran (THF) in 15 min and heated to reflux under nitrogen. Metal ion (10-15 eq.) was dissolved in dry THF, added into the solution, and stirred until reaction was completed (2-24 h., monitored by TLC). The solvents were removed from reaction mixture by rotary evaporator under reduced pressure. The obtained crude was dissolved in dichloromethane or ethyl acetate and extracted with water two times in order to eliminate metal salt. The organic layer was dried over anhydrous Na$_2$SO$_4$ and concentrated *in vacuo*. The

crude product was purified by column chromatography on G60 silica gel and recrystallized in DCM and ethanol to afford the porphyrin metal complexes.

Cobalt (II) complexes (7-9, a)

5,10,15,20-*Tetra*(4-dodecylcarbonyloxyphenyl) porphyrin Co (II) (7a): 65 mg, yield 91 %, R_f = 0.22 (19:1, Hexane: EtOAc), the red crystals.

MALDI-TOF (m/z): calcd. for $C_{92}H_{116}CoN_4O_8$ = 1463.81, found = 1464.675 [M+H$^+$].

FT-IR, ν_{max} (cm^{-1}): 2920.61, 2850.82, 1754.00, 1498.99, 1348.66, 1195.22, 1162.99, 1135.99, 1001.32, 793.85, 717.97.

UV-vis, λ_{max} (nm): 413, 527.

5,10,15,20-*Tetra*(4-hexadecylcarbonyloxyphenyl) porphyrin Co (II) (8a): 98 mg, yield 89.9 %, R_f = 0.27 (19:1, Hexane: EtOAc), the red crystals.

MALDI-TOF (m/z): calcd. for $C_{108}H_{148}CoN_4O_8$ = 1688.06, found = 1689.990 [M+H$^+$].

FT-IR, ν_{max} (cm^{-1}): 2918.11, 2849.97, 1752.63, 1499.50, 1349.03, 1197.33, 1163.25, 1136.44, 1001.57, 793.93, 717.92.

UV-vis, λ_{max} (nm): 412, 527.

5,10,15,20-*Tetra*(4-octadecylcarbonyloxyphenyl) porphyrin Co (II) (9a): 80 mg, yield 90.9 %, R_f = 0.35 (19:1, Hexane: EtOAc), the red crystals.

MALDI-TOF (m/z): calcd. for $C_{116}H_{166}CoN_4O_8$ = 1800.19, found = 1801.045 [M+H$^+$].

FT-IR, ν_{max} (cm^{-1}): 2919.37, 2849.92, 1753.83, 1499.81, 1349.14, 1198.71, 1163.50, 1136.92, 1001.90, 749.11, 717.84.

UV-vis, λ_{max} (nm): 412, 526.

Nickel (II) complexes (7-9, b)

5,10,15,20-*Tetra*(4-dodecylcarbonyloxyphenyl) porphyrin Ni (II) (7b): 95 mg, yield 87 %, R_f = 0.30 (19:1, Hexane: EtOAc), the red crystals.

^{1}H-NMR (500 MHz, CDCl$_3$, TMS, **δ**): 8.76 (s, 8H, **β**-H), 8.00 (d, *J* = 8.5 Hz, 8H), 7.41 (d, *J* = 8.5 Hz, 8H), 2.71 (t, *J* = 7.5 Hz, 8H), 1.91-1.85 (m, 8H), 1.51-1.29 (m, 64H), 0.89 (t, *J* = 7.0 Hz, 12H).

MALDI-TOF (m/z): calcd. for $C_{92}H_{116}NiN_4O_8$ = 1462.81, found = 1464.557 [M+H$^+$]

FT-IR, ν_{max} (cm^{-1}): 2920.62, 2850.51, 1751.06, 1499.61, 1461.04, 1350.62, 1194.07, 1162.28, 1133.65, 1001.95, 795.09, 713.60.

UV-vis, λ_{max} (nm): 415, 524.

5,10,15,20-*Tetra*(4-hexadecylcarbonyloxy)phenylporphyrin Ni (II) (8b): 97 mg, yield 94 %, R_f = 0.35 (19:1, Hexane: EtOAc), the red crystals.

^{1}H-NMR (500 MHz, CDCl$_3$, TMS, **δ**): 8.76 (s, 8H, **β**-H), 8.00 (d, J = 8.5 Hz, 8H), 7.41 (d, J = 8.5 Hz, 8H), 2.71 (t, J = 7.5 Hz, 8H), 1.91-1.85 (m, 8H), 1.51-1.30 (m, 96H), 0.86 (t, J = 7.0 Hz, 12H).

MALDI-TOF (m/z): calcd. for C$_{108}$H$_{148}$NiN$_4$O$_8$ = 1688.07, found = 1689.038 [M+H$^+$]

FT-IR, **ν**$_{max}$ (cm^{-1}): 2917.50, 2849.50, 1752.34, 1499.45, 1465.51, 1351.00, 1195.01, 1162.56, 1134.51, 1001.73, 795.05, 713.94.

UV-vis, λ$_{max}$ (nm): 415, 525.

5,10,15,20-*Tetra*(4-octadecylcarbonyloxy)phenylporphyrin Ni (II) (9b): 111 mg, yield 89 %, R_f = 0.45 (19:1, Hexane: EtOAc), the red crystals.

^{1}H-NMR (500 MHz, CDCl$_3$, TMS, **δ**): 8.76 (s, 8H, **β**-H), 8.00 (d, J = 8.5 Hz, 8H), 7.41 (d, J = 8.5 Hz, 8H), 2.71 (t, J = 7.5 Hz, 8H), 1.91-1.85 (m, 8H), 1.51-1.25 (m, 112H), 0.86 (t, J = 6.88 Hz, 12H).

MALDI-TOF (m/z): calcd. for C$_{116}$H$_{166}$NiN$_4$O$_8$ = 1799.19, found = 1801.352 [M+H$^+$]

FT-IR, **ν**$_{max}$ (cm^{-1}): 2916.07, 2849.03, 1753.09, 1499.81, 1465.48, 1350.85, 1196.77, 1162.62, 1134.80, 1001.95, 795.59, 713.36.

UV-vis, λ_{max} (nm): 414, 527.

Iron (III) complexes (7-9, c)

5,10,15,20-*Tetra*(4-dodecylcarbonyloxy)phenylporphyrin Fe (III) (7c): 95 mg, yield 91 %, R_f = 0.30 (19:1, Hexane: EtOAc), the purple crystals.

MALDI-TOF (m/z): calcd. for $C_{92}H_{116}FeN_4O_8$ = 1460.81, found = 1461.481 [M+]

UV-vis, λ_{max} (nm): 415, 515, 574, 617.

5,10,15,20-*Tetra*(4-hexadecylcarbonyloxy)phenylporphyrin Fe(III) (8c): 97 mg, yield 94 %, R_f = 0.35 (19:1, Hexane: EtOAc), the purple crystals

MALDI-TOF (m/z): calcd. for $C_{108}H_{148}FeN_4O_8$ = 1685.06, found = 1685.748 [M+]

UV-vis, λ_{max} (nm): 415, 514, 576, 617.

5,10,15,20-*Tetra*(4-octadecylcarbonyloxy)phenylporphyrin Fe(III) (9c): 111 mg, yield 89 %, R_f = 0.45 (19:1, Hexane: EtOAc), the purple crystals

MALDI-TOF (m/z): calcd. for $C_{116}H_{164}FeN_4O_8$ = 1797.19, found = 1798.663 [M+]

FT-IR, ν_{max} (cm^{-1}): 2916.48, 2849.14, 1758.84, 1494.23, 1466.58, 1201.28, 1165.28, 1138.29, 1107.19, 998.47, 796.59, 718.09.

UV-vis, λ_{max} (nm): 414, 516, 574, 616.

3.3.3 Preparation of *meso-tetra*(*N*-alkyl-*N*-phenylurea)porphyrin

I. Synthesis of *meso-tetra*(4-aminophenyl)porphyrin (10)
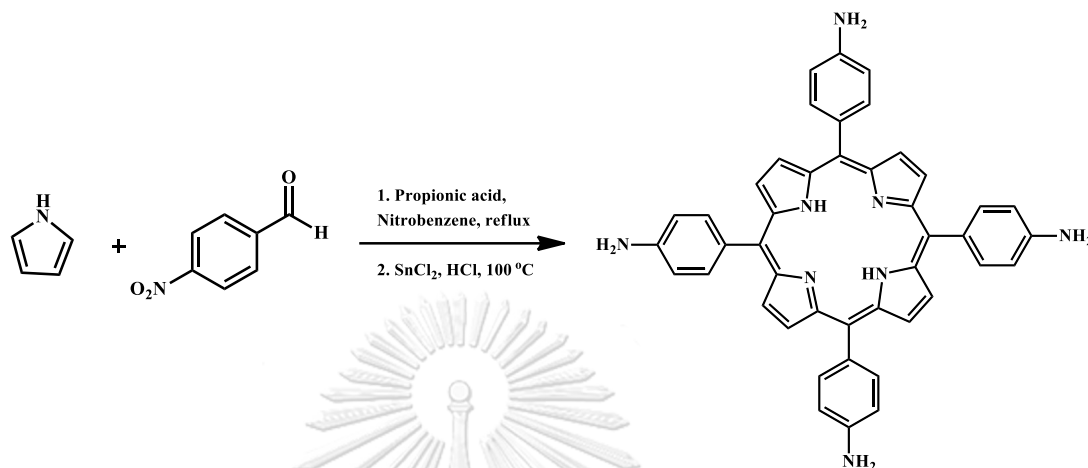
4-Nitrobenzaldehyde 2.00 g (16.38 mmol) was dissolved in 20 mL of a mixture of propionic acid and nitrobenzene (9:1 v/v). The solution of pyrrole (1.14 mL, 16.38 mmol) in 5 mL of propionic acid was added into reaction mixture. The reaction mixture was stirred and heated at reflux for 1 h. After reaction completion, the reaction mixture was cool-down to 40 °C, added methanol (100 mL) and stirred for 2 h at room temperature. The product was filtered and washed by methanol to give black solid. The crude product was refluxed in pyridine (40 mL) for 3 h to remove impurities. After cooling to room temperature, the desired product was filtered and washed with acetone to obtain the purple solid. The obtained *meso-tetra*(4-nitrophenyl) porphyrin (1.50 g, 32.75 mmol) was dissolved in concentrated HCl (20 mL), stirred, and heated at 90 °C. The solution of 9.00 g (40 mmol, 12 eq) of $SnCl_2.2H_2O$ in concentrated HCl (15 mL) was added into the mixture and was continued heating for additional 3 h. The reaction mixture was dissolved in water (50 mL) and neutralized by NH_4OH solution, then the suspension was filtrated and

washed with water to give dark clay. The crude product was extracted by acetone (50 mL, 3-4 times) and filtrated. and the obtained solid was purified by column chromatography on G60 silica gel and recrystallized to obtain the purple microcrystal; in yield 13% for two steps, R_f = 0.40 (Hexane: Acetone, 3:2).

^{1}H-NMR (500 MHz, DMSO-D_6, δ (ppm)) 8.87 (s, 8H, β-H), 7.84 (d, J = 8.3 Hz, 8H), 7.00 (d, J = 8.3 Hz, 8H), 5.57 (s, 8H, NH_2), -2.75 (s, 2H, N-H).

^{13}C-NMR (500 MHz, DMSO-D_6, δ (ppm)): 149.06, 136.01, 129.22, 121.10, 113.02.

MALDI-TOF (m/z): calcd. for $C_{44}H_{34}N_8$ = 674.29, found = 675.435. [M+H$^+$]

FT-IR, ν_{max} (cm^{-1}): 3351.57, 1604.79, 1509.71, 1466.69, 1347.54, 1279.85, 1177.79, 966.33, 803.95.
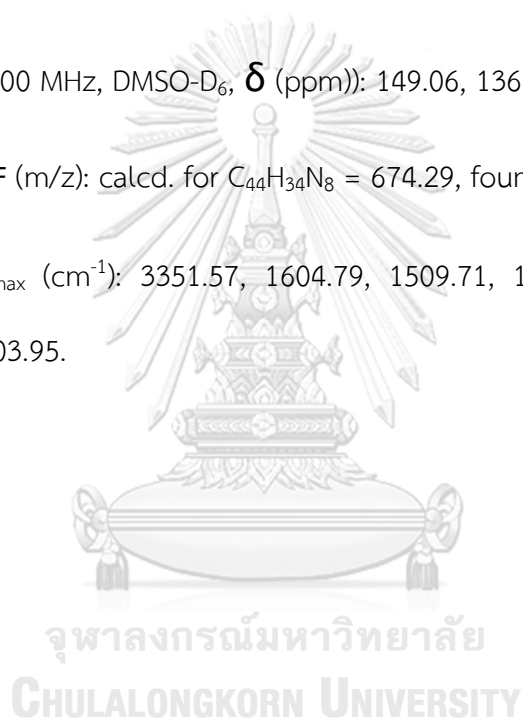
II. Synthesis of *meso-tetra*(*N*-octadecyl-*N*-phenylurea) porphyrin (11)
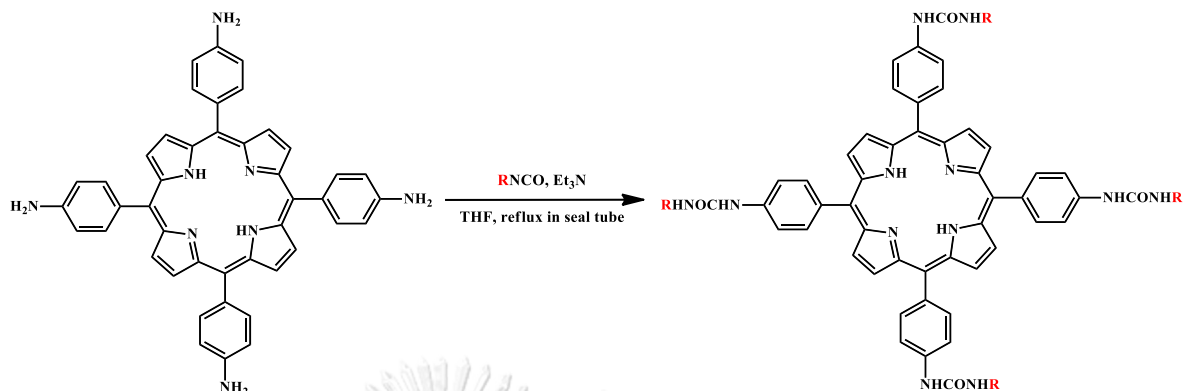
meso-tetra(4-aminophenyl) porphyrin 0.05 g (0.074 mmol) and triethylamine 62 μL (0.45 mmol, 6 eq.) were dissolved with 10 mL of dry THF in pressurized seal-tube. The reaction mixture was stirred at room temperature for 10 min. The solution of octadecyl isocyanate 0.44 g (20 eq.) in dry THF (5 mL) was added and heated to reflux under nitrogen atmosphere. The reaction solution was continuously stirred until reaction was completed (3 days). After the reaction mixture was cooled down to room temperature, the solvents were removed from the reaction mixture under reduced pressure. The product was purified by column chromatography on G60 silica gel and crystallized from a mixture of dichloromethane and hexane to give dark-red solid; Yield 17%, R_f = 0.40 (9:1, DCM: MeOH).

^{1}H-NMR (500 MHz, CDCl$_3$, **δ** (ppm)): 8.82 (s, 8H, **β**-pyrrole), 8.01 (d, 8H, *J* = 7.8 Hz), 7.74 (d, 8H, *J* = 7.9 Hz), 7.01 (b, 4H, N-H), 5.75 (b, 4H, N-H), 3.07 (q, 8H, *J* = 5.8 Hz), 1.63-1.56 (m, 30H) 0.81 (t, 12H, *J* = 4.9 Hz), -2.84 (s, 2H, NH).

FT-IR, **ν**$_{max}$ (cm^{-1}): 3341.35, 2955.67, 2920.82, 2848.55, 1614.34, 1571.52, 1468.70, 1237.33, 721.07.

3.3.4 Axial ligand coordination of functionalized porphyrin complexes
General procedure

The axial ligand complexes were prepared by addition of 50 eq. of axial ligand such as imidazole, pyrazine, 4,4'-bipyridyl, or pyridine to a solution of functionalized porphyrin complexes, stirred at room temperature for 24 h. Axial coordinated compounds were obtained by recrystallization (top-up diffusion, slow evaporation) from suitable solvents (CH_2Cl_2, hexane, or ethanol). Only solid complexes were characterized by spectroscopic techniques; ^{1}H-NMR, UV-vis, Mass spectroscopies.

จุฬาลงกรณ์มหาวิทยาลัย
CHULALONGKORN UNIVERSITY

3.3.5 Preparation of asymmetrical *meso*-substituted phenylporphyrin

I. Synthesis of 5,5-dimethyl-2-(4-formylphenyl)-1,3,2-dioxaborinane (12)
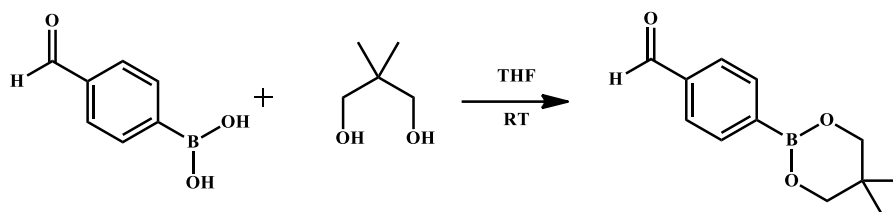
4-Formylphenylboronic acid 1.075 g (7.17 mmol) and 2,2-dimethyl-1,3-propanediol 0.772 g (7.41 mmol, 1.034 eq.) were dissolved in dry THF (15 mL) and stirred at room temperature for 2 h. The solvent was removed from reaction mixture by rotary evaporator under vacuum. The obtained crude was purified by column chromatography on G60 silica gel and crystallized from dichloromethane by hexane to obtain the white needle like crystals; Yield 98 %, R_f = 0.30 (Hexane: EtOAc, 19:1).

^{1}H-NMR (500 MHz, CDCl3, δ (ppm)): 10.04 (s, 1H, C*H*O), 7.95 (d, *J* = 7.9 Hz, 2H), 7.85 (d, *J* = 7.9 Hz, 2H), 3.79 (s, 4H), 1.03 (s, 6H).

^{13}C-NMR (500 MHz, CDCl3, δ (ppm)): 192.93, 137.85, 134.40, 128.73, 72.49, 31.98, 21.94.

DART-TOF-MS (m/z): calcd. for $C_{12}H_{15}BO_3$ = 218.11, found = 219.0925 [M+H$^+$].

II. Synthesis of 4-substituted phenyl terpyridines (13-14)

4-Bromophenylterpyridine (13)
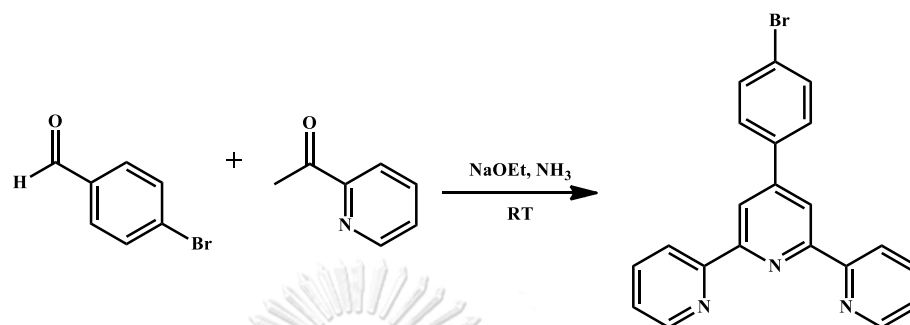
2-Acetylpyridine (0.39 mL, 3.48 mmol) was added into a solution of NaOEt (0.27 g, 4.0 mmol) in 10 mL of ethanol, The reaction mixture was stirred at room temperature for 30 min. The 4-bromobenzaldehyde (0.30 g, 1.62 mmol) was added into the reaction solution and stirred for 1 h, then ammonia solution (10 mL) was added in the reaction mixture. The stirring was continued overnight. The mixture was filtered and washed with water and methanol to provide white solid. The crude product was purified by crystallization to afford white solid. Yield 72 %.

¹H-NMR (500 MHz, CDCl₃, δ (ppm)): 8.75-8.71 (m, 2H,), 8.70 (s, 2H), 8.67 (d, *J* = 8.0 Hz, 2H), 7.89 (dt, *J* = 2.0, 7.8 Hz, 2H), 7.79 (d, *J* = 8.0 Hz, 2H), 7.65 (d, *J* = 8.0 Hz, 2H), 7.36 (dq, *J* = 1.0, 5.0 Hz, 2H).

¹³C-NMR (500 MHz, CDCl₃, δ (ppm)): 156.17, 156.12, 149.23, 137.49, 137.02, 132.19, 128.98, 124.04, 123.56, 121.47, 118.65.

DART-TOF-MS (m/z): calcd. for $C_{21}H_{14}BrN_3$ = 387.04, found = 388.0416 [M+H⁺].

4-Dodecyloxyphenylterpyridine (14)
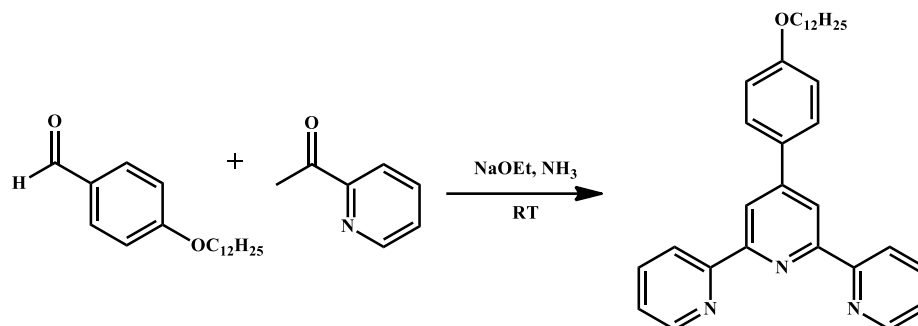
2-Acetylpyridine (0.40 mL, 3.62 mmol) was dissolved into a solution of NaOEt (0.27 g, 4.0 mmol) in 10 mL of ethanol and stirred at room temperature for 30 min. The 4-dodecyloxybenzaldehyde (0.5 g, 1.72 mmol) was added into the reaction solution and stirred further 1 h, then ammonia solution (10 mL) was slowly added in the reaction mixture. The reaction mixture was stirred overnight at room temperature. The solid was filtered and washed with water and methanol to provide white solid. The crude product was purified by crystallization to afford white solid. Yield 63 %.

^{1}H-NMR (500 MHz, CDCl$_3$, δ (ppm)): 8.74-8.71 (m, 2H,), 8.72 (s, 2H), 8.68 (d, J = 8.0 Hz, 2H), 7.91 (d, J = 2Hz, 2H), 7.88 (d, J = 8.0 Hz, 2H), 7.36 (dq, J = 1.0, 5.0 Hz, 2H), 7.02 (d, J = 8.0 Hz, 2H), 4.03 (t, J = 6.4 Hz, 2H), 1.85-1.79 (m, 3H), 1.49-1.28 (m, 20H), 0.88 (t, J = 7.0 Hz, 3H).

^{13}C-NMR (500 MHz, CDCl$_3$, δ (ppm)): 160.20, 156.48, 155.89, 149.90, 149.18, 136.94, 130.52, 128.56,123.83, 121.45, 118.31, 114.91, 68.22, 32.01, 29.76, 29.73, 29.69, 29.68, 29.51, 29.45, 29.36, 26.14, 22.78, 14.22.

DART-TOF-MS (m/z): calcd. for C$_{33}$H$_{39}$N$_3$O = 493.31, found = 494.2823 [M+H$^+$].

III. Synthesis of asymmetrical *meso*-substituted phenylporphyrin

Meso-dodecyloxyphenyldipyrromethane (15)
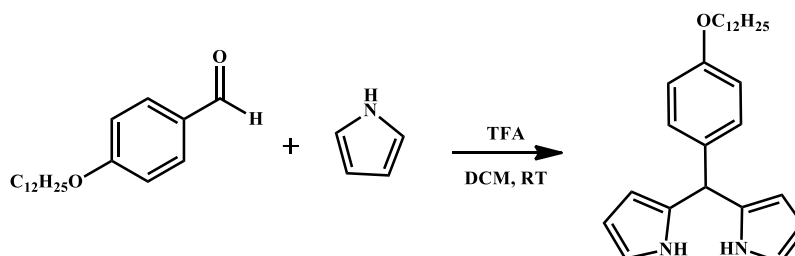
4-*n*-Dodecyloxybenzaldehyde (1.00 g, 3.44 mmol) and pyrrole (0.6 mL, 8.65 mmol) were dissolved in 5 mL of dichloromethane and stirred at room temperature for 10 min, then 2 drops of trifluoroacetic acid were added into the reaction mixture. After reaction completed, 4 mL of diluted NaOH solution were added to the mixture, and then 10 mL of dichloromethane. and the reaction mixture was stirred for further 15 min. After concentration of reaction mixture by rotary evaporator under reduced pressure, the crude product was extracted with DCM (25 mL x 2) and purified by column chromatography on G60 silica gel to obtain the light-brown oil; Yield 65 %, R_f = 0.15 (Hexane: EtOAc, 24:1).

^{1}H-NMR (500 MHz, CDCl$_3$, δ (ppm)): 7.94 (br, 1H, NH), 7.12 (d, *J* = 8.8 Hz, 2H), 6.84 (d, *J* = 8.7 Hz, 2H), 6.69 (t, *J* = 6.6 Hz, 2H), 6.15-6.14 (m, 2H), 5.91(t, *J* = 6.4 Hz, 2H), 5.43 (s, 1H, CH), 3.93 (t, *J* = 6.6 Hz, 2H), 1.79-1.73 (m, 2H), 1.44-1.26 (m, 18H), 0.88 (t, *J* = 7.0 Hz, 3H).

^{13}C-NMR (500 MHz, CDCl$_3$, δ (ppm)): 158.20, 133.96, 132.97, 129.43, 117.14, 114.64, 108.47, 107.08, 68.12, 43.22, 30.01, 29.79, 29.72, 29.69, 29.68, 29.49, 29.44, 29.37, 26.14, 22.78, 14.22.

DART-TOF MS (m/z): calcd. for $C_{27}H_{38}N_2O$ = 406.30, found = 405.2912 [M-H$^+$].

จุฬาลงกรณ์มหาวิทยาลัย
CHULALONGKORN UNIVERSITY

5-Dihydroxaborinatephenyl-10,15,20-tridodecyloxyphenylporphyrin (16)
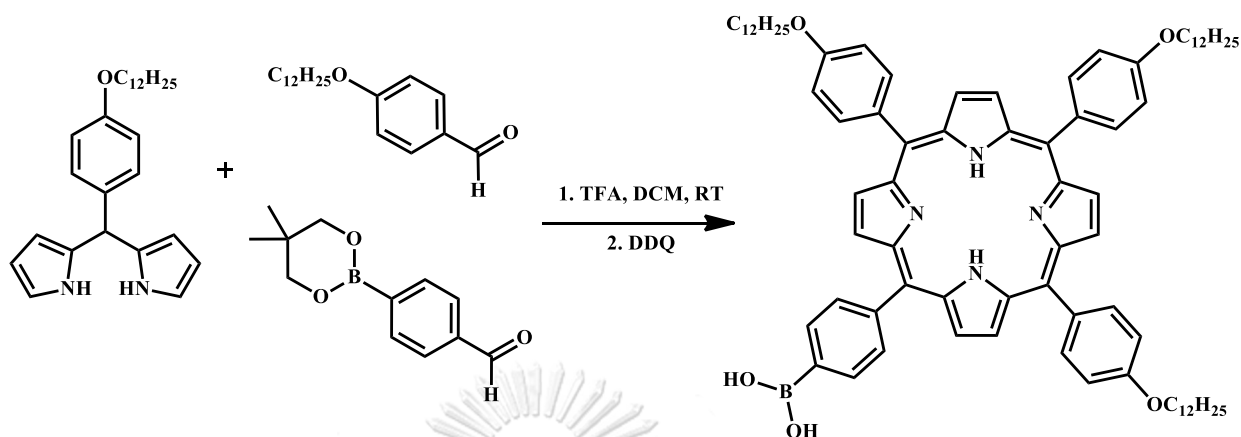
Dodecyloxyphenyldipyrromethane (0.450 g, 1.10 mmol) was dissolved in dry dichloromethane (100 mL) in 250 mL round bottle flask. The mixture of 4-*n*-dodecyloxybenzaldehyde (0.161 g, 0.55 mmol, 0.5 eq.) and 5,5-dimethyl-2-(4-formylphenyl)-1,3,2-dioxaborinane (0.120 g, 0.55 mmol, 0.5 eq.) in dry DCM (120 mL) were added and the reaction mixture was stirred at room temperature for 15 min. The trifluoroacetic acid (TFA) (0.15 mL, 2.0 mmol) was added and the reaction mixture was stirred for 1 hour, then DDQ 0.126 g (1.1 mmol) was added into the solution, which was, then, continuously stirred overnight. Triethylamine was added to neutralize the reaction mixture. After removal of solvents, the obtained crude was purified by column chromatography on G60 silica gel and crystalized by ethanol from dichloromethane to obtain the purple crystals; Yield 13 %, R_f = 0.30 (Hexane: EtOAc, 9:1).

^{1}**H-NMR** (500 MHz, CDCl$_3$, δ (ppm)): 8.88-8.86 (m, 8H, β-H), 8.10 (d, *J* = 8.3 Hz, 6H), 8.07 (d, *J* = 8.25 Hz, 2H), 7.27 (d, *J* = 8.3 Hz, 6H), 7.20 (d, *J* = 8.25 Hz, 2H), 4.25 (t,

J = 6.5 Hz, 6H, OCH$_2$), 2.00-1.59 (m, 6H), 1.49-1.30 (m, 60H), 0.90 (t, J = 7.0 Hz, 9H, CH$_3$), -2.77 (s, NH).

^{13}C-NMR (500 MHz, CDCl$_3$, **δ** (ppm)): 159.04, 135.79, 135.68, 134.94, 134.49, 119.93, 113.53, 113.73, 112.77, 68.42, 32.04, 29.77, 29.64, 29.48, 26.33, 22.81, 14.24.

MALDI-TOF-MS (m/z): calcd. for C$_{80}$H$_{103}$BN$_4$O$_5$ = 1210.80, found = 1212.768.

FT-IR, **ν**$_{max}$ (cm^{-1}): 3413.85, 2922.13, 2851.32, 1605.66, 1508.27, 1466.21, 1243.96, 1174.43, 1095.93, 966.42, 803.32.

5-Dihydroxaborinatephenyl-10,15,20-tridodecyloxyphenylporphyrin zinc complex (17)
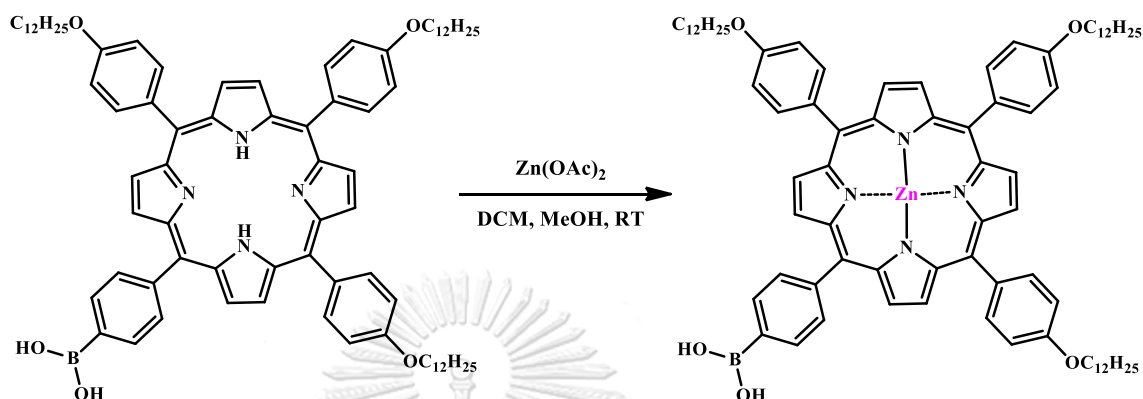
5-Dihydroxaborinatephenyl-10,15,20-tridodecyloxyphenylporphyrin (0.150 g, 0.123 mmol (1.0 eq) and Zn (II) acetate dihydrate (0.09 g, 0.14 mmol, 1.1 eq) were dissolved in a mixture of dry dichloromethane (30 mL) and methanol (5 mL). The reaction mixture was stirred at room temperature overnight. The mixture was extracted with water and brine. After removal of solvent under reduced pressure, and the obtained crude product was purified by column chromatography on G60 silica gel to obtain the purple solid; Yield 86 %, R_f = 0.27 (Hexane: EtOAc, 9:1).

^{1}H-NMR (500 MHz, CDCl$_3$, δ (ppm)): 8.97 (m, 8H, β-H), 8.11 (d, J = 8.3 Hz, 6H), 8.07 (d, J = 8.2 Hz, 2H), 7.27 (d, J = 8.3 Hz, 6H), 7.20 (d, J = 8.2 Hz, 2H), 4.25 (t, J = 6.5 Hz, 6H, OCH_2), 1.99-1.49 (m, 6H), 1.34-1.26 (m, 60H), 0.89 (t, J = 7.0 Hz, 9H, CH_3).

^{13}C-NMR (500 MHz, CDCl$_3$, δ (ppm)): 158.85, 155.38, 150.57, 150.49, 135.59, 135.48, 135.31,135.13, 131.98, 131.87, 129.57, 125.10, 120.89, 120.61, 113.60, 112.62, 68.40, 37.18, 32.84, 32.28, 32.05, 30.14, 29.79, 29.63, 29.49, 26.48. 26.35, 23.54, 22.82, 14.25.

MALDI-TOF-MS (m/z): calcd. for $C_{80}H_{101}BN_4O_5Zn$ = 1272.72, found = 1271.664.

5-[4'-(terpyridinyl)-1,1'-biphenyl]-10,15,20-tridodecyloxyphenylporphyrin zinc complex (18)
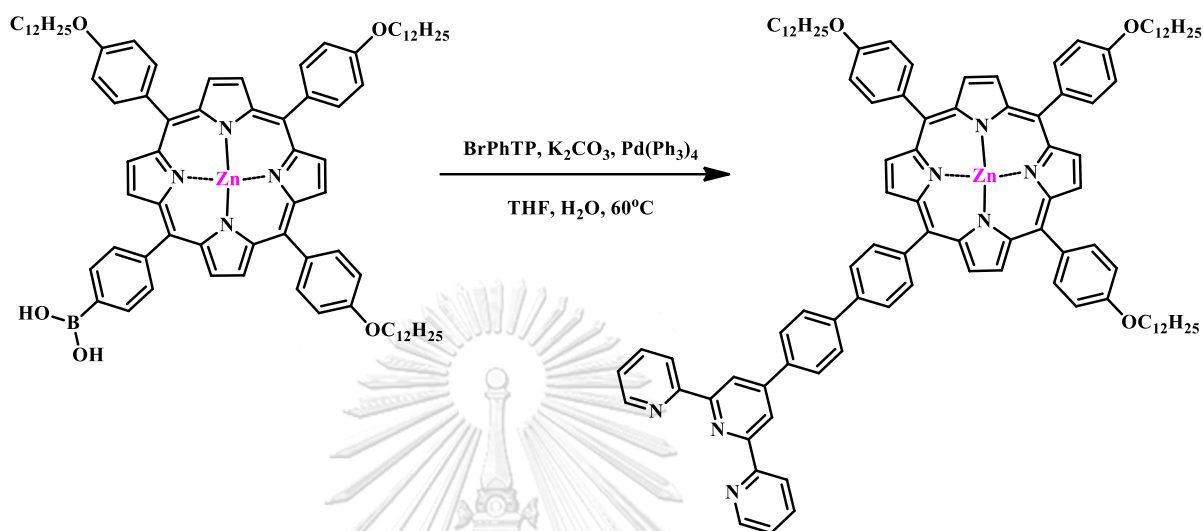
The terpyridinyl biphenyl boronic acid porphyrin Zn complex (0.050 g, 39.3 µmol), 4-bromophenylterpyridine (0.018 g, 43.3 µmol, 1.1 eq.), potassium carbonate (0.038 g, 80 µmol, 2 eq.) and Pd(PPh$_3$)$_4$ (0.005 g, 8 µmol, 0.2 eq.) were dissolved in 15 mL of THF and 2 mL of deionized water in pressurized tube. The reaction mixture was stirred and heated up to 60 °C overnight. The solvent of mixture was removed by rotary evaporator under reduced pressure. The obtained crude product was extracted with dichloromethane (3 x 20 mL) and dried over anhydrous sodium sulfate. The crude product was purified by column chromatography on G60 silica gel to afford the purple solid; Yield 68 %, R$_f$ = 0.25 (Hexane: EtOAc, 9:1).

^{1}H-NMR (500 MHz, CDCl$_3$, δ (ppm)): 8.96-8.94 (m, 8H, β-*H*), 8.72-8.69 (m, 2H), 8.70 (s, 2H), 8.66 (d, *J* = 8.1 Hz, 2H), 8.10 (d, *J* = 8.3 Hz, 6H), 8.05 (d, *J* = 8.2 Hz, 2H), 7.88 (dt, *J* =2.0, 7.5 Hz, 2H), 7.78 (d, *J* = 8.2 Hz, 2H), 7.64 (d, *J* = 8.2 Hz, 2H), 7.38-7.35

(m, 2H), 7.26 (d, J = 8.3 Hz, 6H), 7.19 (d, J = 8.2 Hz, 2H), 4.25 (t, J = 6.5 Hz, 6H, OCH_2), 2.0-1.95 (m, 6H), 1.59-1.26 (m, 60H), 0.90 (t, J = 7.0 Hz, 9H, CH_3).

^{13}C-NMR (500 MHz, CDCl$_3$, δ (ppm)): 158.86, 156.15, 156.11, 150.57, 150.50, 149.22, 137.47, 137.07, 135.60, 135.48, 135.12, 132.20, 131.97, 131.87, 128.99, 124.07, 123.58, 121.51, 120.91, 118.67, 113.65, 112.63, 68.40, 32.04, 29.78, 29.65, 29.49, 26.35, 22.81, 14.25.

MALDI-TOF-MS (m/z): calcd. for $C_{101}H_{113}N_7O_3Zn$ = 1536.82, found = 1536.87.

5-[4'-(terpyridinyl)-1,1'-biphenyl]-10,15,20-tridodecyloxyphenylporphyrin zinc

complex: Dodecyloxyphenyl terpyridine iron (II) hexafluorophosphate (19)
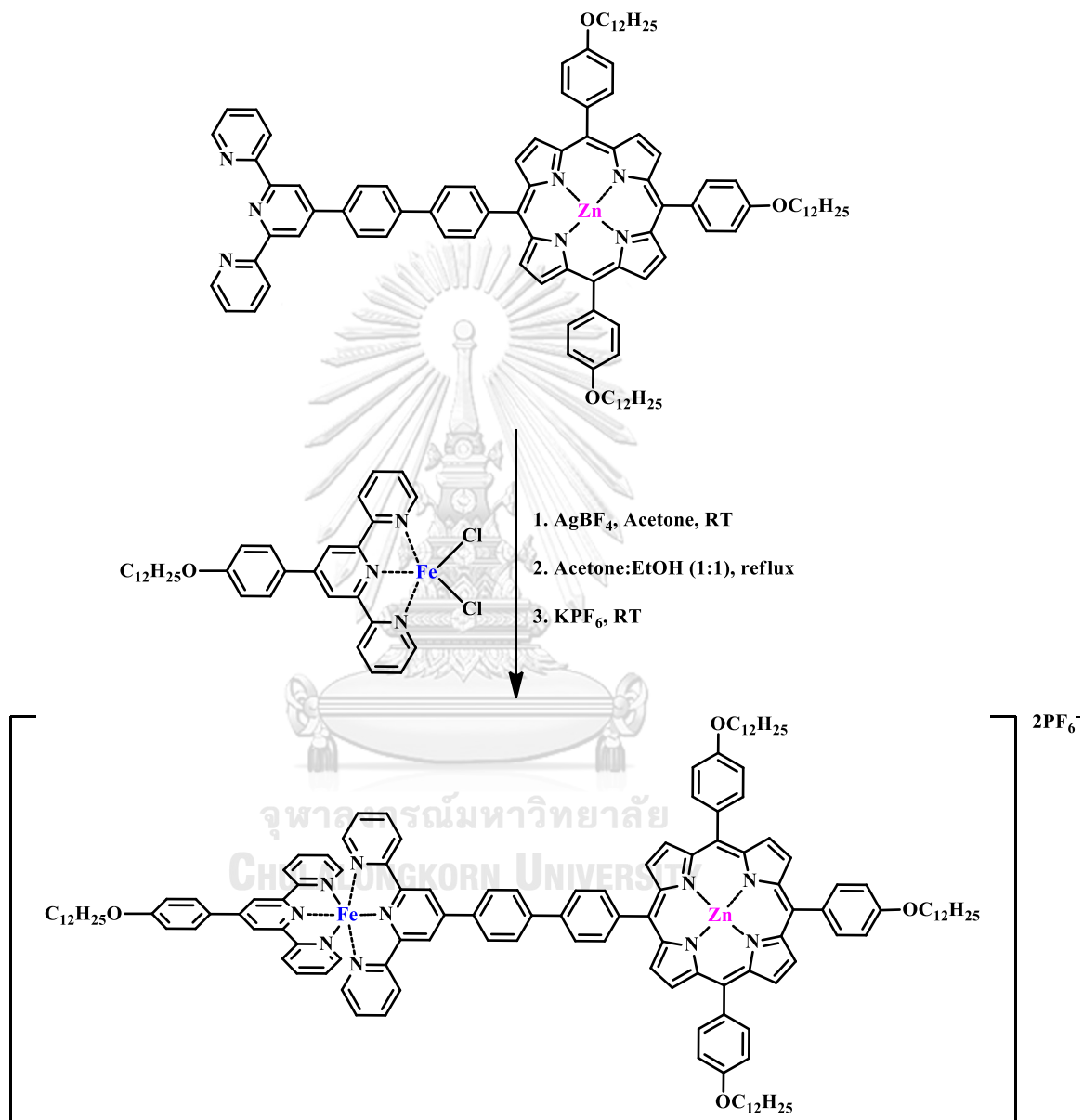
Into the solution of dodecyloxyphenyl terpyridine (14) (25 mg, 51 μmol) in absolute ethanol (10 mL), was added iron (II) chloride (6.5 mg, 57 μmol, 1.1 eq). The reaction mixture color changed to violet, and it was stirred at room temperature for

3 h. The solvent of reaction mixture was reduced to ~5 mL, then diethyl ether (20 mL) was added to precipitate the iron complex. The reaction mixture was filtered to get violet solid.

Anion (Cl⁻) exchange was carried out by re-dissolving the iron complex with acetone (10 mL) and added silver tetrafluoroborate (40 mg, 0.21 mmol, 4 eq). The reaction mixture was stirred at room temperature for 2 h. The AgCl was removed by celite pad filtration, and the solvents were removed *in vacuo* to obtain iron-terpyridine complex.

Into the solution of Zn complex (18) (50 mg, 33 μmol) in 15 mL of absolute ethanol, iron-terpyridine complex from the previous step was added. The reaction mixture was heated to reflux for 24 h. After cooling down to room temperature, the solvents were removed by rotary evaporator under reduced pressure. The crude product was purified by column chromatography on silica gel (acetone : water : sat. KNO_3 = 10:1:0.02), and subsequently treated with 2 mL of 0.2 M KPF_6 in acetone to obtain the violet solid, Yield 15%.

MALDI-TOF-MS (m/z): calcd. for $C_{134}H_{152}FeN_{10}O_4Zn$ = 2086.07, found = 2086.846 $[M^{2+}]$

EA: calcd. for $C_{134}H_{152}F_{12}FeN_{10}O_4P_2Zn$: C, 67.68; H, 6.44; N, 5.89; O, 2.69. found: in progress.

3.3.6 Mesophase and magnetic properties

I. Mesomorphic behaviors

The phase transition of all solid coordination complexes was analyzed on differential scanning calorimetry (DSC) -- NETZSCH DSC 204 F1 Phoenix calorimeter. DSC curves were recorded by thermal process (-50 to 300 $^{\circ}$C) with scanning rate of 10 $^{\circ}$C/min.

II. Magnetic susceptibilities

The desired compounds were measured for solid samples on the superconducting quantum interference device (SQUID) magnetometer. Susceptibilities data were obtained in temperature range from 5 to 300 K and the applied field at 5000 Oe for a crystal or solid sample.
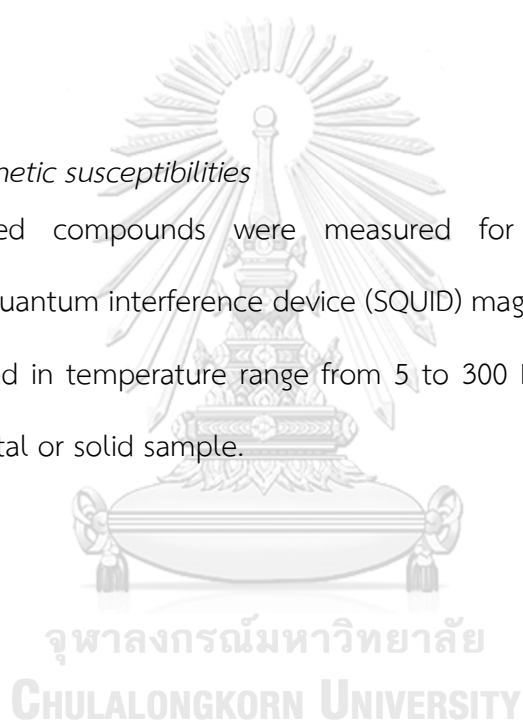
CHAPTER 4

RESULTS AND DISCUSSION

4.1 Synthesis

The functionalized porphyrin derivatives in this work were synthesized in various methods.
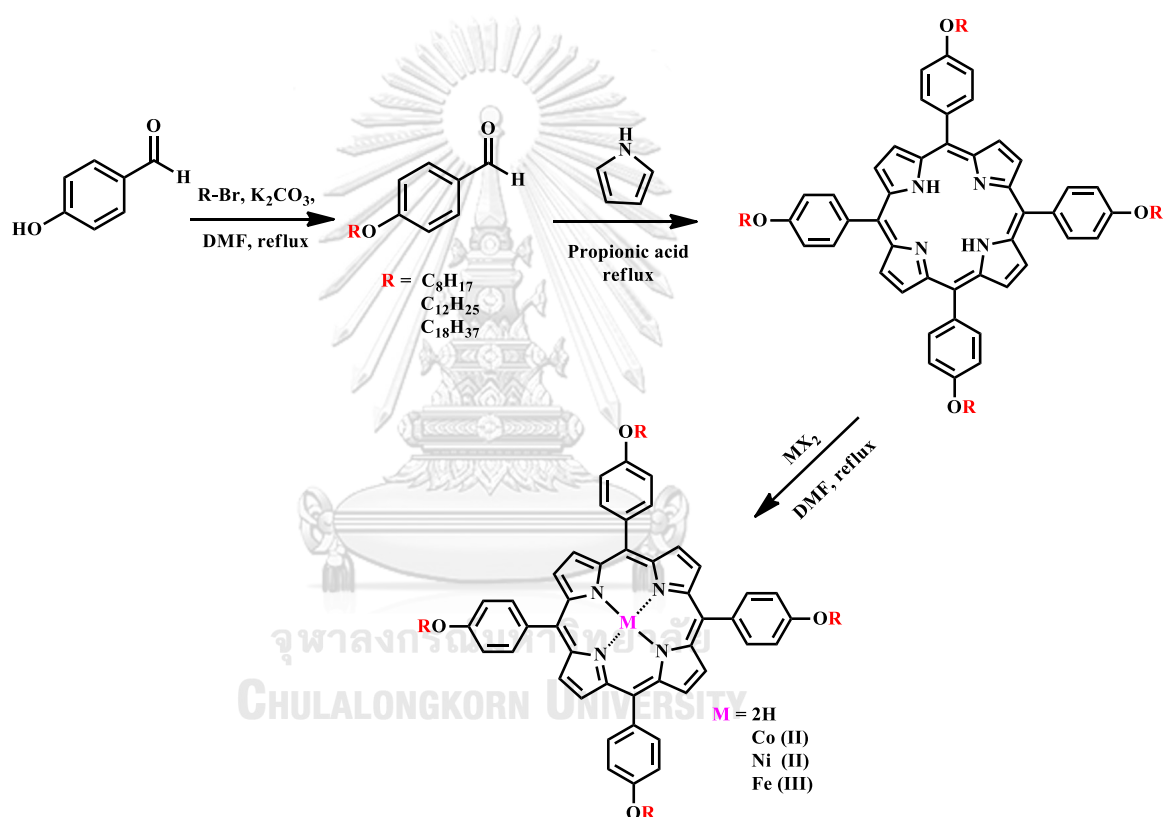
Scheme 4.1 Synthetic route of etherated phenyl porphyrins (**3-5, a-c**)

Etherated phenyl porphyrins (**3-5**) were prepared by Adler method through the condensation of 4-substituted benzaldehyde and pyrrole in refluxing propionic acid with air oxidant in good yield. The long alkyl etherated with phenyl ring at *meso*-position was clearly confirmed by ^{1}H-NMR technique; the **β**-proton of pyrrole

on macrocycle showed strong singlet at ~ 8.87 ppm, oxymethylene proton of *meso*-substituted phenyl revealed triplet signal at 4.23 ppm, and the N-H proton on pyrrole residue displayed at -2.73 ppm by anisotropic effect on aromatic macrocycle. The FT-IR technique revealed N-H, C-H and O-C stretching peaks at ~ 3,315, 2,900 and 1,605 cm^{-1}, respectively. UV-visible spectroscopic data were showed strong characteristic peaks; the Soret band at 423 nm and the Q bands at 520, 557, 595 and 652 nm[11, 35, 36]. These analyses confirmed that ether functionalized porphyrin ligands were successfully synthesized. The Ni(II), Co(II) and Fe(III) complexes of etherated porphyrin were prepared in high yield by Adler and Longo method[39]. All complexes were characterized by spectroscopic analyses; NMR, IR, UV-vis, and MS techniques. UV-visible spectra of metal complexes showed the blue shift about 2-7 nm compared to porphyrin metal free[31, 35, 36].
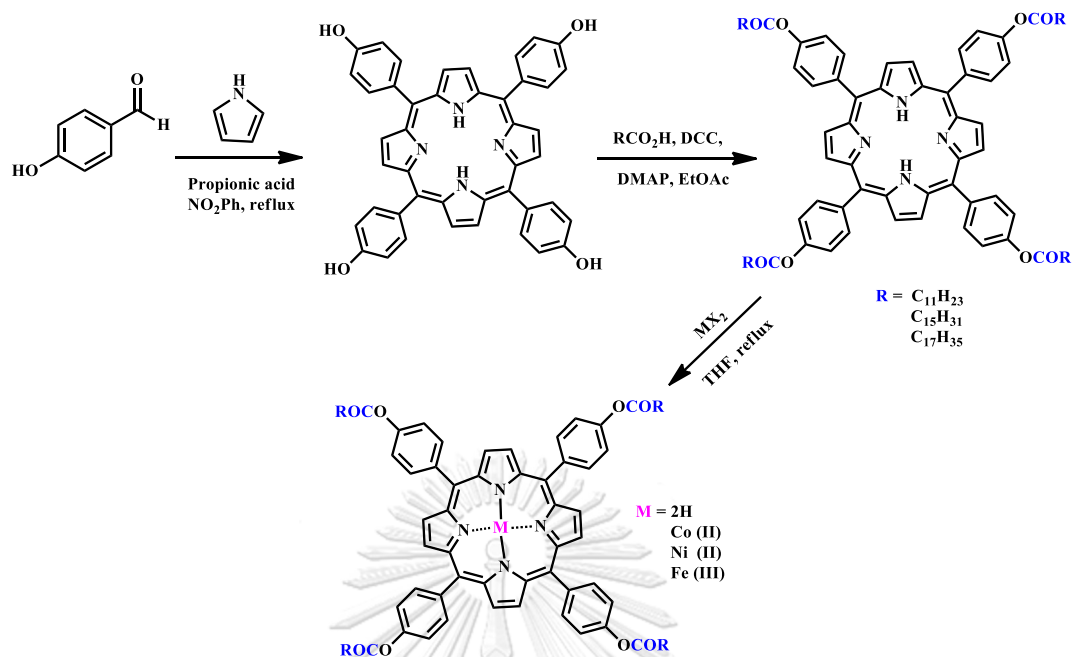
Scheme 4.2 Synthetic route of esterated phenyl porphyrins (**7-9, a-c**)

Esterated phenyl porphyrins (**7-9**) were synthesized starting from tetrahydroxyphenyl porphyrin (HPP) (**6**) scaffold with modified Valentina protocol[29] and long alkyl ester chains were introduced by Steglich esterification[45] by using saturated fatty acid, DCC and DMAP in EtOAc at room temperature for 2-3 days in high yields. The ester bond on *meso*-phenyl position was proved by using ^{1}H-NMR and IR techniques. From NMR spectra, the triplet peak at 2.75 ppm implied that methylene proton connected to carbonyl residue and singlet peak at -2.82 ppm confirmed the existence of porphyrin ring. The IR analysis found the stretching of carbonyl moiety of ester group is a strong band around 1,758 cm^{-1} [12, 25, 31, 32, 34]. The Ni(II), Co(II) and Fe(III) complexes of esterated porphyrin (**7-9**) were prepared by metalation with acetate salts in refluxing THF[33] in. All complexes were characterized

by NMR, IR, UV-vis, and MS analysis. UV-visible spectra of metal complexes showed the blue shift about 4-7 nm compared to porphyrin ligand[12, 16, 31, 33].
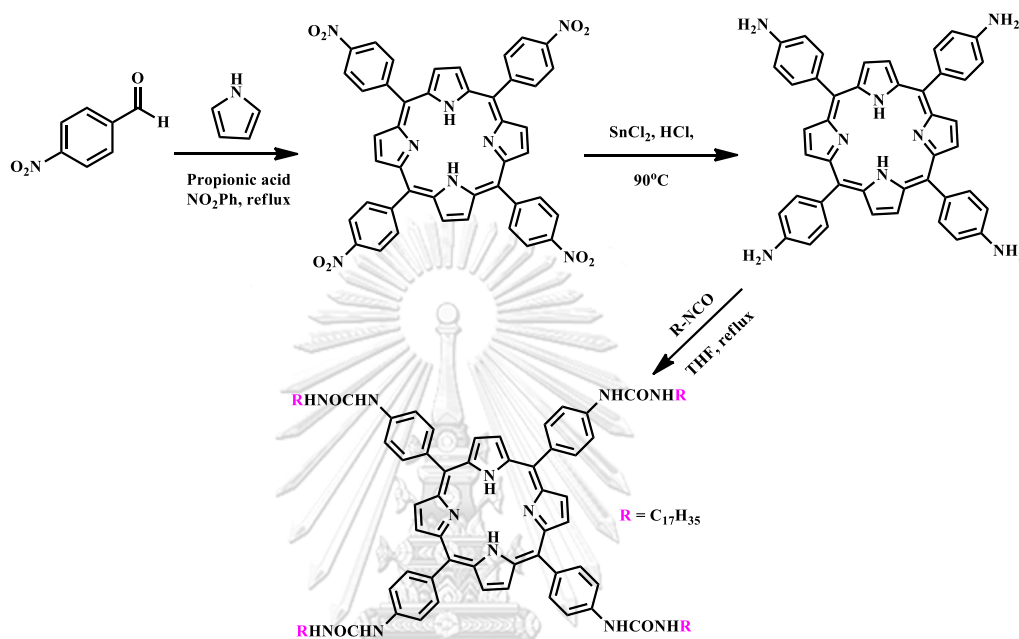
Scheme 4.3 Synthetic route of urea phenyl porphyrin (**11**)

Urea functionalized porphyrins were prepared through tetra-aminophenyl porphyrin (APP) (**10**)[23, 24] which was derived from a reduction of tetra-nitrophenyl porphyrin (NPP) intermediate by tin (II) chloride in concentrated hydrochloric acid. The urea derivative was prepared by amination of long alkyl isocyanate in refluxing THF and triethylamine (TEA) as catalyst for 3 days[38] to obtain deep-red powder. The obtained urea porphyrin ligand is hardly soluble in single organic solvents like hexane, DCM or EtOAc but insoluble in acetone, DMSO, EtOH. The structure characterization of this urea derivative was determined by ^{1}H-NMR in mixed deuterated chloroform and DMSO and the NMR results found N-H protons at 7.01

and 5.75 ppm which indicated urea residue. IR spectra showed N-H at ~3,340 and C=O at ~1,610 cm^{-1}.
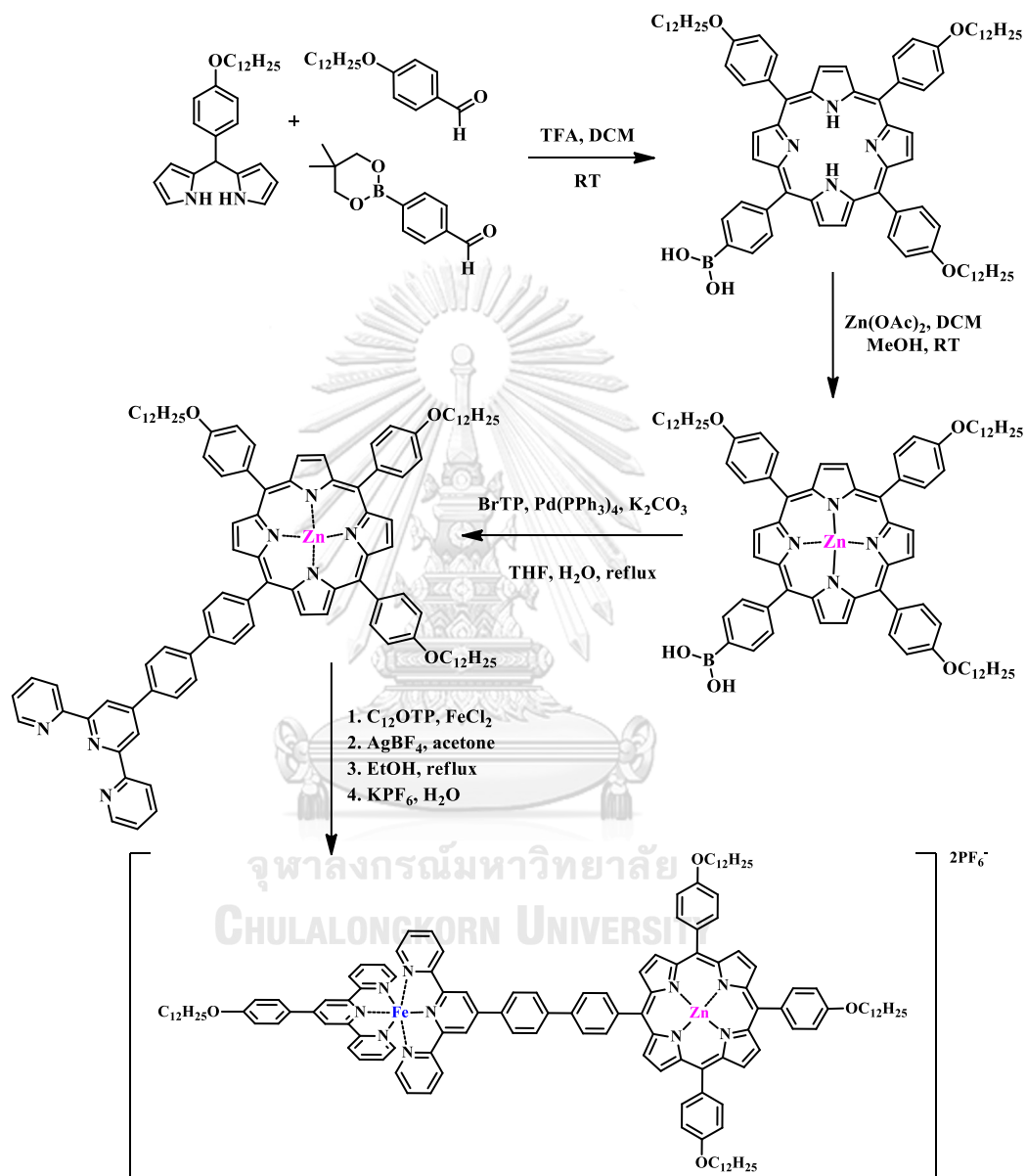
Scheme 4.4 Synthetic route of unsymmetrical porphyrin (**19**)

The A$_3$B system was designed by combination of long alkyl chains and terpyridine residue on *meso*-substituted phenyl porphyrin to provide mesomorphic and magnetic properties of functionalized porphyrin complex. Firstly, phenylterpyridine derivatives (**13-14**) were prepared by aldol condensation between 2-acetylpyridine and substituted benzaldehydes in a presence of sodium ethoxide and ammonia solution at mild condition in moderate yields[41]. Secondly, asymmetrical borylated porphyrin was synthesized by modified Lindsey method[43, 44] and metalized with Zn (II) acetate[8, 46, 47]. Terpyridine functionalized porphyrin (TPPP) was prepared by Suzuki coupling between bromophenylterpyridine (**13**) and borylated porphyrin (**16**)[43]. The iron *bis*-terpyridine target compound (**19**) was obtained by termination of the TPPP and iron terpyridine derivative[40, 48, 49] to get violet microcrystal[43, 44]. The ^{1}H-NMR and MS techniques were elucidated the molecular structure of all synthesized compounds, which data were present in Appendix figure. S22-S24.

4.2 Axial coordination

      Nitrogen heterocyclic aromatic compounds were employed to prepare axial ligand coordinated complexes in suitable organic solvents at room temperature. The metal porphyrin complexes were reacted with excess axial ligands to provide the desired axial ligand coordinated complexes as solid compounds. UV-visible spectroscopy was used to investigate the complexation process.

      Nickel (II) functionalized porphyrin complexes (**3b**-**5b** and **7b**-**9b**) reacted with various axial ligands in dichloromethane (DCM), or toluene as shown in Table 4.1.

Table. 4.1 Coordination of nickel (II) porphyrins with axial ligands.

Compound	Py	4-CNPy	4-MePy	DMAP	Pyz	Bpy
3b	^{b}NR	-	-	-	^{a}NR	^{a}NR
4b	-	-	-	-	-	-
5b	^{a}NR	-	-	-	-	-
7b	^{a}NR	-	^{a}NR	^{a}NR	-	-
8b	^{a}NR	-	-	^{a}NR	-	-
9b	^{a}NR	^{a}NR	-	^{a}NR	-	-

NR:No reaction, Reaction solvent: ^{a}DCM, ^{b}Toluene.

The UV-vis spectra of nickel porphyrin complexes were preliminary investigated their reaction behaviors. The results indicate that axial coordination could not be accomplished as the obtained spectra were similar to those from Ni (II) porphyrin complexes. Examples of reaction spectra are shown in Fig.4.1a-d.

This unsuccessful pyridyl axial ligand coordination to nickel (II) porphyrin complexes may come from the steric effect of long alkyl chains of *meso*-substituted phenyl ring and the electronic effect on nickel (II) metal which flavors in square planar geometry than octahedral geometry[21, 50-53].
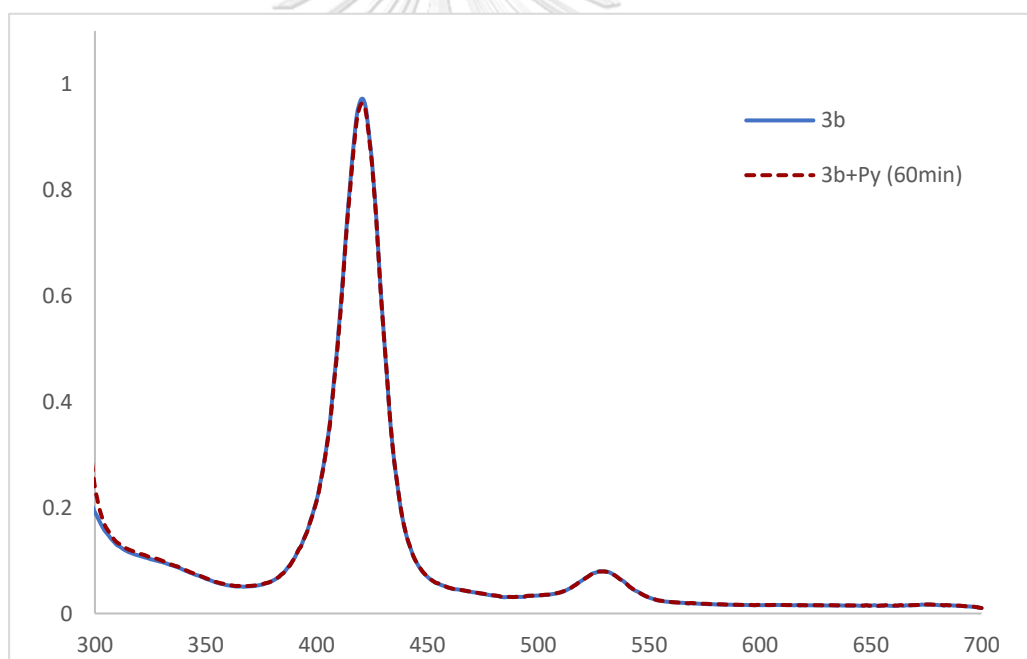
Fig. 4.1a UV-vis spectrum of reaction between **3b** and pyridine in toluene.
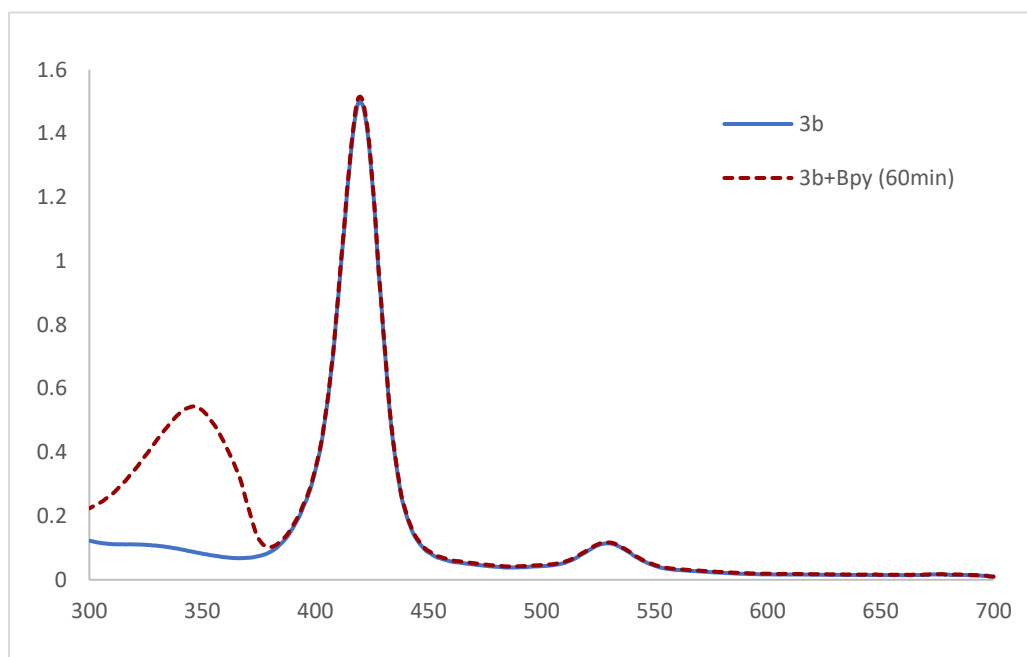
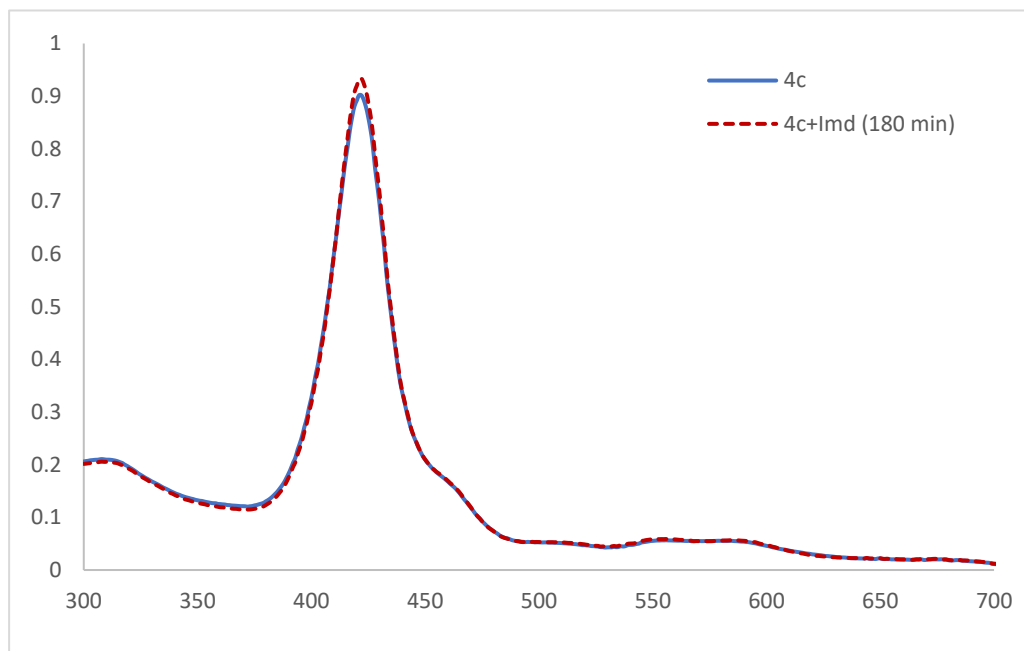**Fig. 4.1b** UV-vis spectrum of reaction between **3b** and 4,4'-bipyridine in DCM.
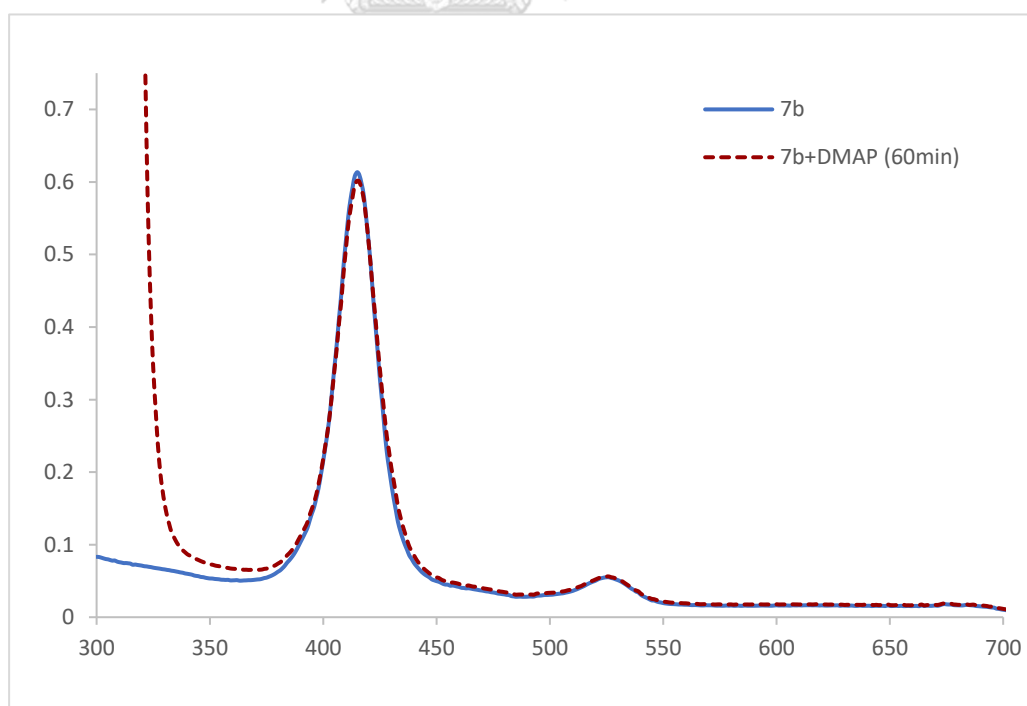
Fig. 4.1c UV-vis spectrum of reaction between **7b** and DMAP in DCM.
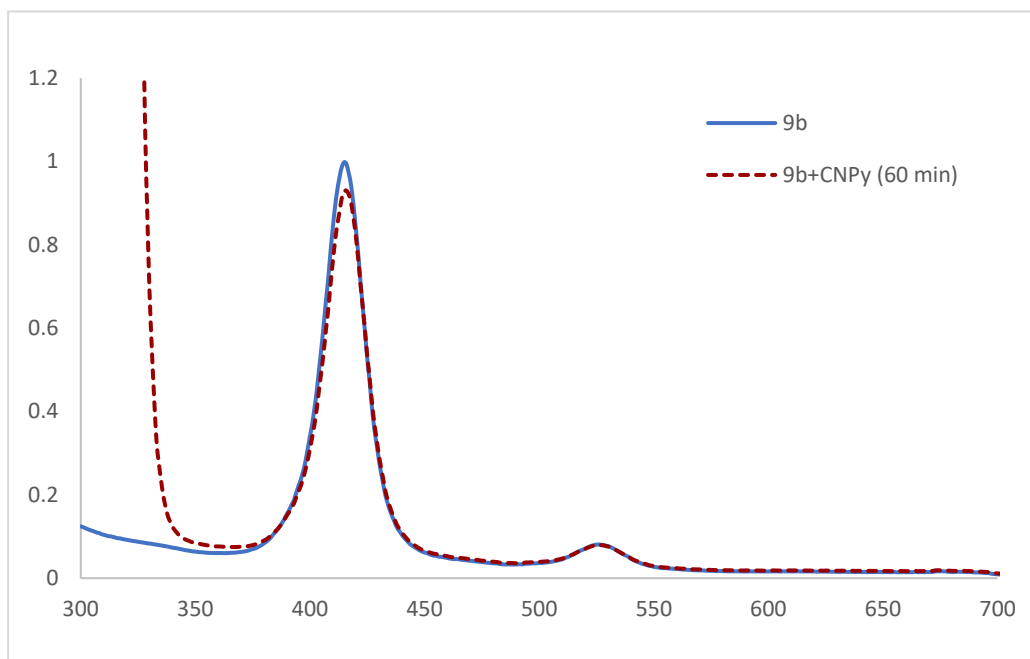
Fig. 4.1d UV-vis spectrum of reaction between **9b** and 4-CNPy in DCM.

The axial coordination of cobalt (II) porphyrin series (**3a**-**5a** and **7a**-**9a**) was examined by UV-visible spectroscopic analysis and the attempts to prepare micro-scale preparation crystal or solid. UV-visible screening test of cobalt (II) functionalized porphyrin complexes with excess axial compounds was conducted in DCM at room temperature for 6-8 h.[54], which results are shown in Table 4.2. and examples of reaction spectra for various times are displayed in Fig. 4.2a-d.

Table. 4.2 Coordination of cobalt (II) porphyrins with axial compounds.

Compound	Imd	Py	Pyz	Bpy
3a	+	[a]+	-	NR
4a	+	[a]+	-	-
5a	+	[a]+	NR	-
7a	+	[a]+	NR	-
8a	+	[a]+	-	-
9a	+	[a]+	-	NR

NR:No reaction, [a]Incomplete in 12 h.

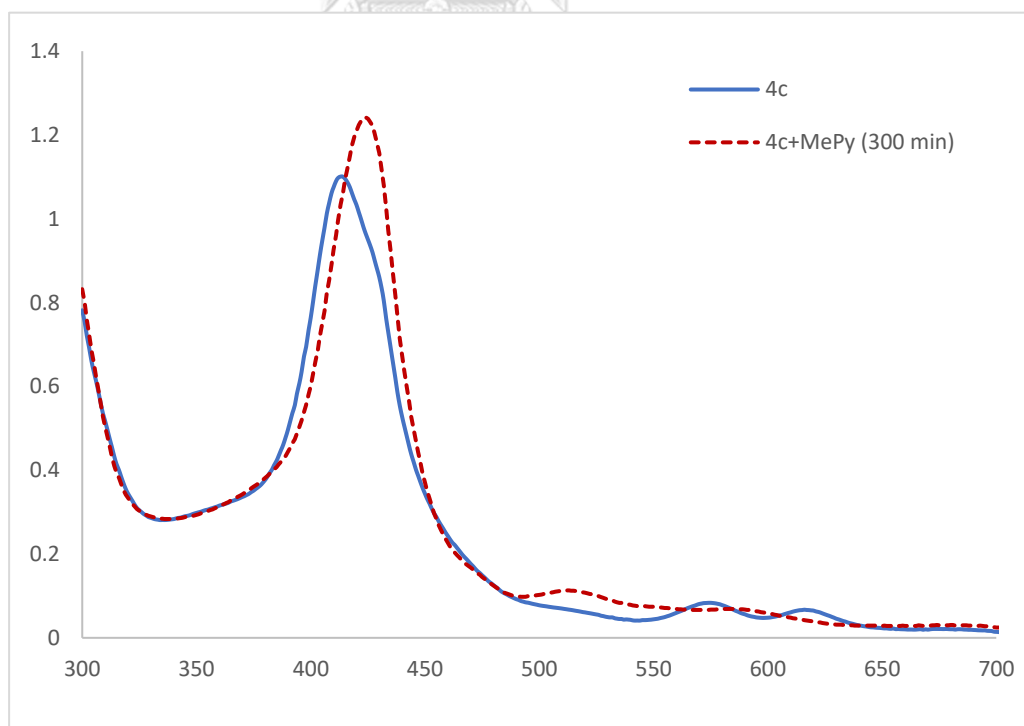จุฬาลงกรณ์มหาวิทยาลัย

CHULALONGKORN UNIVERSITY
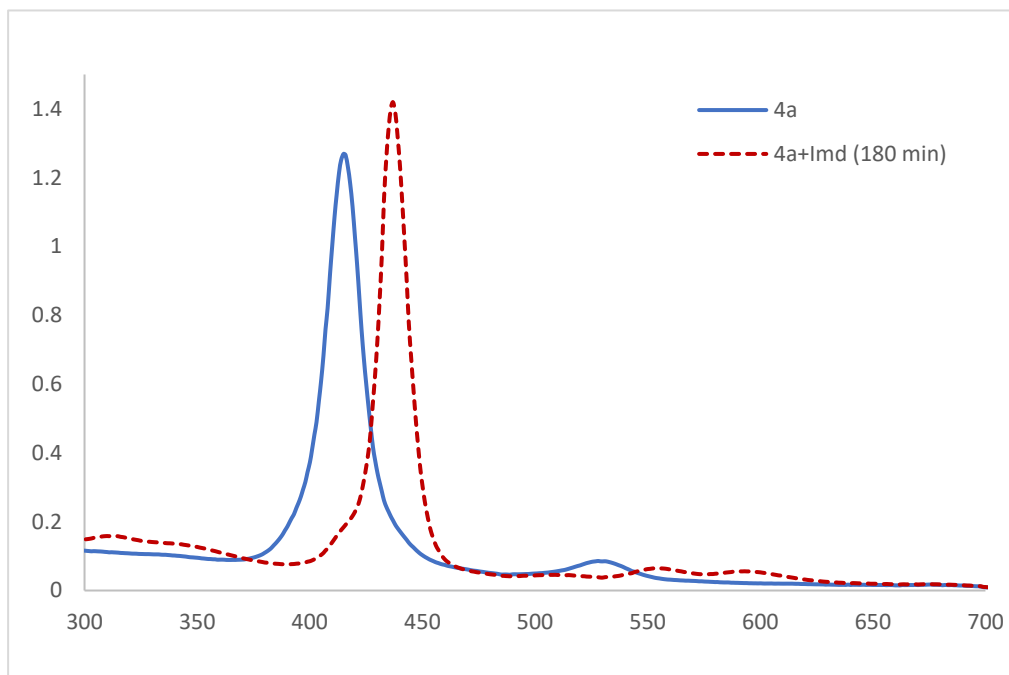
Fig. 4.2a UV-vis spectrum of reaction between **4a** and Imidazole in DCM.
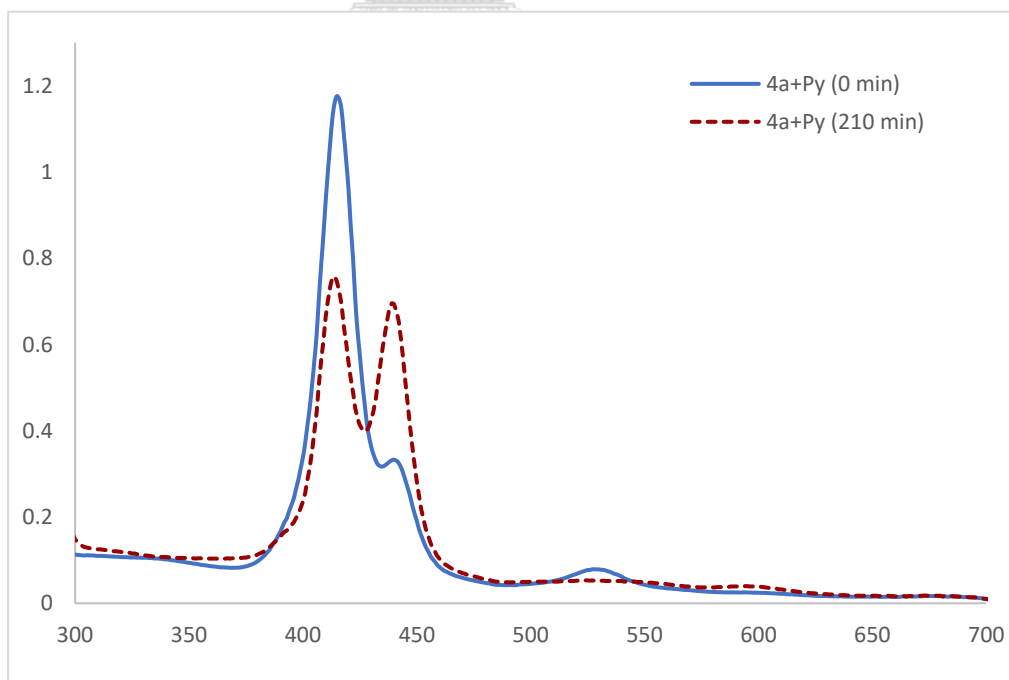
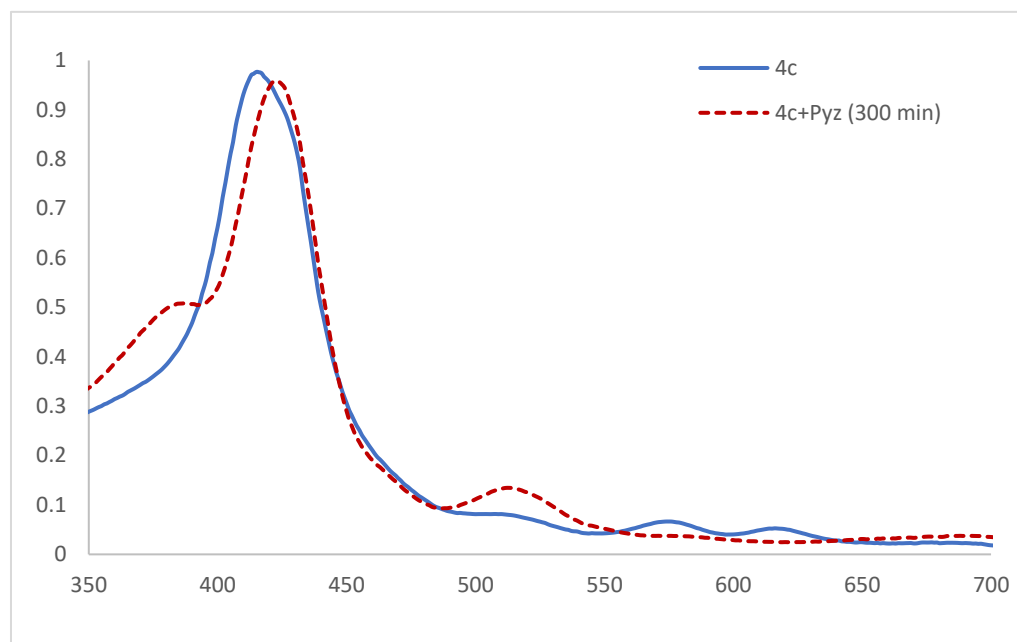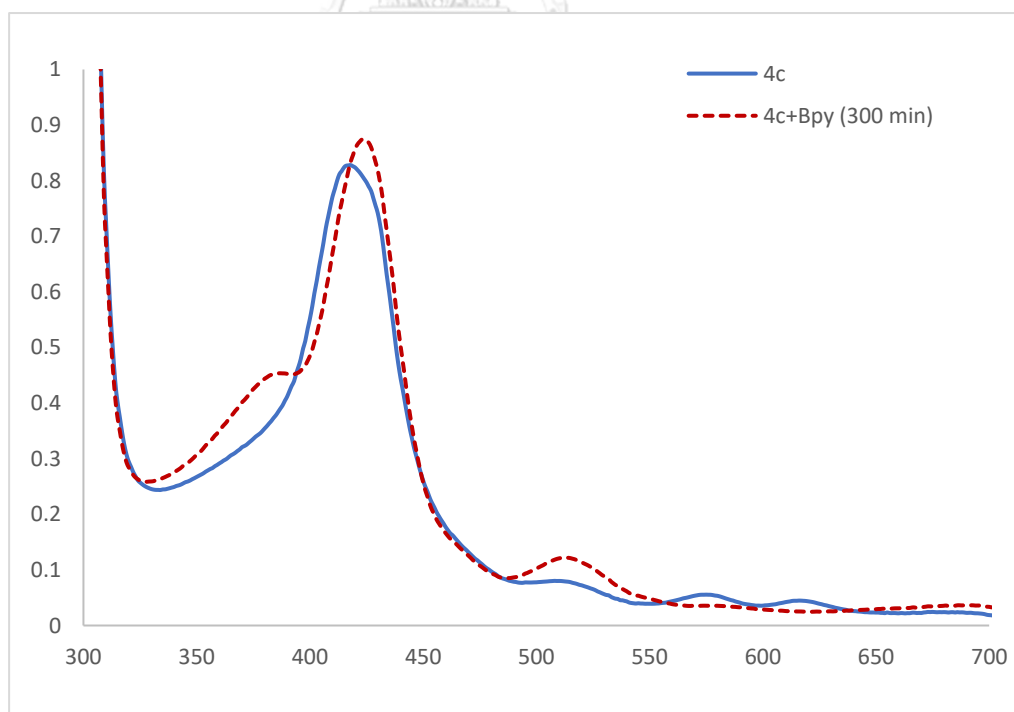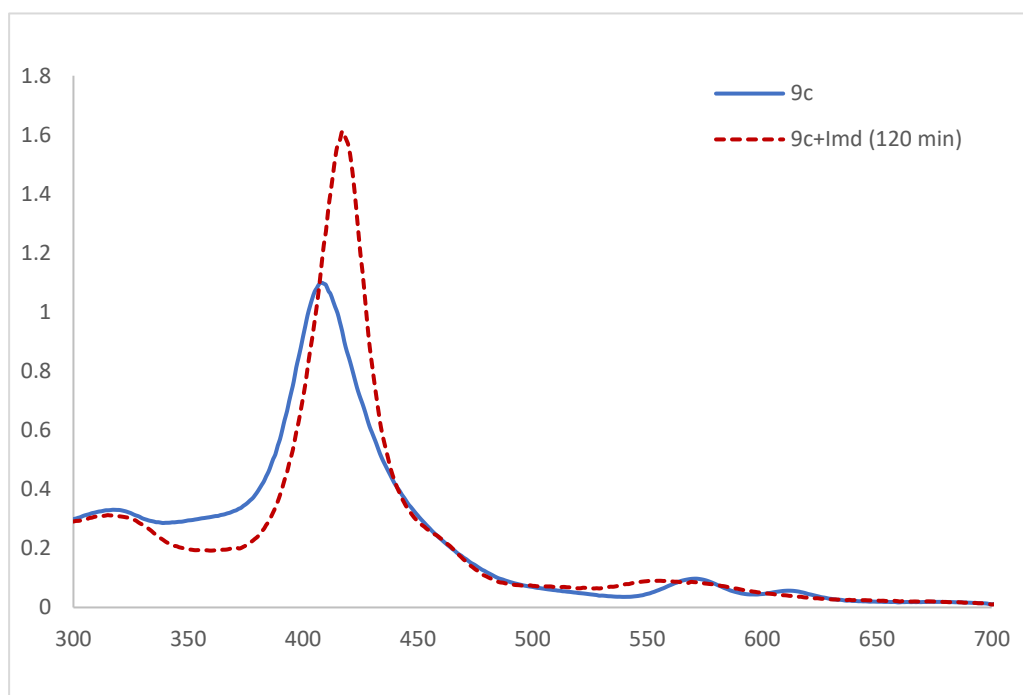**Fig. 4.2b** UV-vis spectrum of reaction between **4a** and pyridine in DCM.
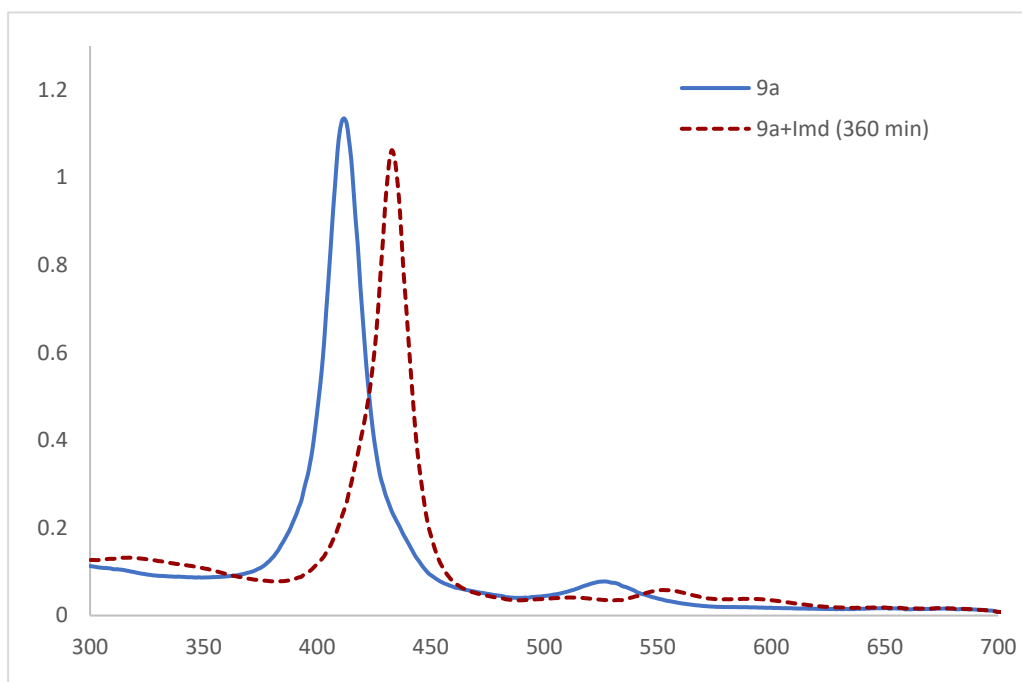
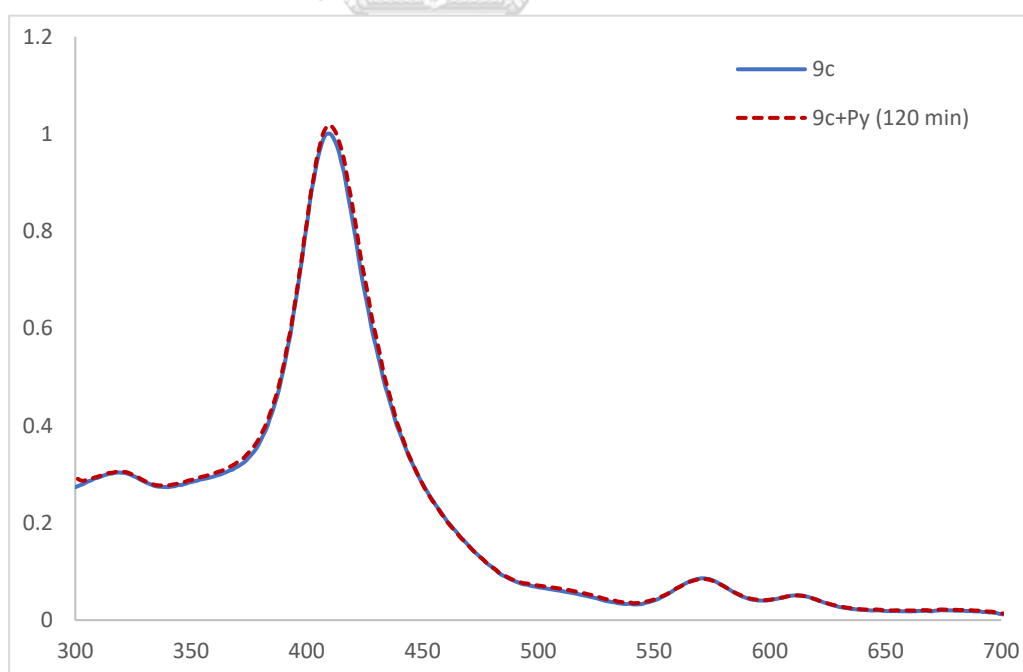**Fig. 4.2c** UV-vis spectrum of reaction between **9a** and Imidazole in DCM.
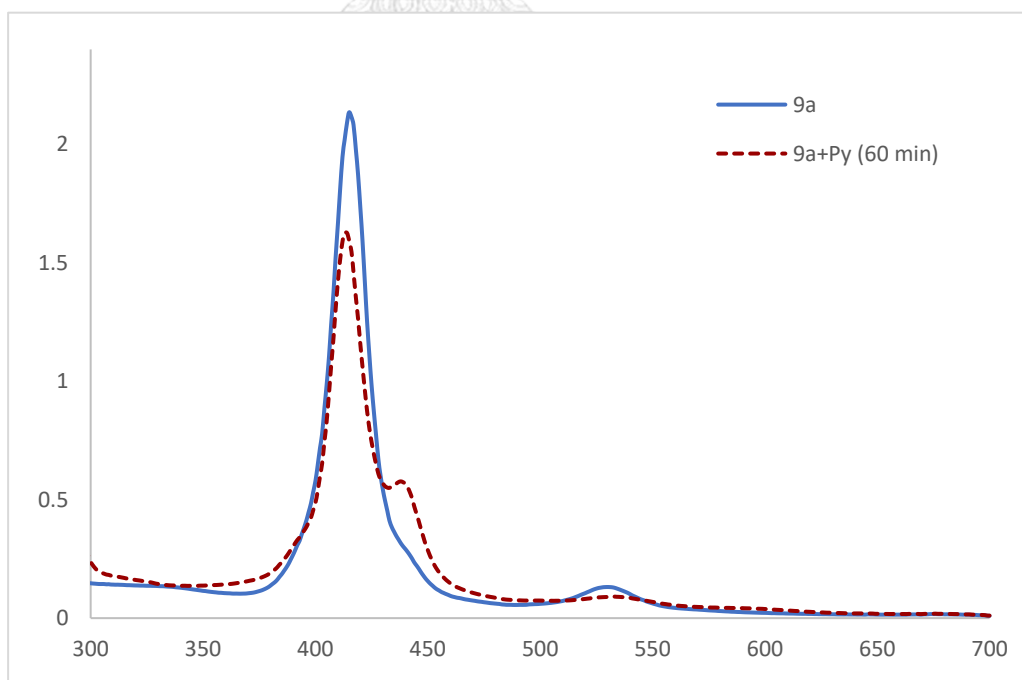
Fig. 4.2d UV-vis spectrum of reaction between **9a** and Pyridine in DCM.

UV-visible spectra results revealed that imidazole and pyridine could coordinate to cobalt atom of the porphyrin complexes to provide new compounds. Imidazole could bind to cobalt porphyrin complexes faster than pyridine in the same reaction time. A micro-scale axial ligand coordination was carried out by the same previously described procedure: in round bottle flask filled by ~50 mg of complex was charged with excess axial ligand, stirred at room temperature for 24-48 h[54]. The reaction color changed from transparent red solution to deep green or purple precipitated solid and crystal of the desirable products which are summarized in Table 4.3.

Table. 4.3 The desire compounds of cobalt (II) porphyrins coordinated with axial ligands.

Compound	Imd	Py	Pyz	Bpy
3a	L	L	-	-
4a	L	L	-	-
5a	L	L	-	-
7a	C	L	-	-
8a	C	L	-	-
9a	C	L	-	-

L: liquid, C: crystalline

The results showed that the products obtained after micro-crystallization were in liquid, solid or crystalline forms but only solid or crystal were kept to reserve liquid crystalline property. Thus, all solid compounds were characterized by UV-visible and mass spectroscopic analysis to confirm the desire products. UV-visible spectra of solids were corresponded to preliminary tests, while MS results were not conformed to the molecular masses of the products. MS data of **7a**, **8a**, and **9a** with imidazole are shown the similar molecular masses at 803.1768, 803.1782, and 803.1789 m/z, respectively. MS results implied that hydrolysis of all ester residues by imidazole on *meso*-functionalized phenyl parts, and imidazole coordinated to cobalt atom of the hydrolyzed complex to obtain the five coordination (undesired) product. This phenomenon might be purposed the mechanism as shown in scheme 4.1.
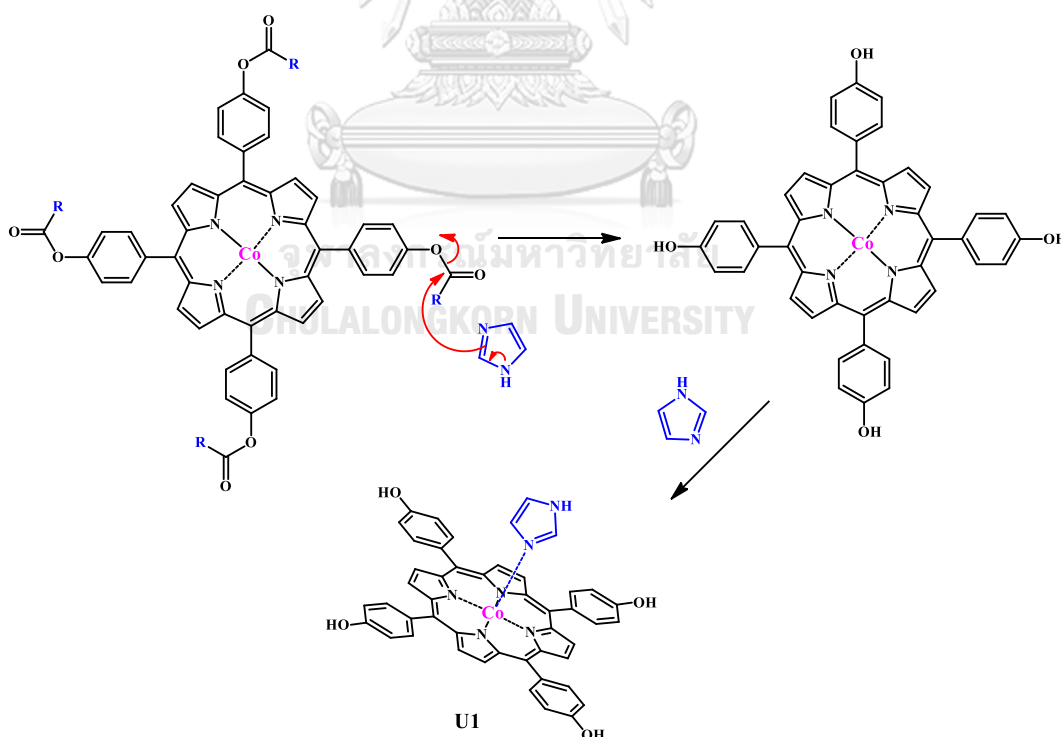
Scheme 4.1 The reaction mechanism of **U1.** [Co(II) ester porphyrin complex and imidazole].

Iron (III) porphyrins (**3c**-**5c** and **7c**-**9c**)-axial ligand coordination were carried out similar to Co (II) porphyrin complexes: by UV-visible spectroscopic technique and a micro-scale synthesis to obtain solid or crystal. UV-visible screening study of iron (III) porphyrin complexes with excess axial ligands was realized in DCM at room temperature for 6-8 h.[18, 55-57] The results are shown in Table 4.4 and examples of reaction spectra for various times are presented in Fig. 4.3a-d.

Table. 4.4 Coordination of iron (III) porphyrins with axial ligands.

Compound	Imd	Py	4-MePy	Pyz	Bpy
3c	-	-	-	-	-
4c	NR	[a]+	[a]+	[b]+	[a]+
5c	NR	[a]+	[a]+	[a]+	[a]+
7c	-	NR	-	NR	-
8c	NR	-	[a]+	-	-
9c	NR	NR	[a]+	-	NR

NR:No reaction, [a]Incomplete in 12 h, [b]complete in 8 h.

Fig. 4.3a UV-vis spectrum of reaction between **4c** and imidazole in DCM.

Fig. 4.3b UV-vis spectrum of reaction between **4c** and 4-picoline in DCM.

Fig. 4.3c UV-vis spectrum of reaction between **4c** and pyrazine in DCM.

Fig. 4.3d UV-vis spectrum of reaction between **4c** and 4,4'-bipyridine in DCM.

Fig. 4.3e UV-vis spectrum of reaction between **9c** and imidazole in DCM.

Fig. 4.3f UV-vis spectrum of reaction between **9c** and pyridine in DCM.

UV-visible spectra revealed that imidazole and pyridine ligands could react with iron atom on the porphyrin complexes to provide the new compounds. The micro-scale axial-ligand complexation was performed as same procedure that used for axial-ligand Co-porphyrin complexes. The resulting compounds are summarized in Table 4.5.

Table. 4.5 The desire compound of iron (III) porphyrins with axial ligands.

Compound	Imd	Py	4-MePy	Pyz	Bpy
3c	-	-	-	-	-
4c	-	L	L	L	L
5c	-	L	L	C	L
7c	-	-	-	-	-
8c	-	-	L	-	-
9c	-	-	L	-	-

L: liquid, C: crystalline

Among the products obtained, only **5c**-pyrazine (**FeE3-Pyrazine**) could crystalize, while other products were exhibited in solutions. The crystal **5c**-pyrazine (**FeE3-Pyrazine**) was characterized by ^{1}H-NMR and MS to confirm the structure. ^{1}H-NMR spectrum displayed protons of pyrazine at 7.05 and 7.47 ppm as presented in Fig. 4.4, and MS result found a m/z peak at 1821.497 which confirmed that the pyrazine ligand coordinated with iron atom on etherate porphyrin ring to provide a five-coordination compound.
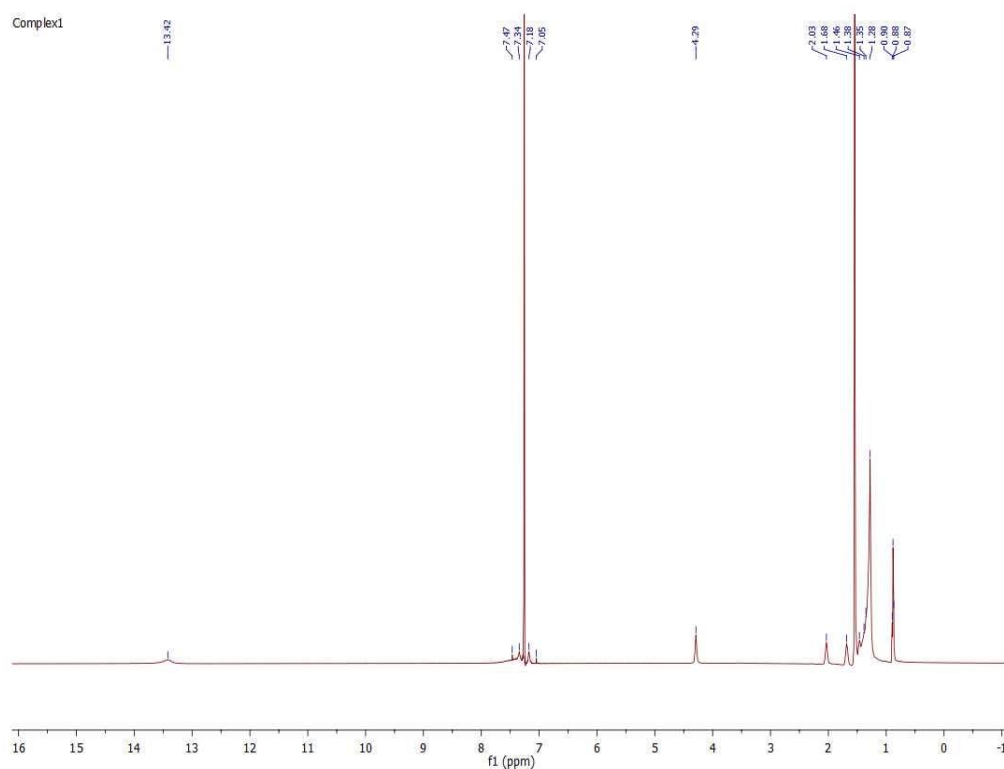
Fig. 4.4 ^{1}H-NMR spectrum of **5c**-pyrazine (**FeE3-Pyrazine**).

4.3 Mesomorphic property

Phase transition is the major feature of liquid crystalline materials, which depends on the nature of core structure (rigid part) and composition of long alkyl chains (soft part) in each compound[47, 58, 59]. All suitable synthesized compounds were investigated the mesophase behaviors by different scanning calorimetry (DSC) and the results are shown in Table 4.6 and 4.7.

Table 4.6 Phase transition of ether porphyrins and their metal complexes.

Compound				T/°C				
3	C	217.8	L					
4	C	138.1	L					
5	C	121.4	L					
4c	C	82.1	MS$_1$	205.6	L			
5c	C	88.9	MS$_1$	149.9	L			
3a	C	231.1	L					
5c-Pz	C	75.0	MS$_1$	90.6	MS$_2$	150.4	L	

C: crystal, MS$_1$: mesophase1, MS$_2$: mesophase2, L: liquid

Metal free ether porphyrins (**3**-**5**) with different side chain lengths had low melting points, whereas the cobalt complex (**3a**) had higher melting point than porphyrin ligand[11, 35, 36]. No liquid crystalline property was observed for these metal free ether porphyrins (**3**-**5**) and cobalt complex (**3a**). Contrastingly, iron complexes (**4c** and **5c**) displayed multi-phase transitions (crystal-mesophase1-liquid) in wide

range temperature (82 to 205 °C), Interestingly, axial ligand coordination could increase number of phase transition but decrease temperature of phase transition. DSC data of this series implied that some metal complexes might have mesophase properties.

Table 4.7 Phase transition of ester porphyrins (**7**-**9**) and their metal complexes.

Compound		T/°C						
7	C	54.3	MS$_1$	153.6	L			
8	C	90.8	MS$_1$	131.2	L			
9	C	93.9	MS$_1$	127.0	L			
7b	C	-18.3	MS$_1$	-9.4	MS$_2$	134.4	L	
8b	C	31.8	MS$_1$	116.1	L			
9b	C	-43.2	MS$_1$	40.0	MS$_2$	112.7	L	
7a	C	155.0	MS$_1$	173.8	L			
8a	C	49.6	MS$_1$	141.1	L			
9a	C	57.0	MS$_1$	135.5	L			
7c	C	113.9	MS$_1$	174.3	L			
8c	C	58.4	MS$_1$	152.8	L			
9c	C	50.5	MS$_1$	64.2	L			

C: crystal, MS$_1$: mesophase1, MS$_2$: mesophase2, L: liquid

For ester porphyrin series (**7**-**9**), DSC results showed mesophase behaviors both ligands and metal complexes. All ester porphyrin ligands (**7**-**9**) showed mesophase temperatures from 54 to 94 °C and transited to liquid phase at 127 to 153 °C[32, 34]. The nickel complexes (**7b**-**9b**) revealed lower mesomorphic temperatures than cobalt (**7a**-**9a**) and iron (**7c**-**9c**) complexes with the same chain length[33]. Again, the metals on porphyrin demonstrated an effect on mesophase property as previously seen in ether series. Moreover, all nickel complexes (**7b**-**9b**) exhibited liquid crystalline materials at room temperature[31]. The effect of alkyl chain length was demonstrated. While the chain length increased, the transition temperature decreased in both metal free porphyrins and their transition metal complexes.

4.4 Magnetic property

All four undesired products (**7a**-imidazole, **8a**-imidazole, **9a**-imidazole, and **5c**-pyrazine) were investigated the magnetic property on SQUID magnetometer by collaborating with Professor Shinya Hayami at Kumamoto university, Japan. Magnetic susceptibility data were obtained in the temperature range from 5 to 300 K and applied field at 5000 Oe for all compounds.

The magnetic susceptibility of all cobalt (II) porphyrin imidazole (**7a**-imidazole **8a**-imidazole and **9a**-imidazole) and iron (III) pyrazine (**5c**-pyrazine) complexes displayed the highest value at 5 K, decreased when raise temperature to 60-75 K and kept quite constant from 75 to 300 K as shown in Fig. 4.5a-d. These results indicate that all these compounds exhibit as paramagnetic materials with no spin-crossover property[20, 60-63].
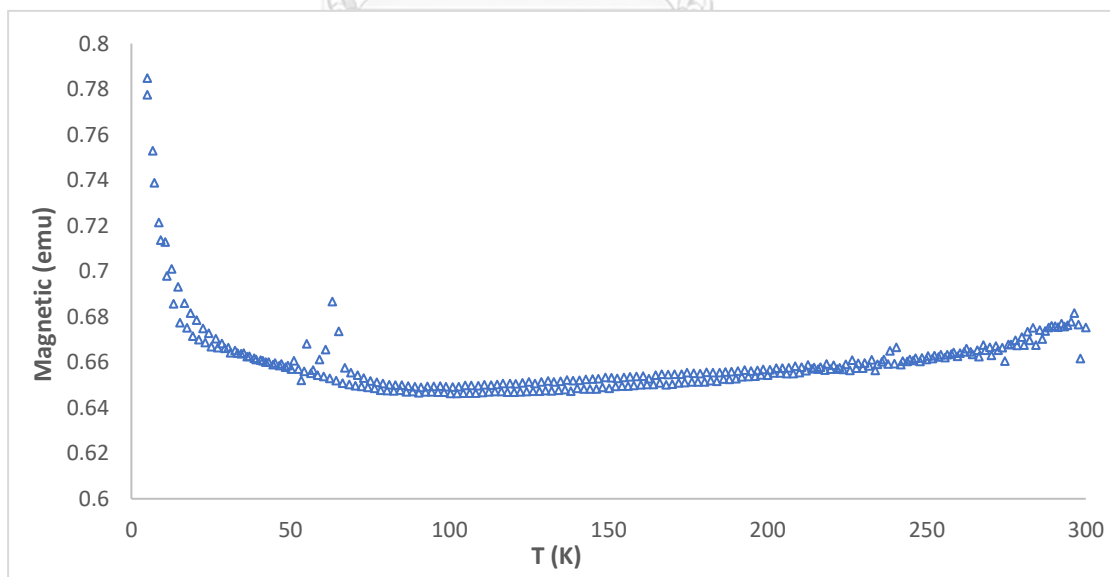
Fig. 4.5a Temperature dependence of the magnetic moment of **7a**-imidazole.
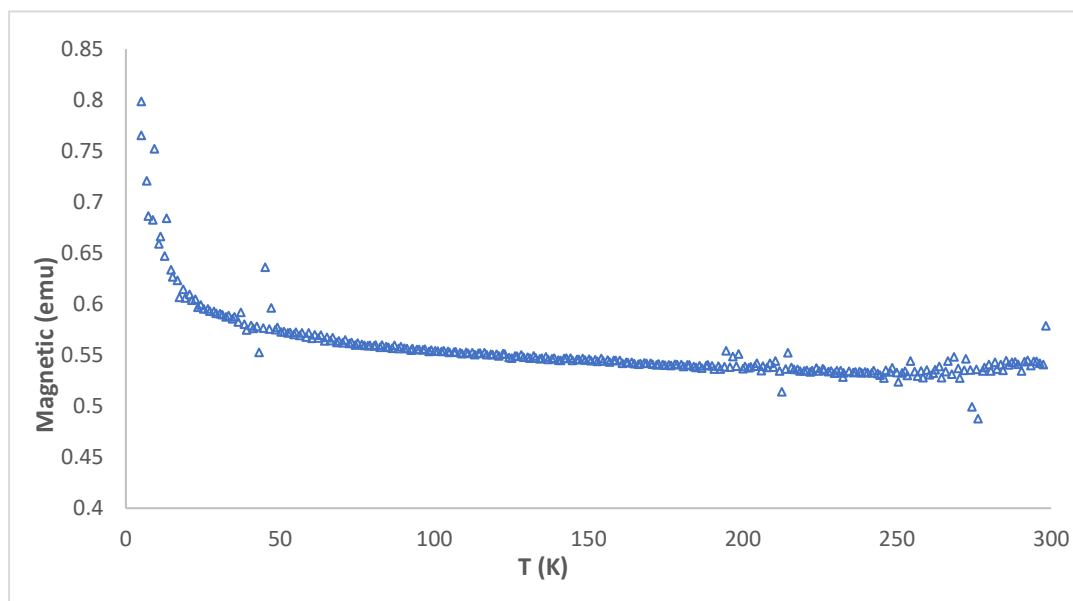
Fig. 4.5b Temperature dependence of the magnetic moment of **8a**-imidazole.
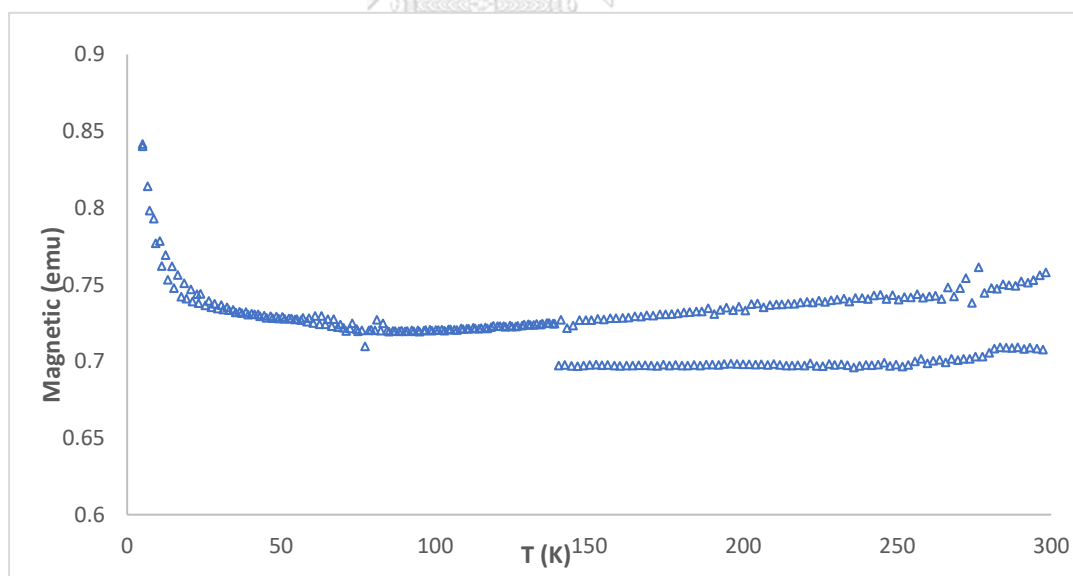
Fig. 4.5c Temperature dependence of the magnetic moment of **9a**-imidazole.
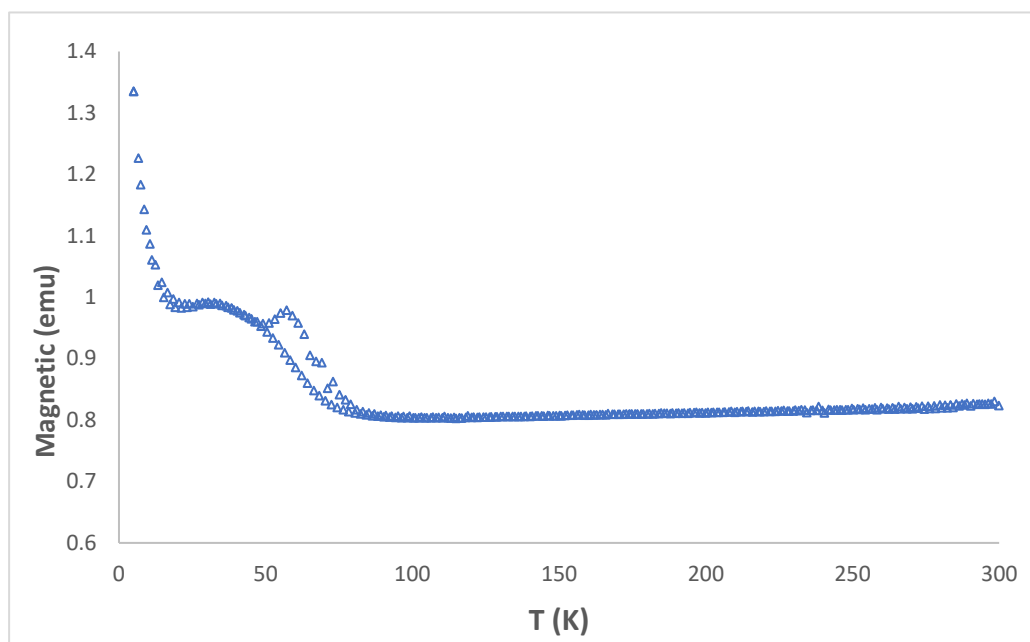
Fig. 4.5d Temperature dependence of the magnetic moment of **5c**-pyrazine.

CHAPTER 5

CONCLUSION

Three series of functionalized porphyrins and metalloporphyrins were designed and synthesized to serve as the soft materials; liquid crystal and studied magnetic properties by spin-crossover phenomenon of suitable complexes. The core porphyrin macrocycles were prepared *via* macrocyclization between 4-substituted benzaldehydes and pyrrole, followed by modified Adler method to obtain purple crystals in moderate yields. In the first series, ether derivatives (**3-5**), were prepared by alkylation of 4-hydroxylbenzaldehyde with long chain alkyl bromide by using K_2CO_3 as a base, then macrocyclization with pyrrole in refluxing propanoic acid. For second series, ester derivatives (**7-9**), were synthesized by Steglich esterification on 4-hydroxyphenyl groups in the presence of DCC and DMAP in ethyl acetate. And in the last series, urea porphyrin (**11**), was achieved in three steps; synthesis of *tetrakis*(4-nitroophenyl) porphyrin, reduction of nitro groups by $SnCl_2$ in concentrated hydrochloric acid to provide *tetrakis*(4-aminophenyl) porphyrin, and then condensation with active alkyl isocyanate and TEA in refluxing THF. Metalloporphyrins were achieved by metalation with metal acetate or chloride in refluxing DMF or THF in high yields.

Nickel ester complexes (**7-9, b**) were exhibited the liquid crystalline property at room temperature, but their axial coordination could not be achieved to provide spin-crossover property. Some cobalt (**7-9, a**) and iron (**4-5, 7-9, c**) complexes showed mesophase property in wide ranges. Most axial coordination compounds showed liquid crystal property at room temperature, whereas the spin-crossover

phenomenon by octahedral complexation with axial ligand of ether and ester porphyrin complexes cannot successfully realized due to the nature of long alkyl chains of porphyrins that might be effect on axial ligand coordination with saddle-shape long alkyl chain metalloporphyrins to provide spin-crossover property.

The asymmetrical terpyridyl-ether porphyrin Zn-Fe complex (**19**) was designed and synthesized to develop the desirable product for soft material with spin-crossover property. The hybrid desired compound was successfully synthesized and elucidated the structure. The mesomorphic and magnetic properties are in progress.

จุฬาลงกรณ์มหาวิทยาลัย

CHULALONGKORN UNIVERSITY
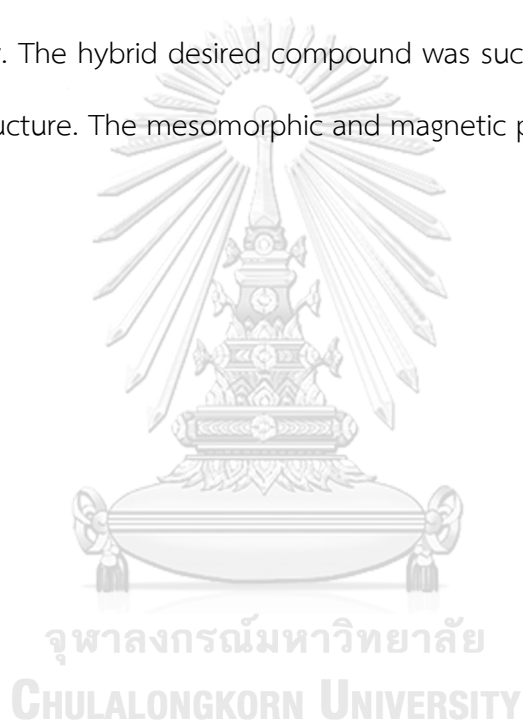
REFERENCES

1. S. Tang, Z. Davoudi, G. Wang, Z. Xu, T. Rehman, A. Prominski, B. Tian, K. M. Bratlie, H. Peng and Q. Wang, *Chemical Society Reviews*, 2021, **50**, 12679-12701.

2. F.-J. Valverde-Muñoz, M. Seredyuk, M. C. Muñoz, G. Molnár, Y. S. Bibik and J. A. Real, *Angewandte Chemie International Edition*, 2020, **59**, 18632-18638.

3. S. Ito, *Journal of Photochemistry and Photobiology C: Photochemistry Reviews*, 2022, **51**, 100481.

4. M. Nakaya, K. Shimayama, K. Takami, K. Hirata, S. A. Amolegbe, M. Nakamura, L. F. Lindoy and S. Hayami, *Crystals*, 2014, **4**, 104-112.

5. R. Akiyoshi, R. Ohtani, L. F. Lindoy and S. Hayami, *Dalton Transactions*, 2021, **50**, 5065-5079.

6. A. Ruaudel-Teixier, A. Barraud, P. Coronel and O. Kahn, *Thin Solid Films*, 1988, **160**, 107-115.

7. H. Eichhorn, *Journal of Porphyrins and Phthalocyanines*, 2000, **04**, 88-102.

8. C. Arunkumar, P. Bhyrappa and B. Varghese, *Tetrahedron Letters*, 2006, **47**, 8033-8037.

9. M. Ichihara, M. Miida, B. Mohr and K. Ohta, *Journal of Porphyrins and Phthalocyanines*, 2006, **10**, 1145-1155.

10. J. M. Warman, J. E. Kroeze, P. G. Schouten and A. M. v. d. Craats, *Journal of Porphyrins and Phthalocyanines*, 2003, **07**, 342-350.

11. I. N. Fedulova, N. A. Bragina, N. V. Novikov, A. F. Mironov, V. V. Bykova, N. V. Usol'tseva and G. A. Ananieva, *Mendeleev Communications*, 2008, **18**, 324-326.

12. W. Liu and T. Shi, *Science in China Series B: Chemistry*, 2007, **50**, 488-493.

13. H. K. Bisoyi and Q. Li, *Progress in Materials Science*, 2019, **104**, 1-52.

14. A. Ş. Ahsen, A. Segade, D. Velasco and Z. Z. Öztürk, *Journal of Porphyrins and Phthalocyanines*, 2009, **13**, 1188-1195.

15. J. W. Goodby, P. S. Robinson, B.-K. Teo and P. E. Cladi, *Molecular Crystals and Liquid Crystals*, 1980, **56**, 303-309.

16. Z.-C. Sun, Y.-B. She, Y. Zhou, X.-F. Song and K. Li, *Molecules*, 2011, **16**, 2960-2970.

17. K. Takahashi, *Inorganics*, 2018, **6**, 32.

18. T. Ikeue, Y. Ohgo, O. Ongayi, M. G. H. Vicente and M. Nakamura, *Inorganic Chemistry*, 2003, **42**, 5560-5571.

19. M. Nakamura, Y. Ohgo and A. Ikezaki, *Journal of Inorganic Biochemistry*, 2008, **102**, 433-445.

20. Y. Ide, N. Murai, H. Ishimae, M. Suzuki, S. Mori, M. Takahashi, M. Nakamura, K. Yoshino and T. Ikeue, *Dalton Transactions*, 2017, **46**, 242-249.

21. Y. Ide, T. Kuwahara, S. Takeshita, R. Fujishiro, M. Suzuki, S. Mori, H. Shinokubo, M. Nakamura, K. Yoshino and T. Ikeue, *Journal of Inorganic Biochemistry*, 2018, **178**, 115-124.

22. A. D. Adler, F. R. Longo, J. D. Finarelli, J. Goldmacher, J. Assour and L. Korsakoff, *The Journal of Organic Chemistry*, 1967, **32**, 476-476.

23. A. Bettelheim, B. A. White, S. A. Raybuck and R. W. Murray, *Inorganic Chemistry*, 1987, **26**, 1009-1017.

24. R. Luguya, L. Jaquinod, F. R. Fronczek, M. G. H. Vicente and K. M. Smith, *Tetrahedron*, 2004, **60**, 2757-2763.

25. W. Liu, Y. Shi, T. Shi, G. Liu, Y. Liu, C. Wang and W. Zhang, *Liquid Crystals*, 2003, **30**, 1255-1257.

26. Y. D. Liu Jiepin, Cao Hua, Zhao Hongbin, *Chinese Journal of Organic Chemistry*, 2012, **32**, 709-713.

27. E.-j. Sun, X.-l. Cheng, D. Wang, X.-x. Tang, S.-j. Yu and T.-s. Shi, *Solid State Sciences*, 2007, **9**, 1061-1068.

28. E. Sun, Y. Shi, P. Zhang, M. Zhou, Y. Zhang, X. Tang and T. Shi, *Journal of Molecular Structure*, 2008, **889**, 28-34.

29. V. D. Rumyantseva, *Macroheterocycles*, 2013, **6**, 59-61.

30. X. Zhang, Y. Xia, L. Zhou, P. Liu and W. Deng, *Tetrahedron*, 2017, **73**, 558-565.

31. J. Li, T. Tang, F. Li and M. Li, *Dyes and Pigments*, 2008, **77**, 395-401.

32. L. Li, S. W. Kang, J. Harden, Q. Sun, X. Zhou, L. Dai, A. Jakli, S. Kumar and Q. Li, *Liquid Crystals*, 2008, **35**, 233-239.

33. E. Tsuchida, T. Komatsu, E. Hasegawa and H. Nishide, *Journal of the Chemical Society, Dalton Transactions*, 1990, 2713-2718.

34. I. N. Fedulova, N. A. Bragina, N. V. Novikov, O. A. Ugol'nikova and A. F. Mironov, *Russian Journal of Bioorganic Chemistry*, 2007, **33**, 589-593.

35. K. A. Formirovsky, N. A. Bragina, A. F. Mironov, G. A. Anan'eva, V. V. Bykova and N. V. Usol'tseva, *Mendeleev Communications*, 2012, **22**, 278-280.

36. W. Q. Zheng, W. Y. Liu and M. Yu, *Synthesis and Reactivity in Inorganic, Metal-Organic, and Nano-Metal Chemistry*, 2013, **43**, 175-177.

37. A. Alliband, F. A. Meece, C. Jayasinghe and D. H. Burns, *The Journal of Organic Chemistry*, 2013, **78**, 356-362.

38. S.-i. Tamaru, S.-y. Uchino, M. Takeuchi, M. Ikeda, T. Hatano and S. Shinkai, *Tetrahedron Letters*, 2002, **43**, 3751-3755.

39. A. D. Adler, F. R. Longo, F. Kampas and J. Kim, *Journal of Inorganic and Nuclear Chemistry*, 1970, **32**, 2443-2445.

40. Y. H. Lee, M. R. Karim, Y. Ikeda, T. Shimizu, S. Kawata, A. Fuyuhiro and S. Hayami, *Journal of Inorganic and Organometallic Polymers and Materials*, 2013, **23**, 186-192.

41. A. Jouaiti, *Synthetic Communications*, 2021, **51**, 1547-1555.

42. T. J. Cho, C. D. Shreiner, S.-H. Hwang, C. N. Moorefield, B. Courneya, L. A. Godínez, J. Manríquez, K.-U. Jeong, S. Z. D. Cheng and G. R. Newkome, *Chemical Communications*, 2007, 4456-4458.

43. I. M. Dixon, J.-P. Collin, J.-P. Sauvage and L. Flamigni, *Inorganic Chemistry*, 2001, **40**, 5507-5517.

44. F. Odobel, J.-P. Sauvage and A. Harriman, *Tetrahedron Letters*, 1993, **34**, 8113-8116.

45. C.-L. Wang, W.-B. Zhang, X. Yu, K. Yue, H.-J. Sun, C.-H. Hsu, C.-S. Hsu, J. Joseph, D. A. Modarelli and S. Z. D. Cheng, *Chemistry – An Asian Journal*, 2013, **8**, 947-955.

46. G. C. Shearman, G. Yahioglu, J. Kirstein, L. R. Milgrom and J. M. Seddon, *Journal of Materials Chemistry*, 2009, **19**, 598-604.

47. C. J. Wilson, D. A. Wilson, R. W. Boyle and G. H. Mehl, *J. Mater. Chem. C*, 2013, **1**,

144-150.

48. S. Hayami, Y. Kojima, D. Urakami, K. Ohta and K. Inoue, *Polyhedron*, 2009, **28**, 2053-2057.

49. K. Kuroiwa, T. Arie, S. Sakurai, S. Hayami and T. J. Deming, *Journal of Materials Chemistry C*, 2015, **3**, 7779-7783.

50. D. Achey and G. J. Meyer, *Inorg Chem*, 2013, **52**, 9574-9582.

51. F. Gutzeit, M. Dommaschk, N. Levin, A. Buchholz, E. Schaub, W. Plass, C. Näther and R. Herges, *Inorganic Chemistry*, 2019, **58**, 12542-12546.

52. S. Thies, C. Bornholdt, F. Köhler, F. D. Sönnichsen, C. Näther, F. Tuczek and R. Herges, *Chemistry – A European Journal*, 2010, **16**, 10074-10083.

53. M. Dommaschk, V. Thoms, C. Schütt, C. Näther, R. Puttreddy, K. Rissanen and R. Herges, *Inorganic Chemistry*, 2015, **54**, 9390-9392.

54. N. Amiri, S. Nouir, M. Hajji, T. Roisnel, T. Guerfel, G. Simonneaux and H. Nasri, *Journal of Saudi Chemical Society*, 2019, **23**, 781-794.

55. L. Ben Haj Hassen, K. Ezzayani, Y. Rousselin, C. Stern, H. Nasri and C. E. Schulz, *Journal of Molecular Structure*, 2016, **1110**, 138-142.

56. M. K. Peters, C. Nather and R. Herges, *Acta Crystallographica Section E*, 2019, **75**, 762-765.

57. B. Hu, M. He, Z. Yao, C. E. Schulz and J. Li, *Inorganic Chemistry*, 2016, **55**, 9632-9643.

58. A. B. Gaspar and M. Seredyuk, *Coordination Chemistry Reviews*, 2014, **268**, 41-58.

59. D. J. Harding, P. Harding and W. Phonsri, *Coordination Chemistry Reviews*, 2016, **313**, 38-61.

60. S. S. Eaton and G. R. Eaton, *Inorganic Chemistry*, 1980, **19**, 1095-1096.

61. R. T. Pardasani and P. Pardasani, DOI: 10.1007/978-3-662-53971-2_197.

62. H. Nasri, M. K. Ellison, B. Shaevitz, G. P. Gupta and W. R. Scheidt, *Inorg Chem*, 2006, **45**, 5284-5290.

63. C.-C. Chiu, J.-H. Chen, S.-S. Wang and J.-Y. Tung, *Polyhedron*, 2014, **83**, 212-219.

APPENDICES

SPECTROSCOPIC DATA
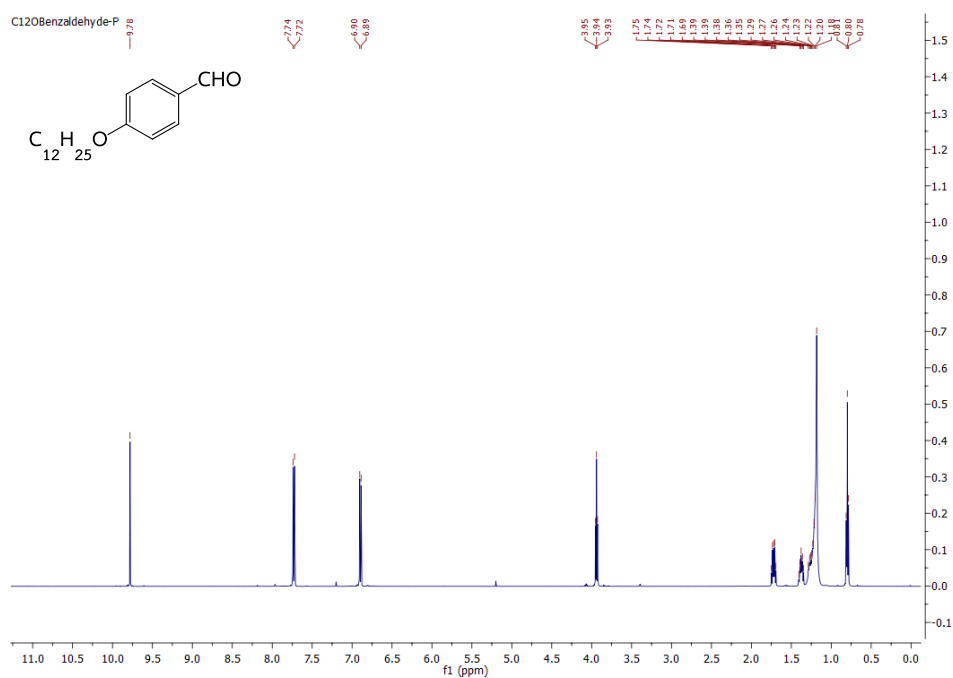
Appendix Figure. S1 ^{1}H NMR spectrum of compound **1**
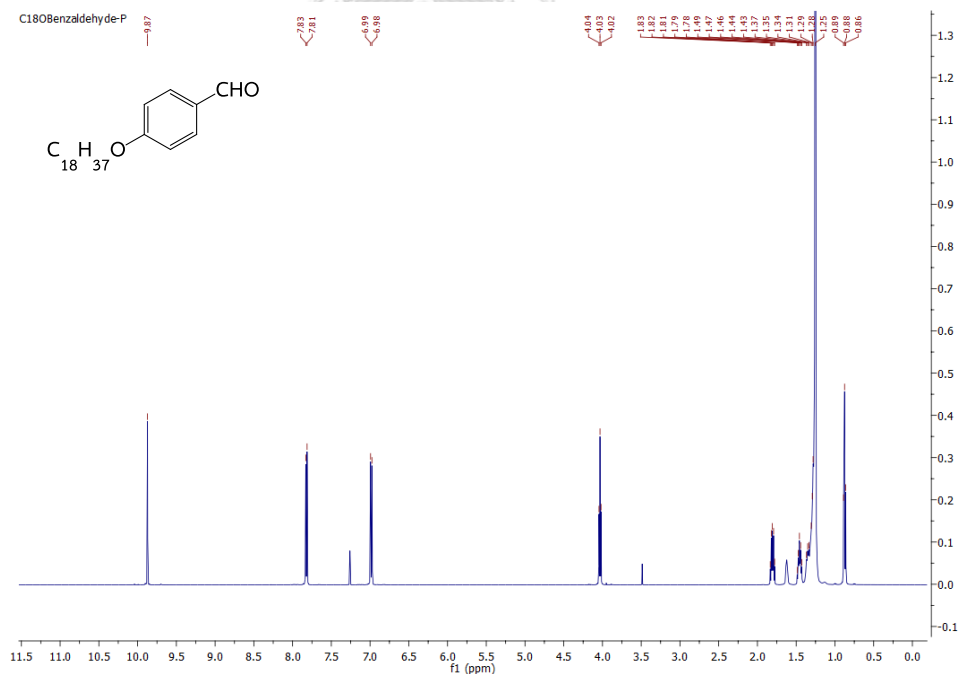
Appendix Figure S2 ^{1}H NMR spectrum of compound **2**
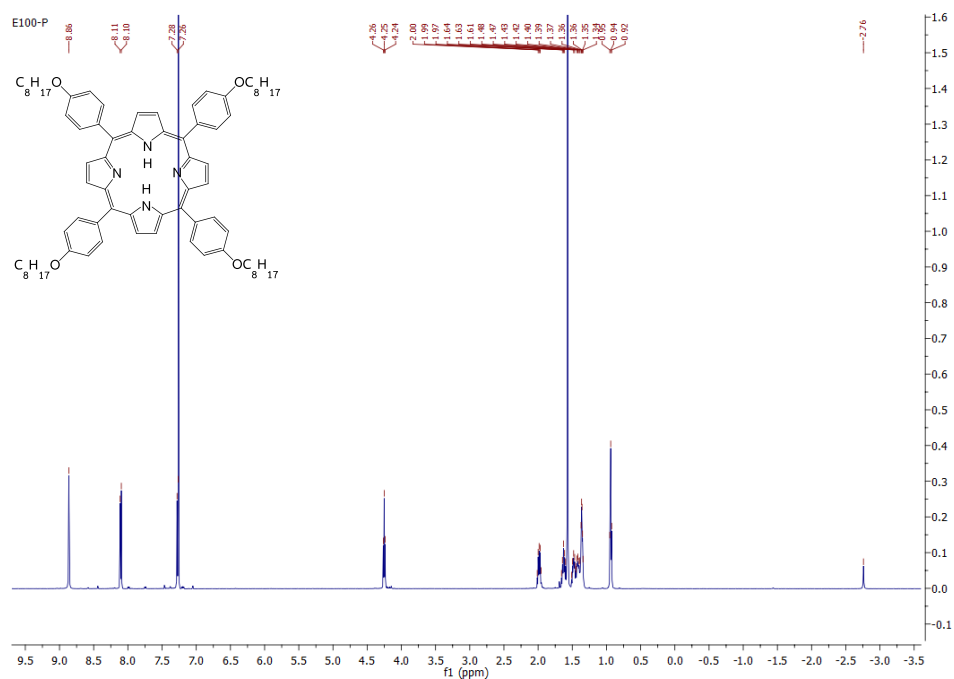
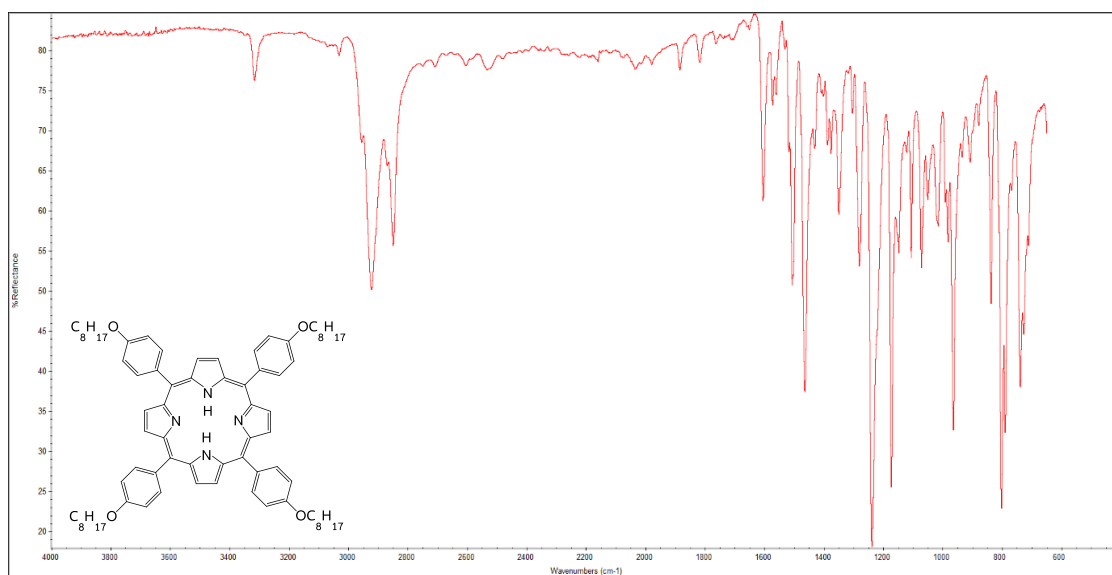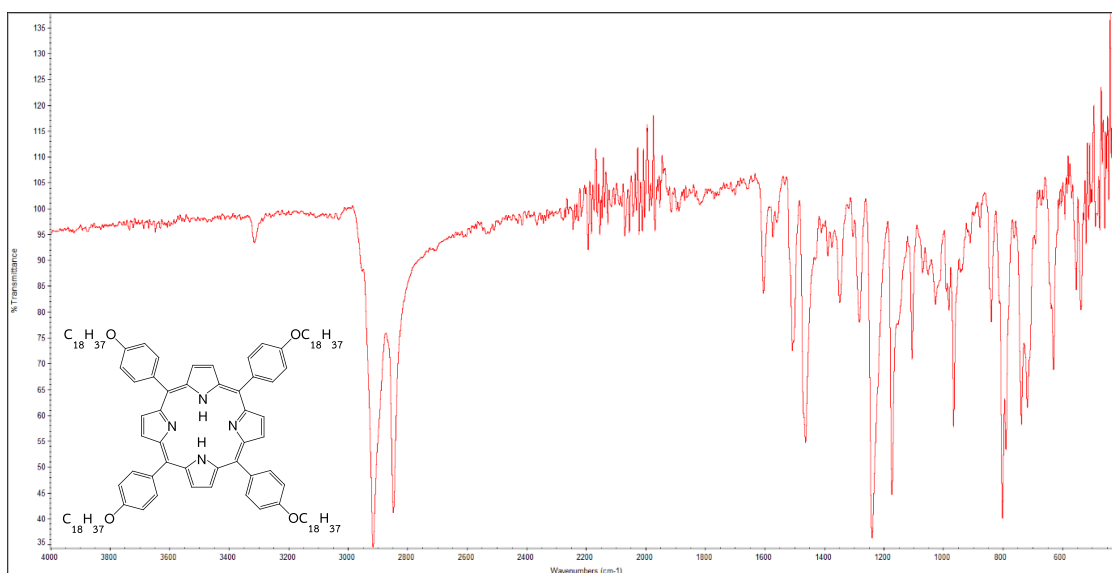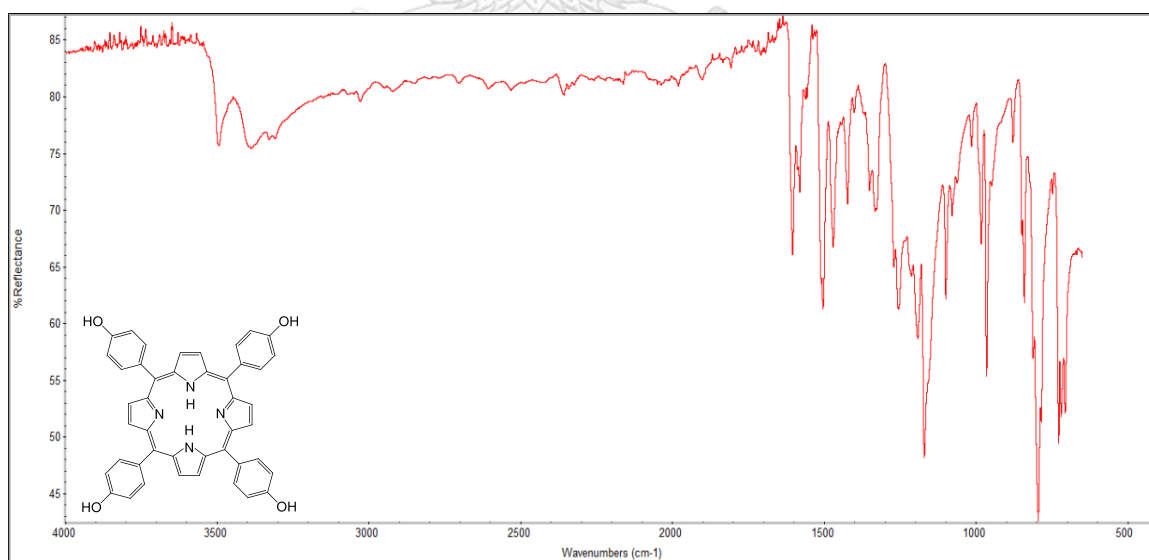**Appendix Figure S3** ^{1}H NMR spectrum of compound **3**
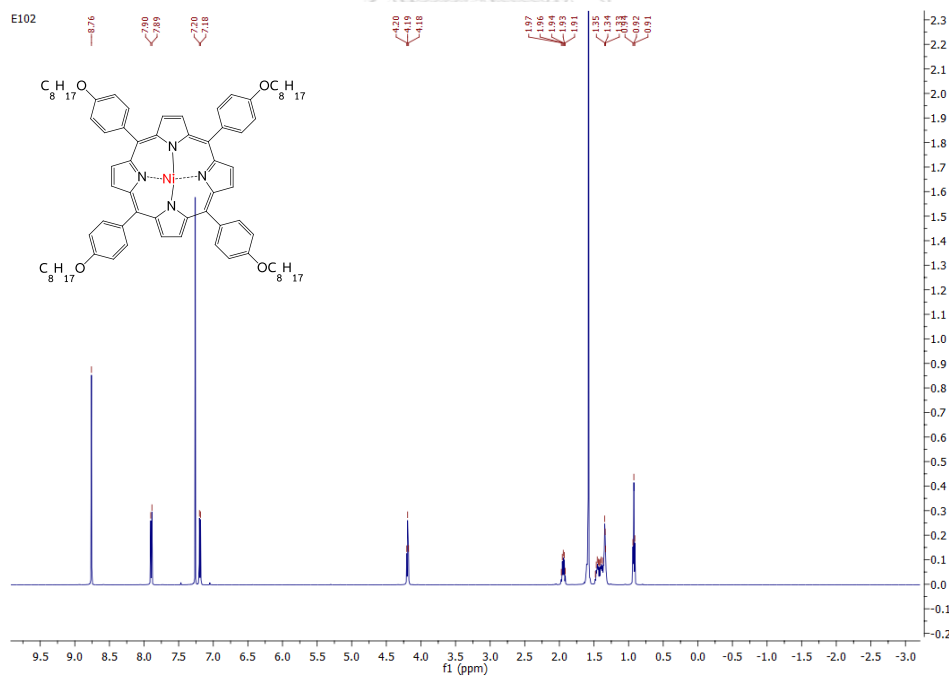
Appendix Figure S4 ^{1}H NMR spectrum of compound **3b**
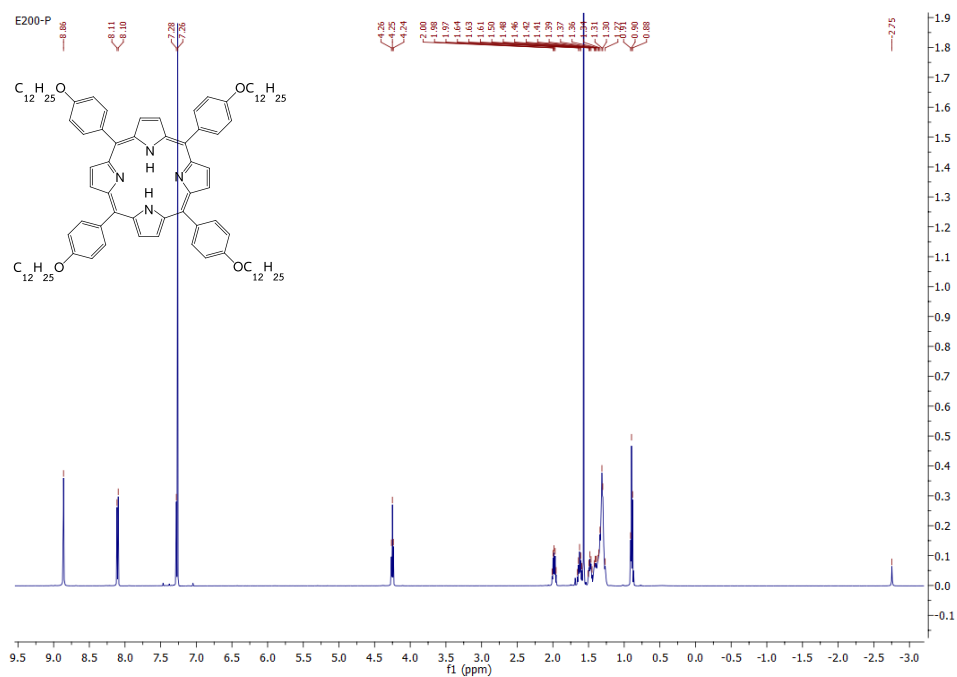
Appendix Figure S5 ^{1}H NMR spectrum of compound **4**
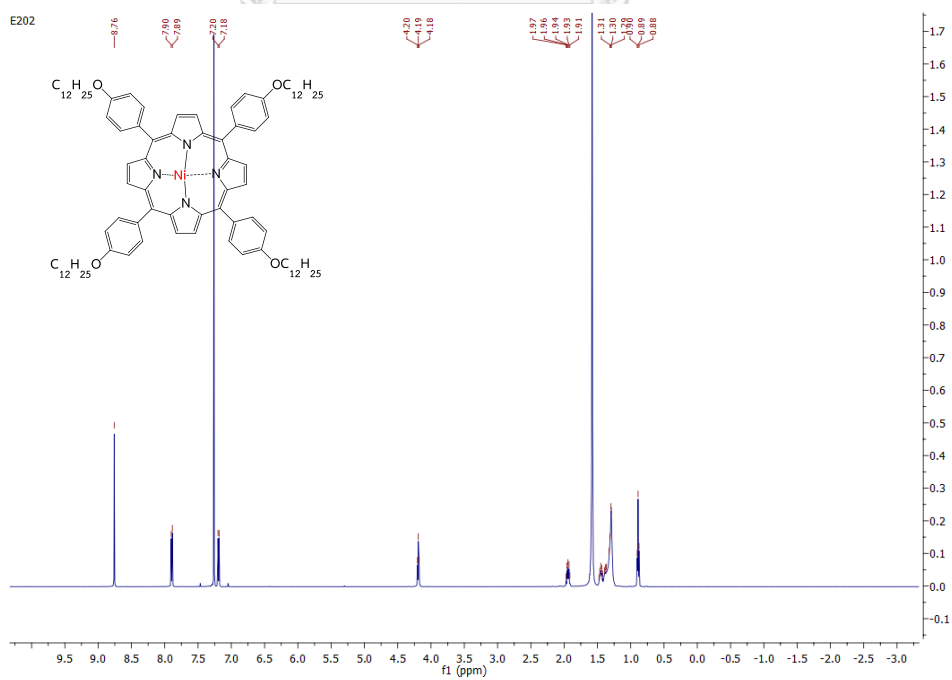
Appendix Figure S6 ^{1}H NMR spectrum of compound **4b**

Appendix Figure S7 ^{1}H NMR spectrum of compound **5**

Appendix Figure S8 ^{1}H NMR spectrum of compound **5b**
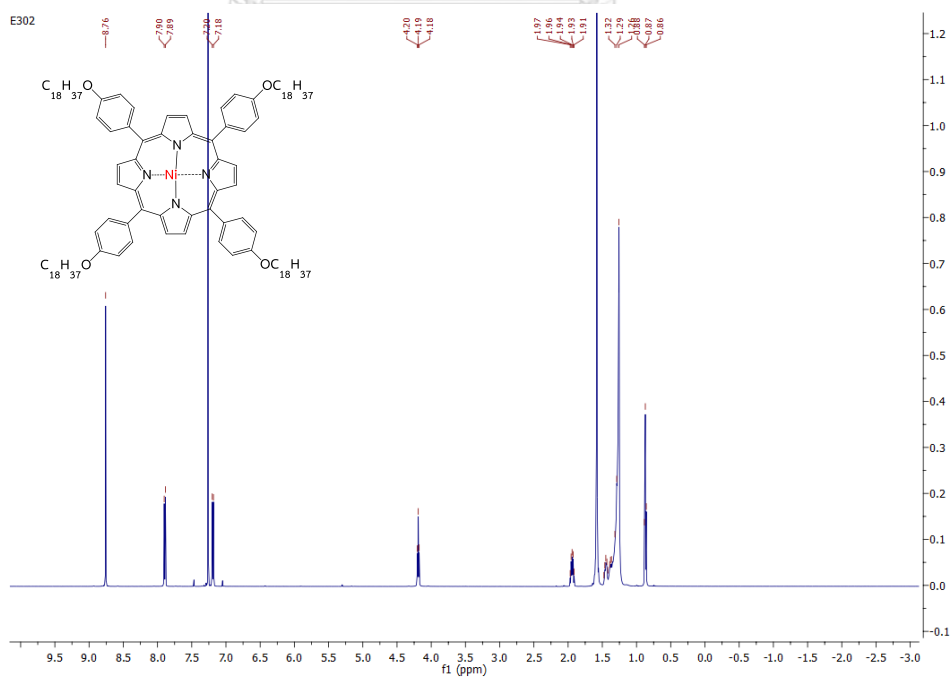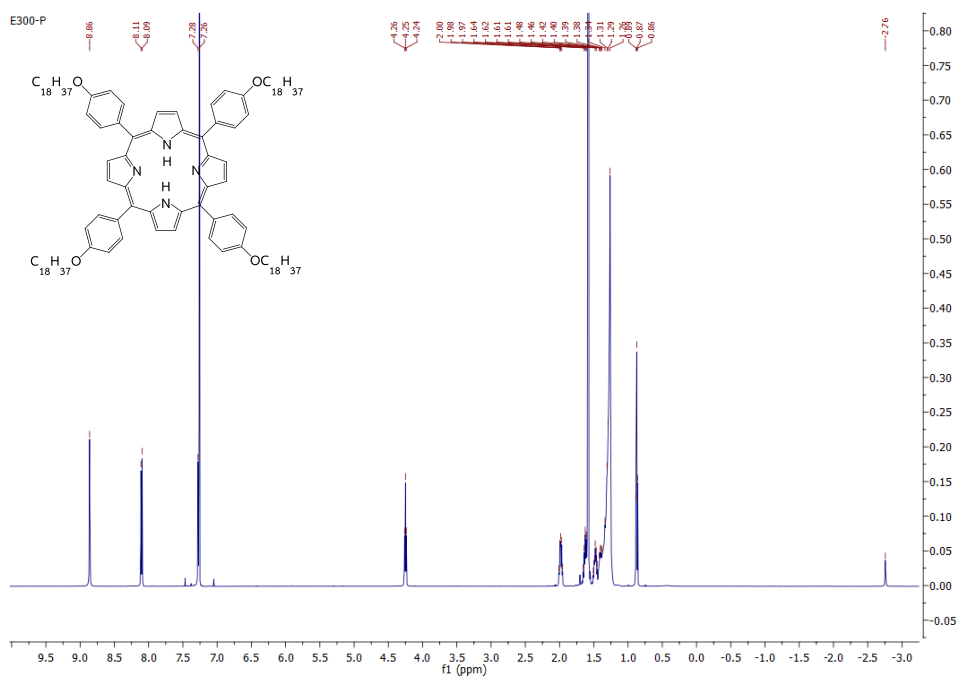
Appendix Figure S9 ^{1}H NMR spectrum of compound **6**
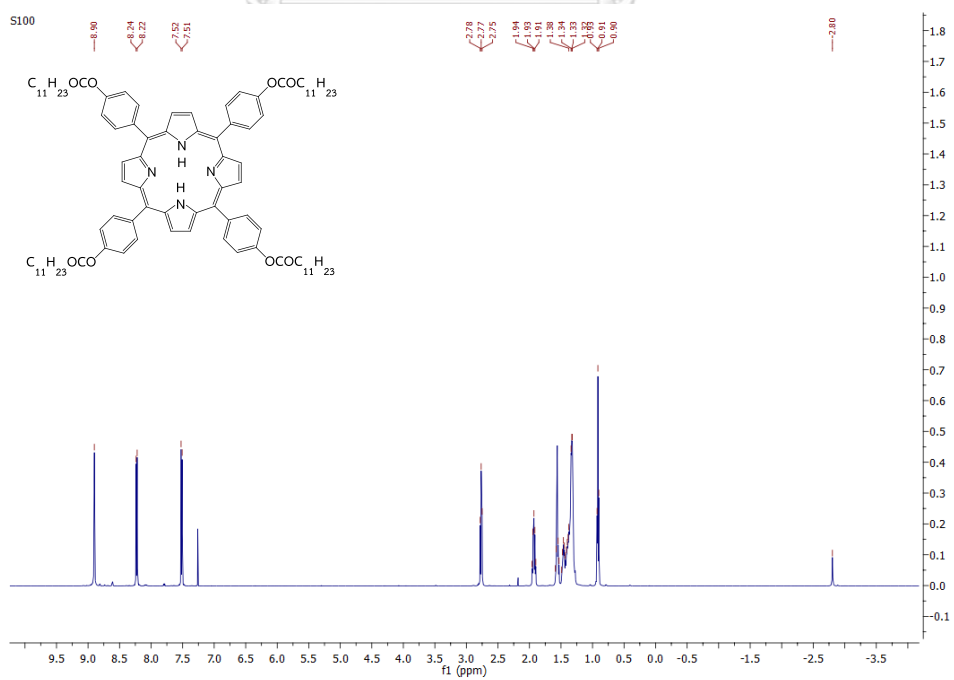
Appendix Figure S10 ^{1}H NMR spectrum of compound **7**
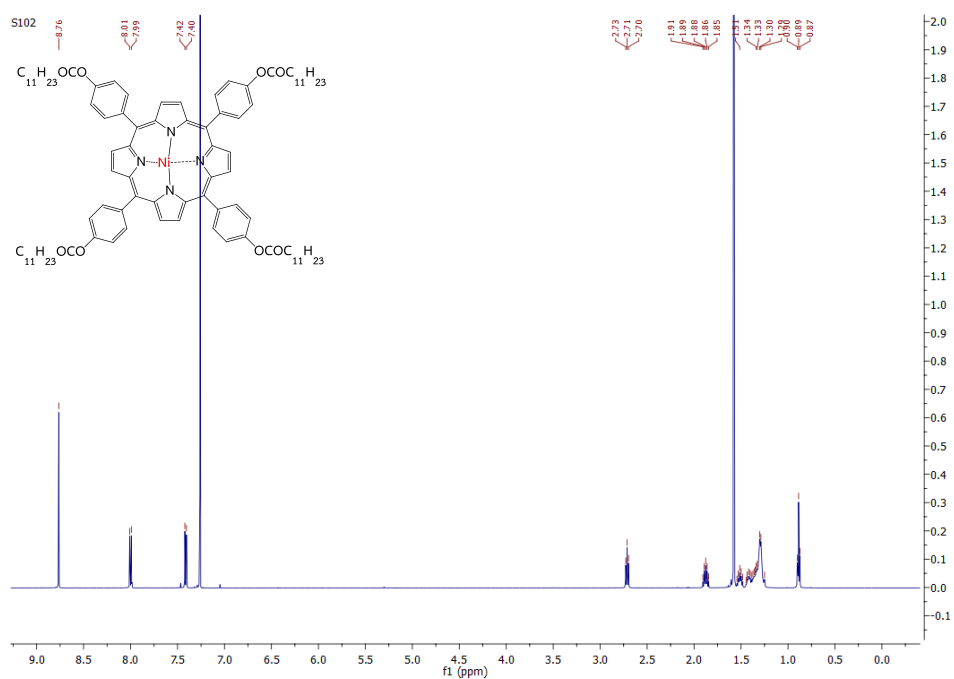
Appendix Figure S11 ^{1}H NMR spectrum of compound **7b**
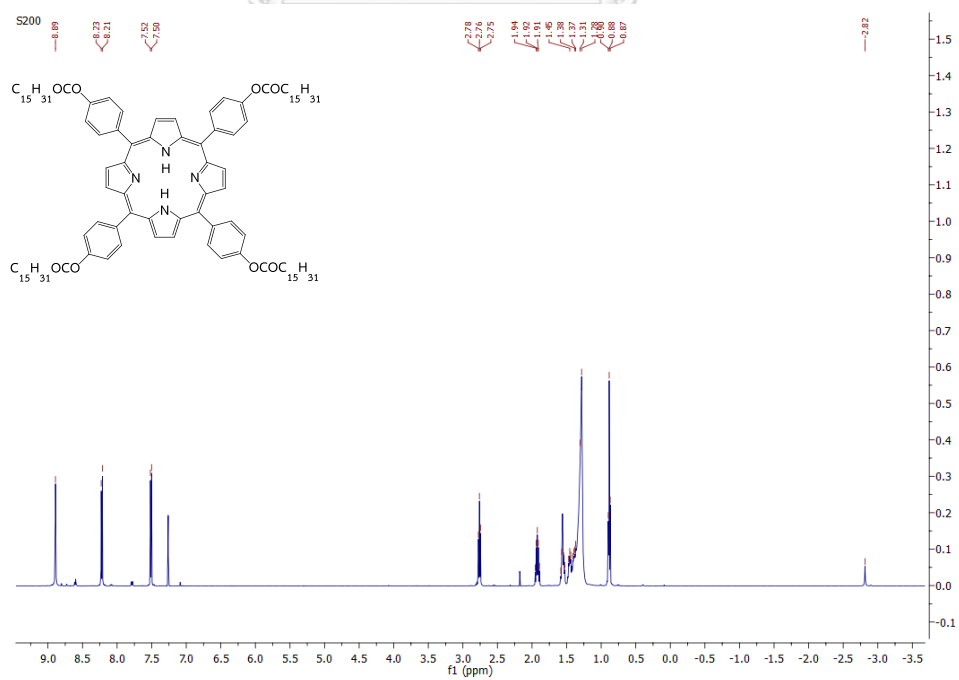
Appendix Figure S12 ^{1}H NMR spectrum of compound **8**
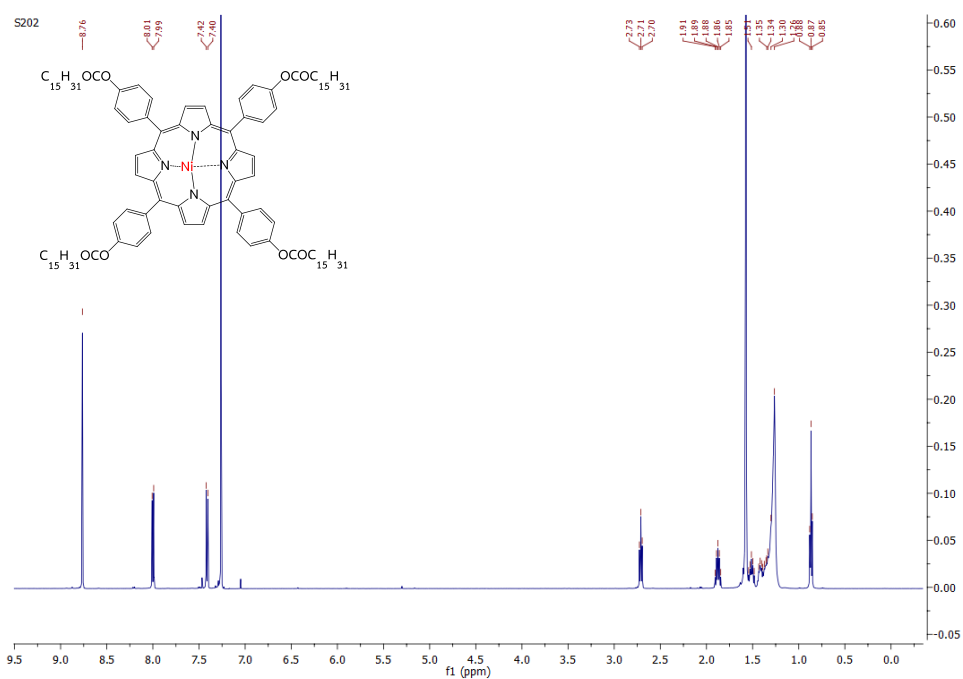
Appendix Figure S13 ^{1}H NMR spectrum of compound **8b**
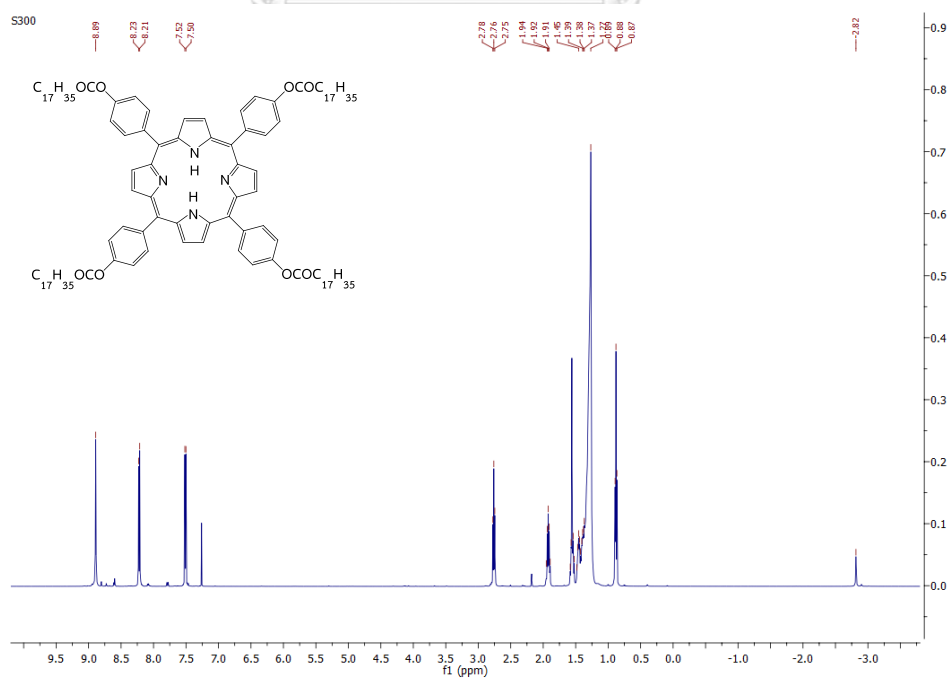
Appendix Figure S14 ^{1}H NMR spectrum of compound **9**
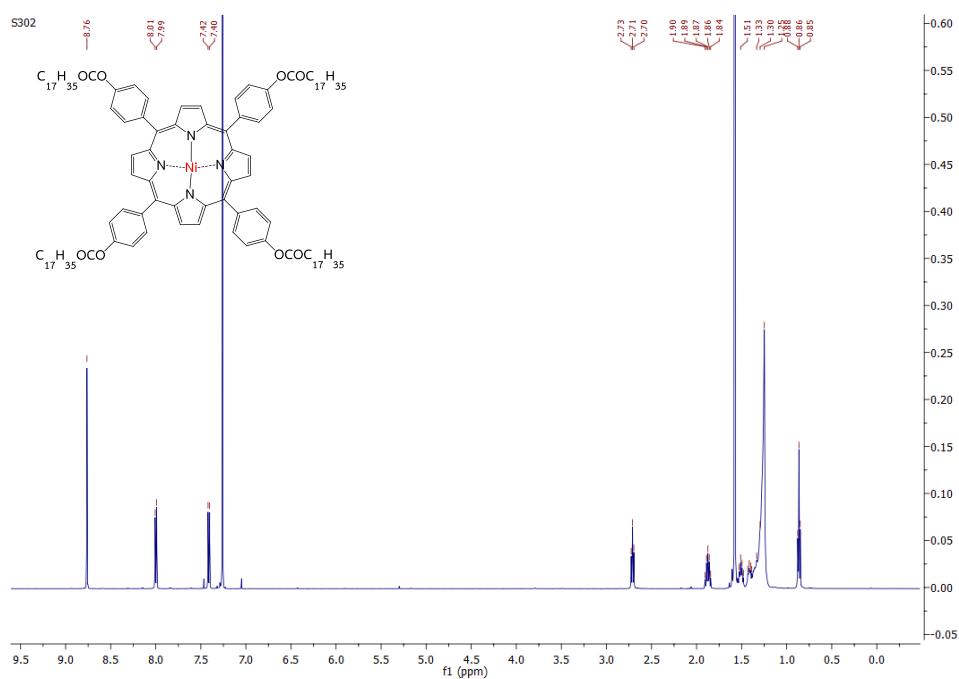
Appendix Figure S15 ^{1}H NMR spectrum of compound **9b**
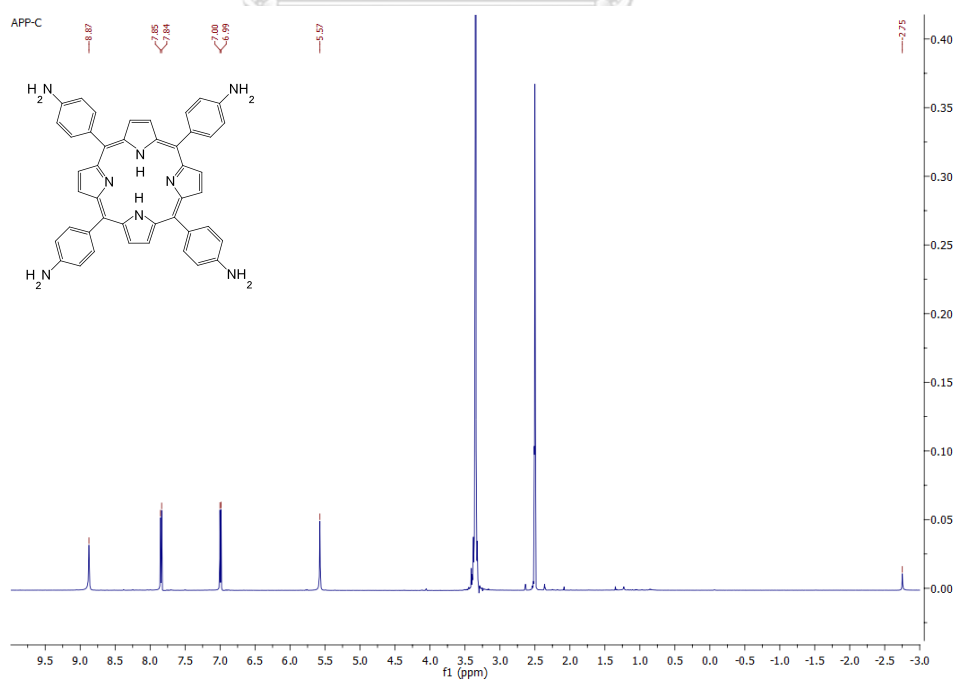
Appendix Figure S16 ^{1}H NMR spectrum of compound **10**
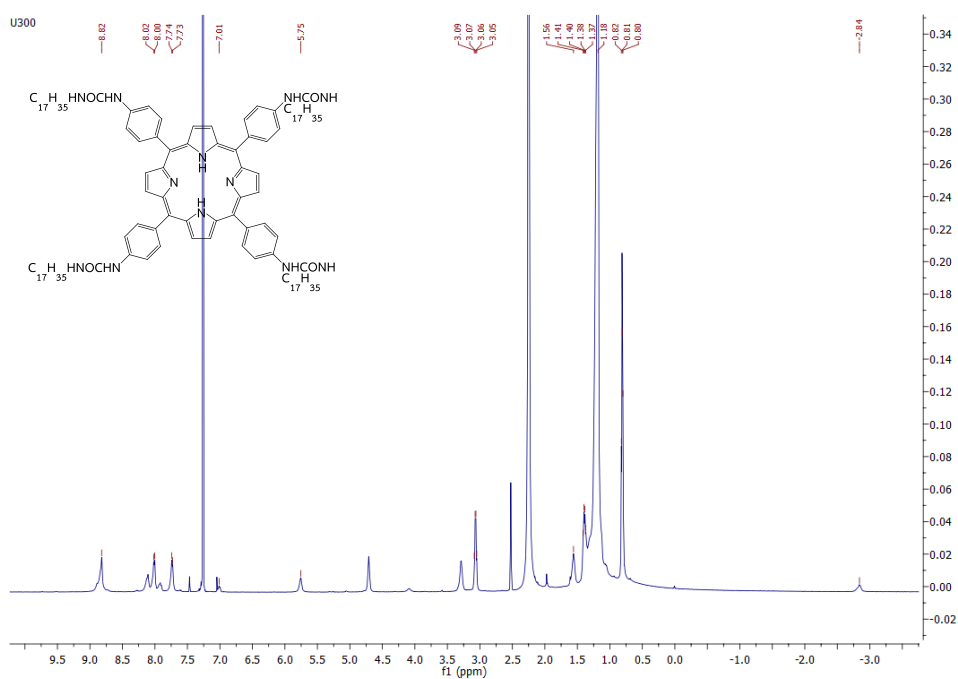
Appendix Figure S17 ^{1}H NMR spectrum of compound **11**
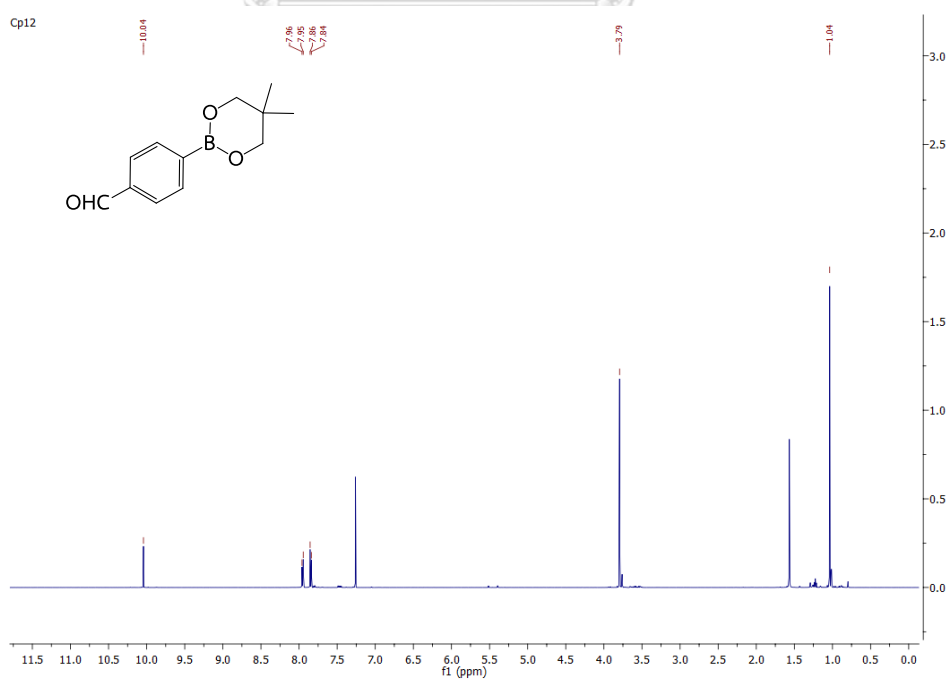
Appendix Figure S18 ^{1}H NMR spectrum of compound **12**
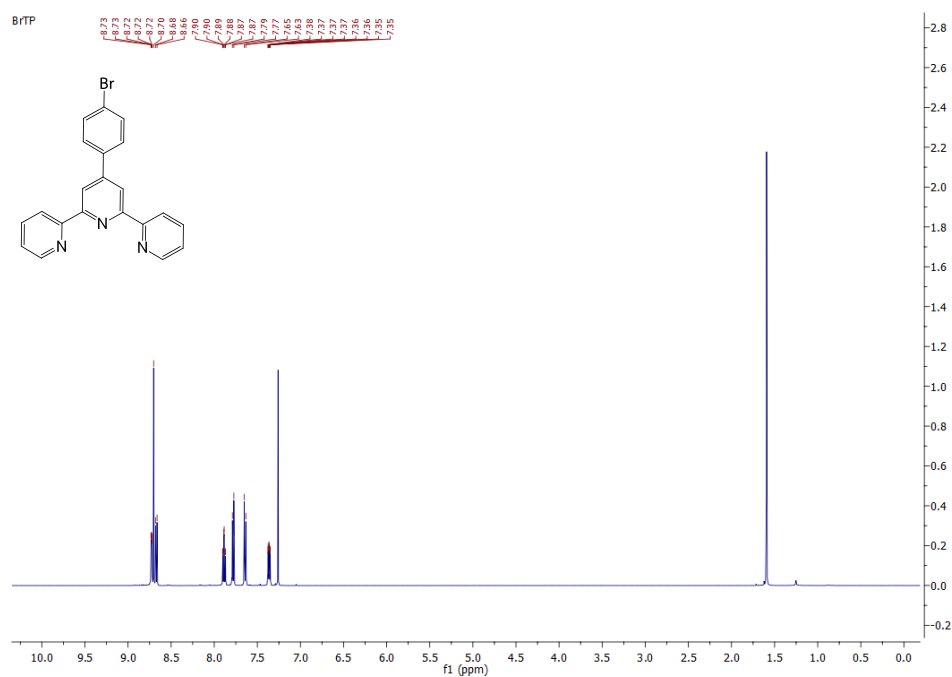
Appendix Figure S19 ^{1}H NMR spectrum of compound **13**
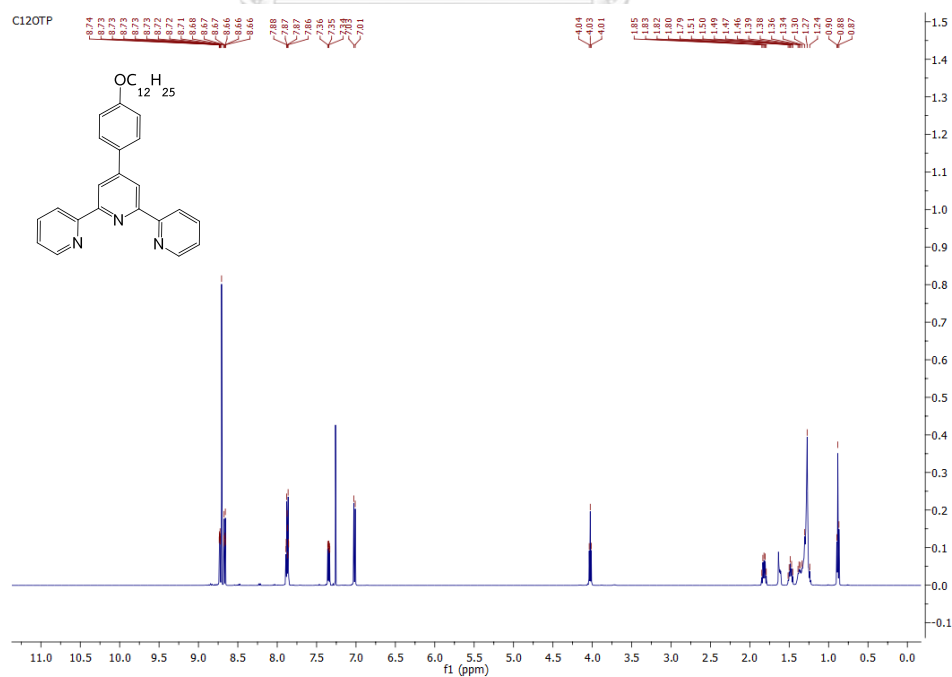
Appendix Figure S20 ^{1}H NMR spectrum of compound **14**
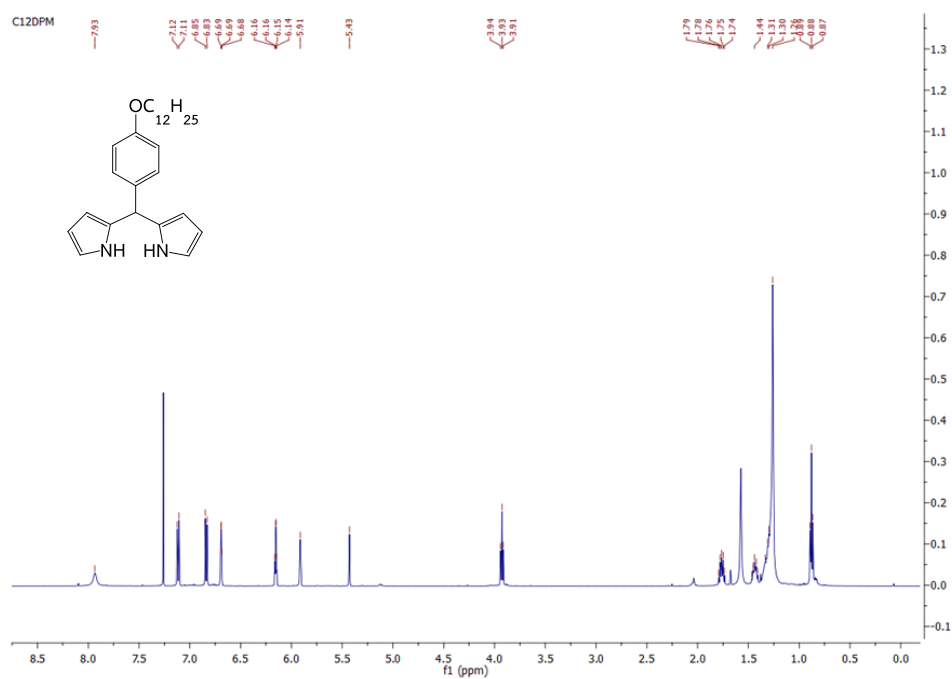
Appendix Figure S21 [^1]H NMR spectrum of compound **15**
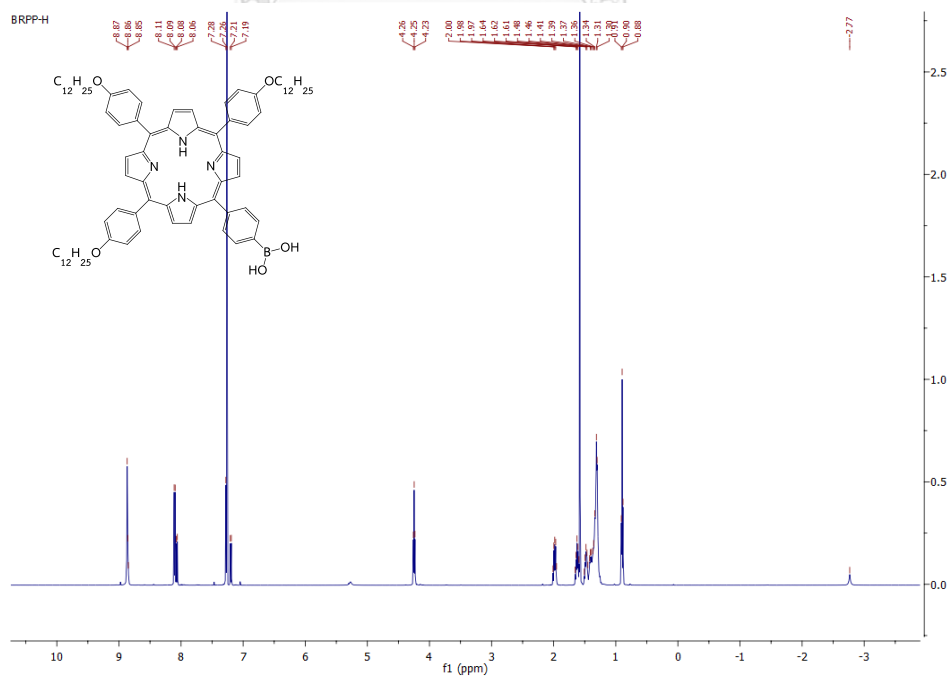
Appendix Figure S22 [^1]H NMR spectrum of compound **16**

Appendix Figure S23 ^{1}H NMR spectrum of compound **17**

Appendix Figure S24 ^{1}H NMR spectrum of compound **18**
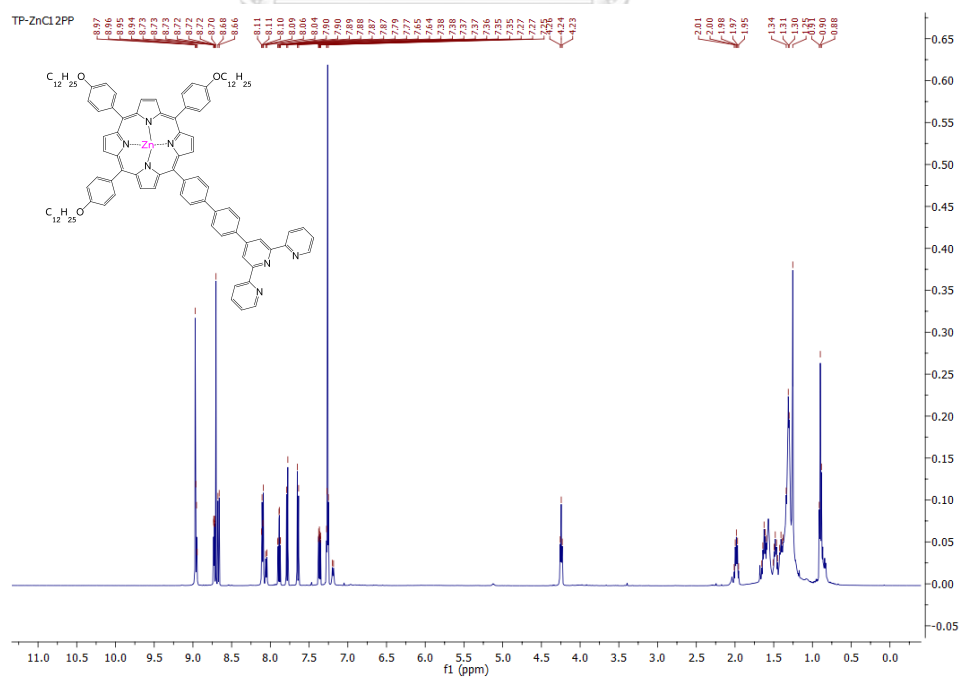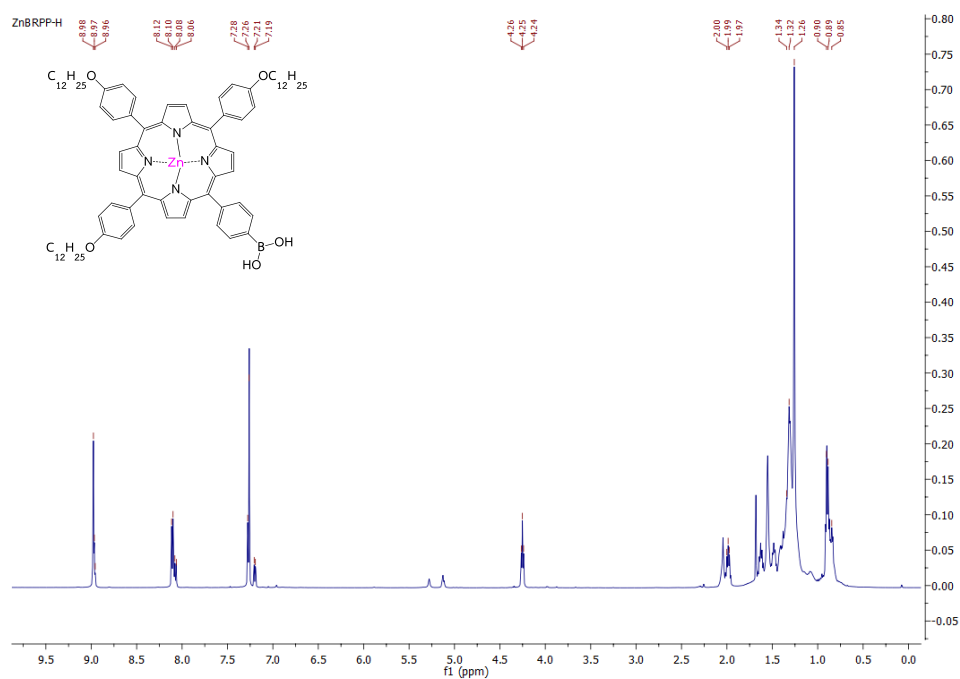
Appendix Figure S25 FTIR spectrum of compound **3**
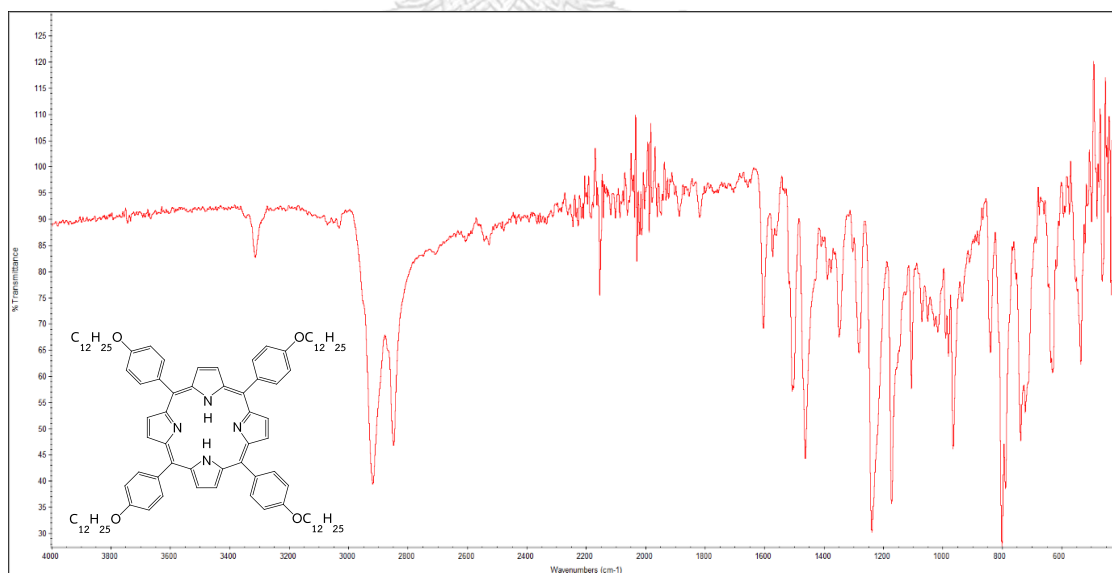
Appendix Figure S26 FTIR spectrum of compound **4**

Appendix Figure S27 FTIR spectrum of compound **5**

Appendix Figure S28 FTIR spectrum of compound **6**
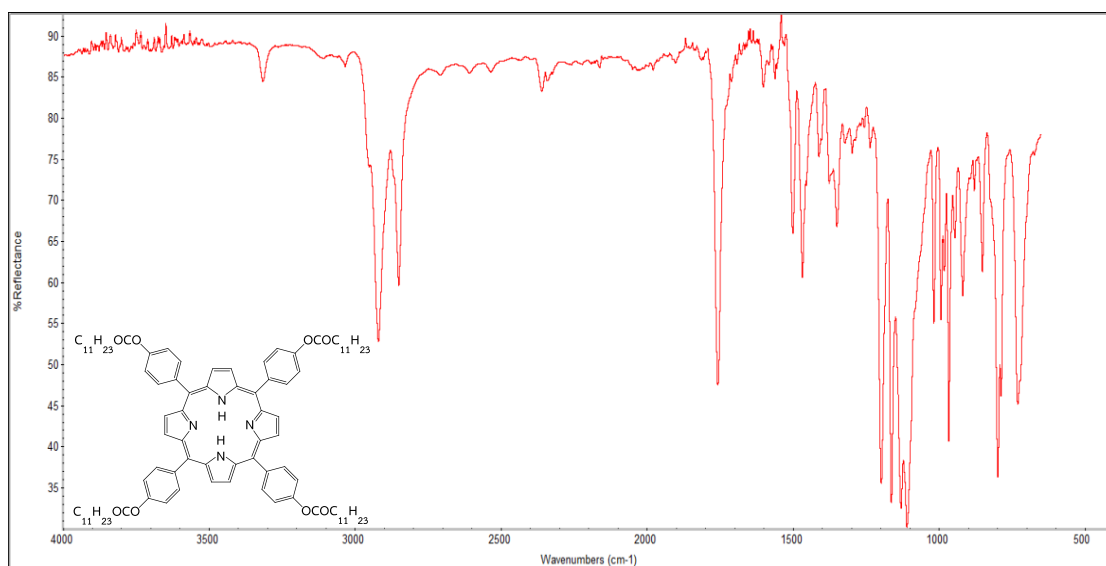
Appendix Figure S29 FTIR spectrum of compound **7**
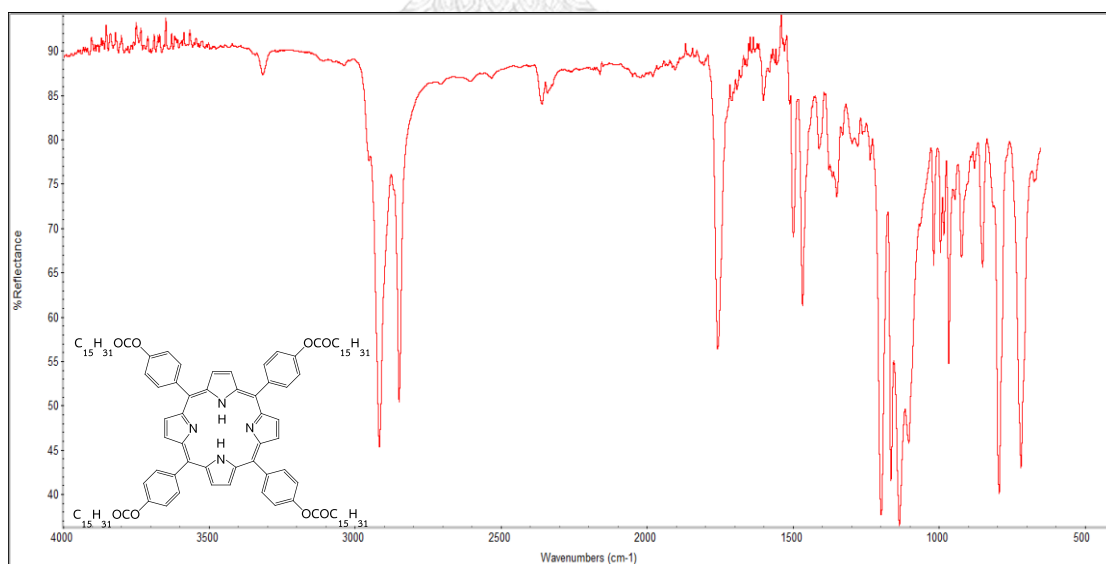
Appendix Figure S30 FTIR spectrum of compound **8**
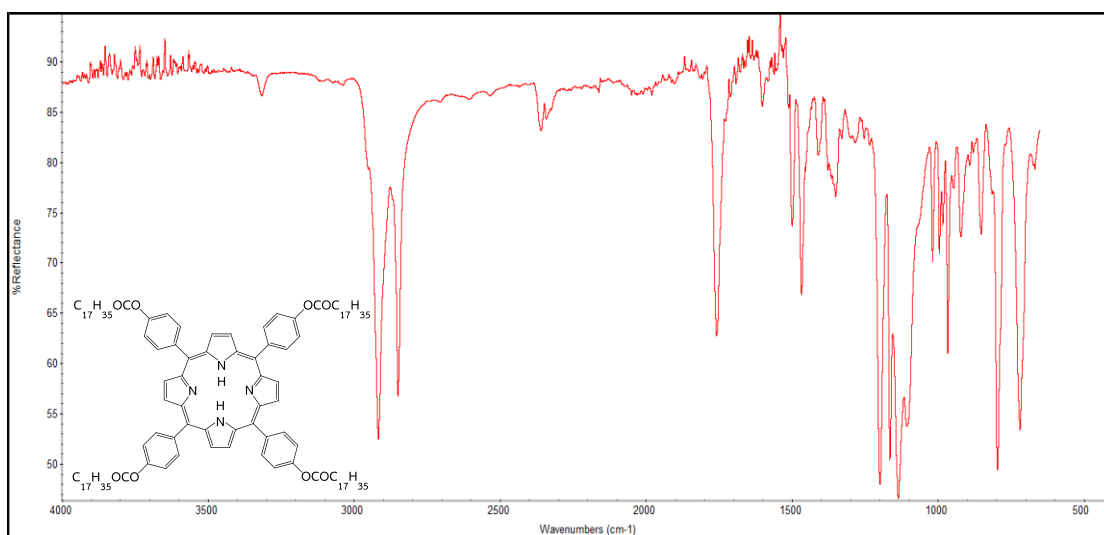
Appendix Figure S31 FTIR spectrum of compound **9**
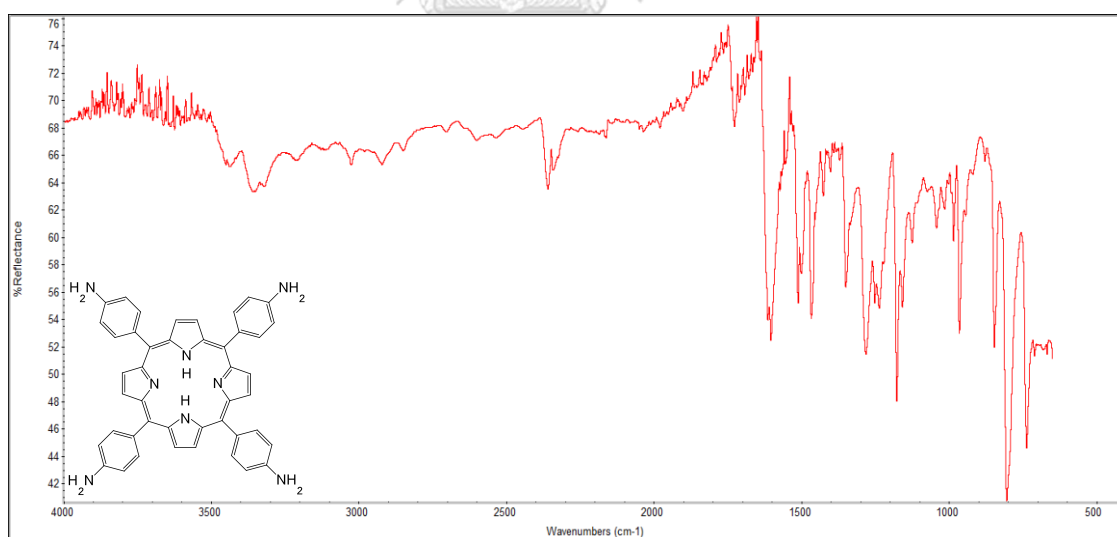
Appendix Figure S32 FTIR spectrum of compound **10**
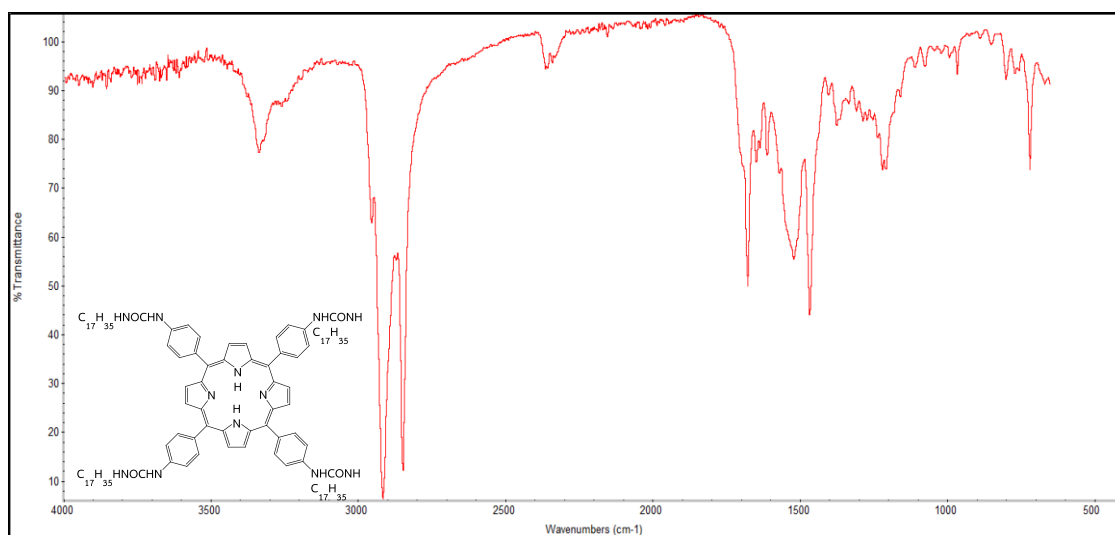
Appendix Figure S33 FTIR spectrum of compound **11**

จุฬาลงกรณ์มหาวิทยาลัย

CHULALONGKORN UNIVERSITY

E100 (3)

Appendix Figure S34 DSC thermogram of compound **3**

E101 (3a)
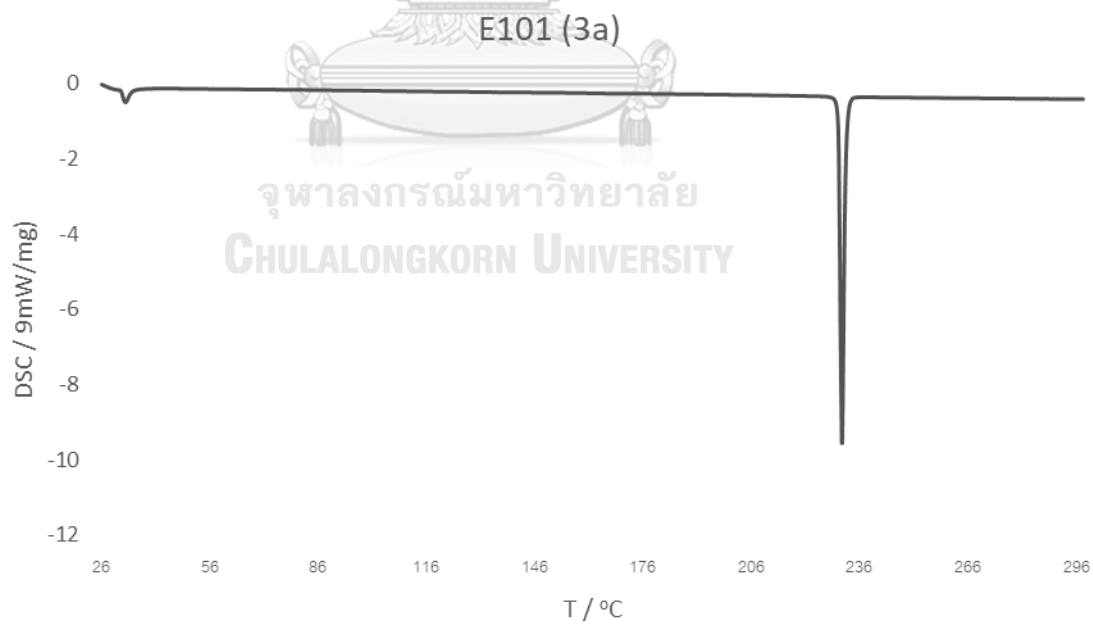
Appendix Figure S35 DSC thermogram of compound **3a**
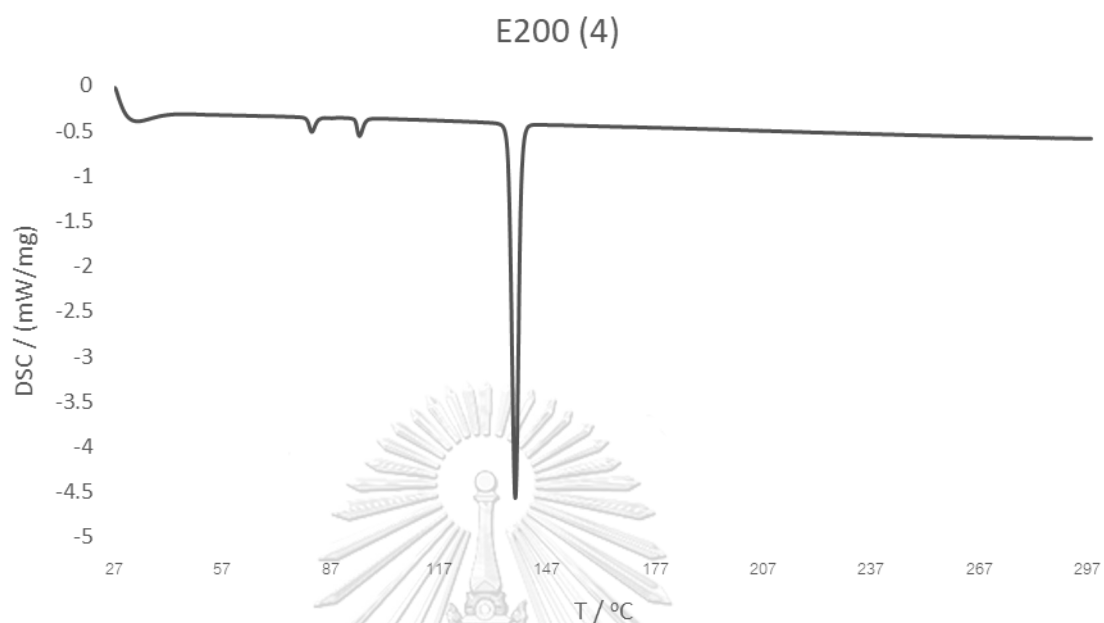
Appendix Figure S36 DSC thermogram of compound **4**
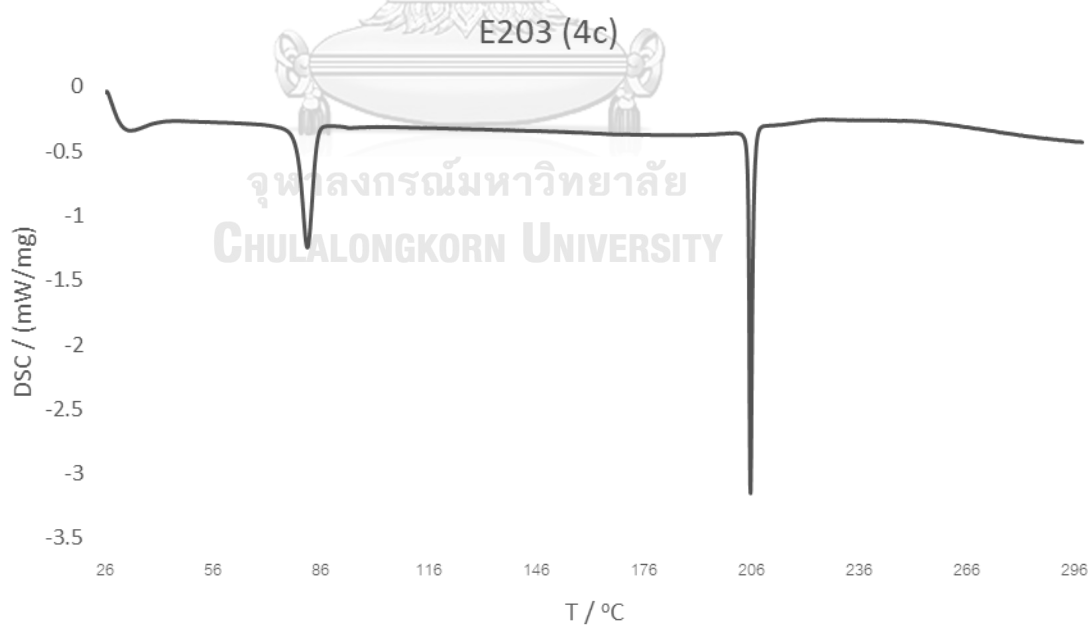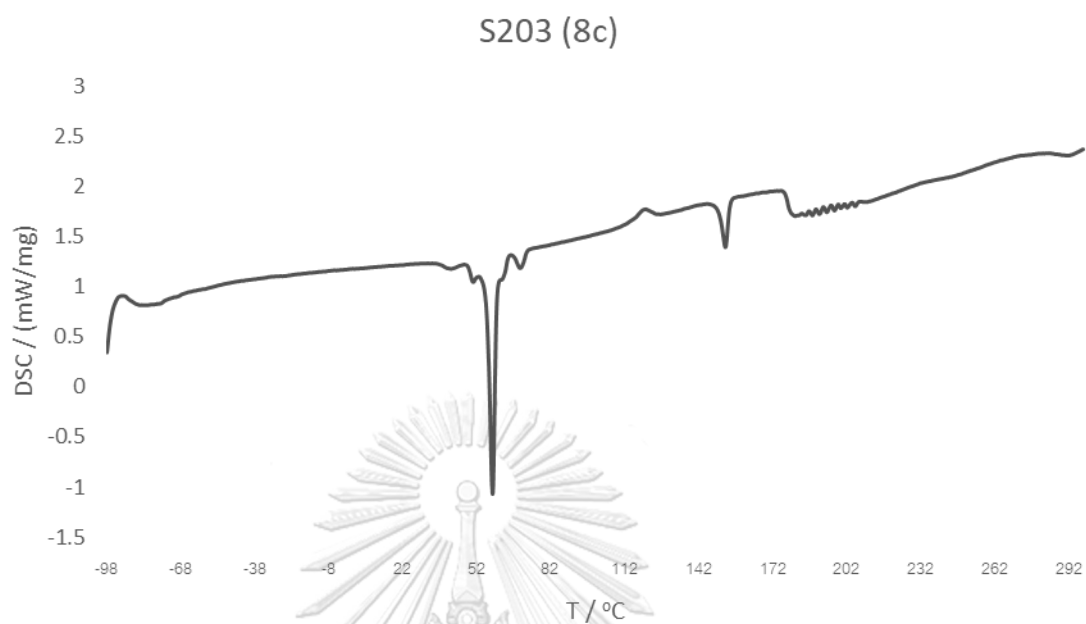

Appendix Figure S37 DSC thermogram of compound **4c**

E300 (5)
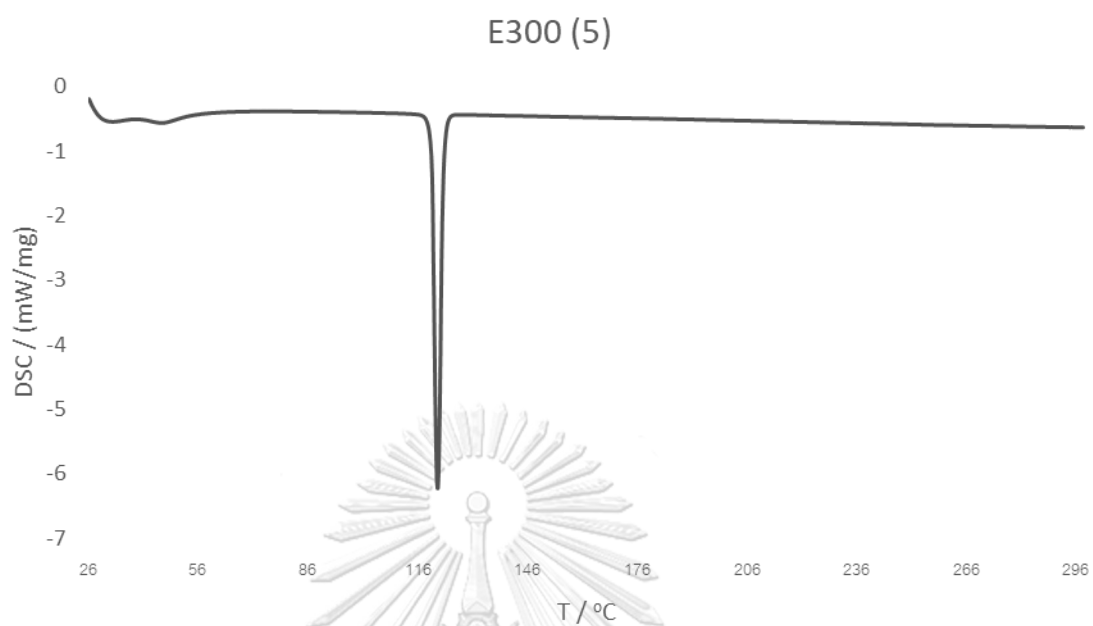
Appendix Figure S38 DSC thermogram of compound **5**

E303 (5c)
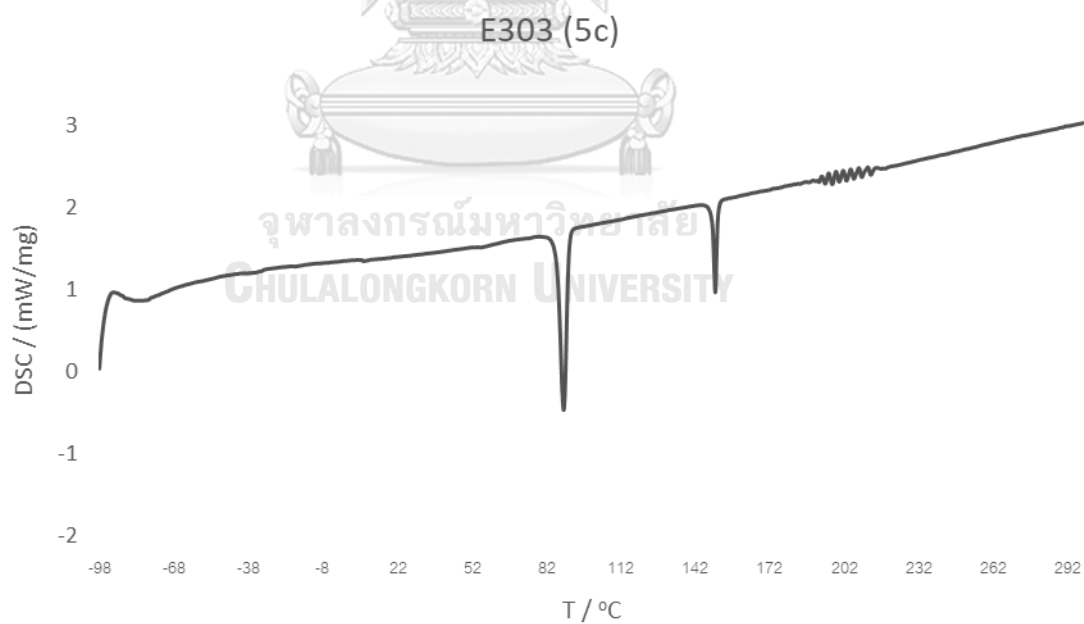
Appendix Figure S39 DSC thermogram of compound **5c**

E303 (5c-Pz)
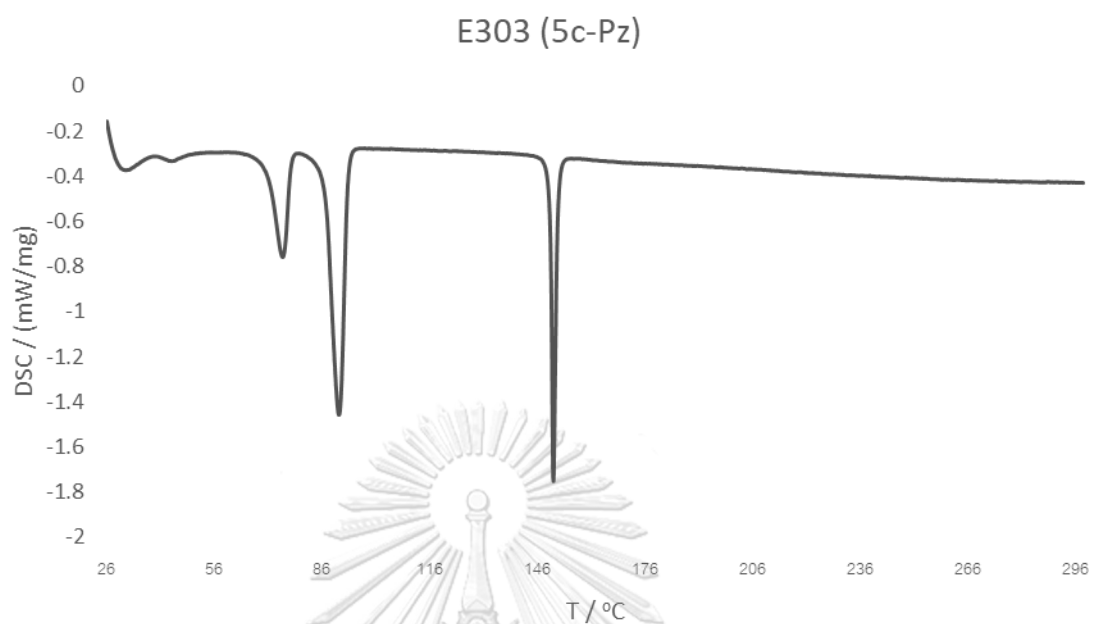
Appendix Figure S40 DSC thermogram of compound **5c-Pz**

S100 (7)
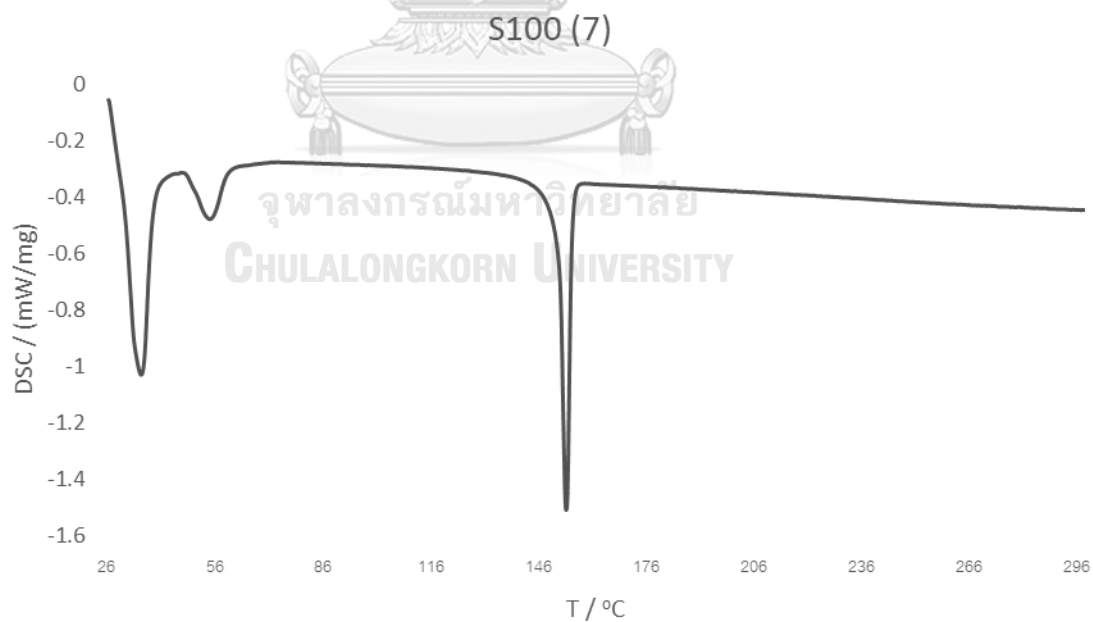
Appendix Figure S41 DSC thermogram of compound **7**

S101 (7a)
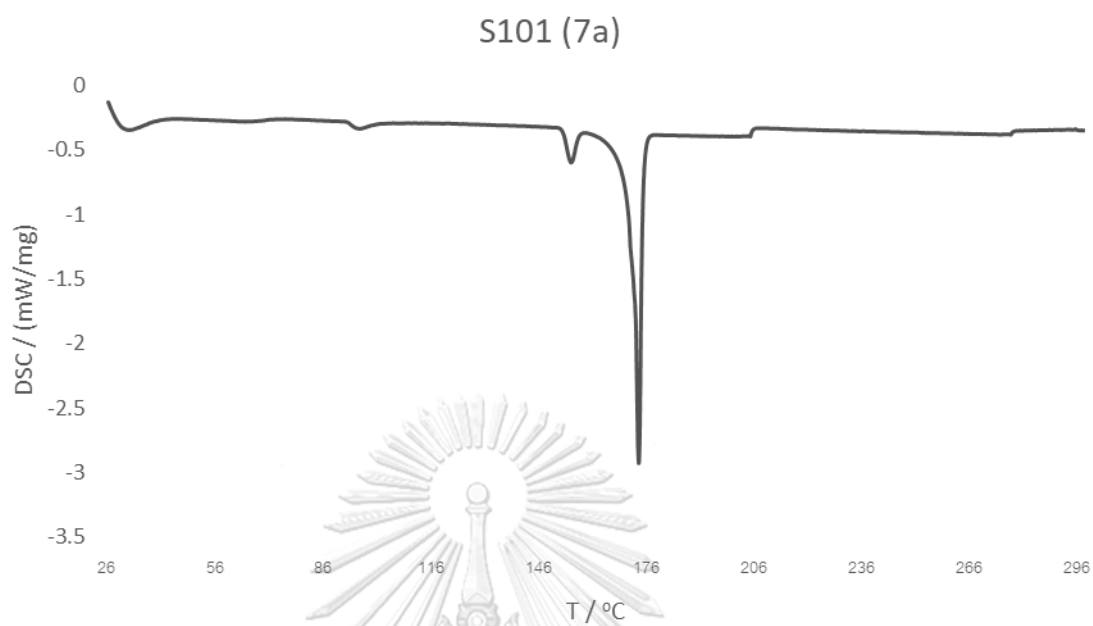
Appendix Figure S42 DSC thermogram of compound **7a**

S102 (7b)
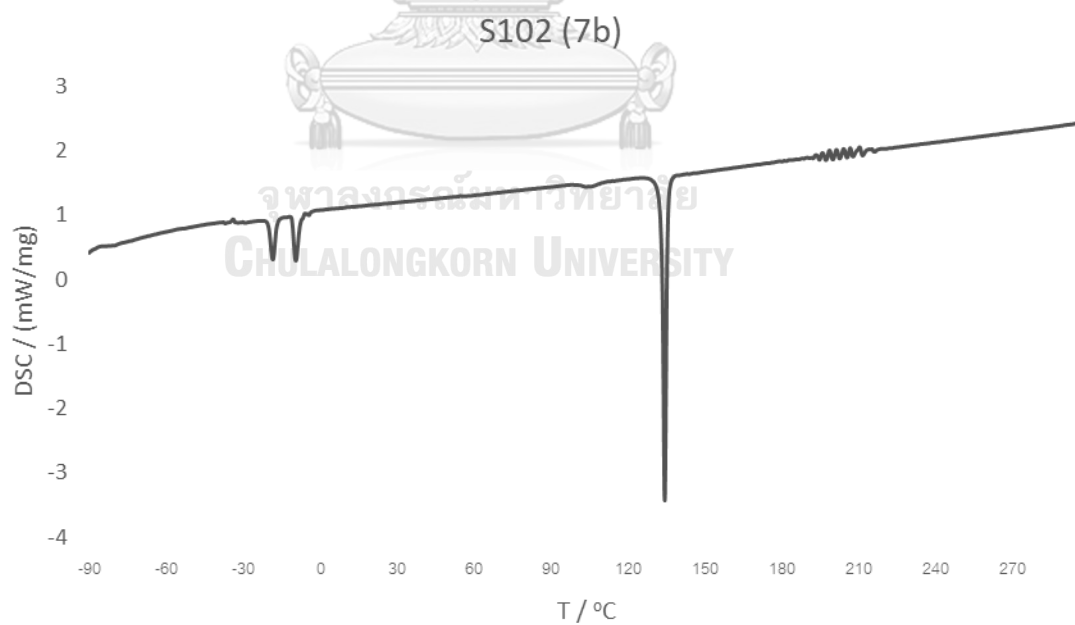
Appendix Figure S43 DSC thermogram of compound **7b**

S103 (7c)
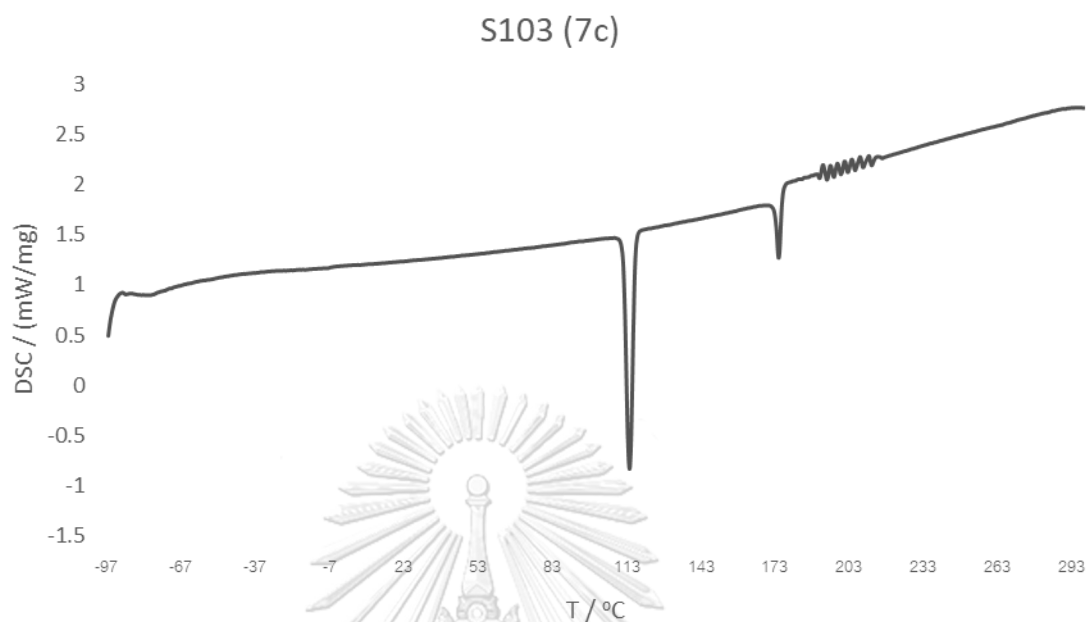
Appendix Figure S44 DSC thermogram of compound **7c**

S200 (8)
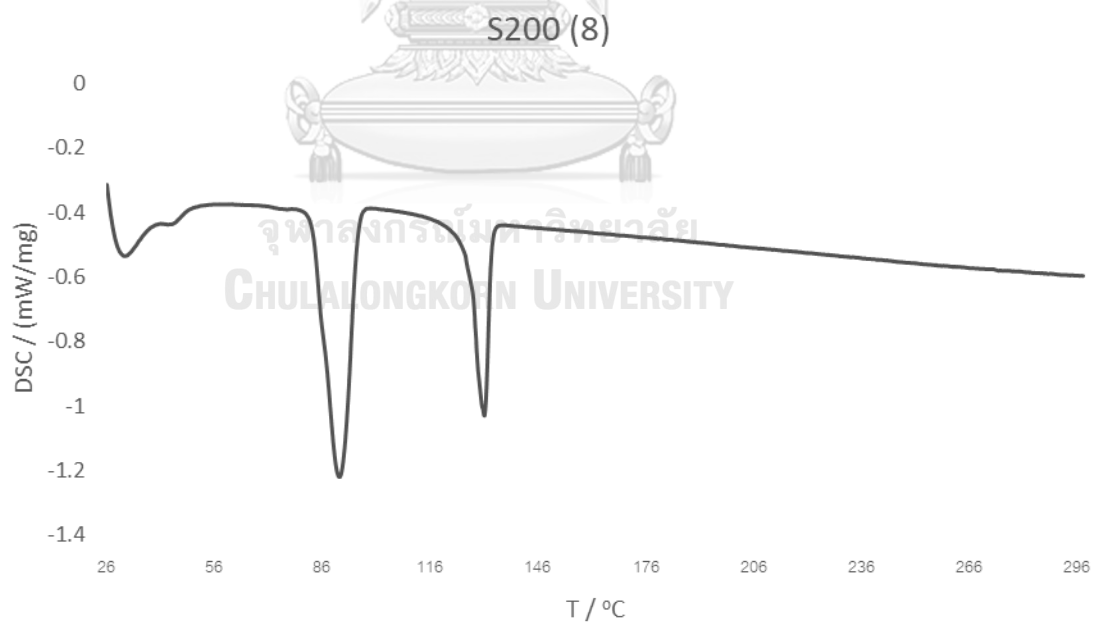
Appendix Figure S45 DSC thermogram of compound **8**

S201 (8a)
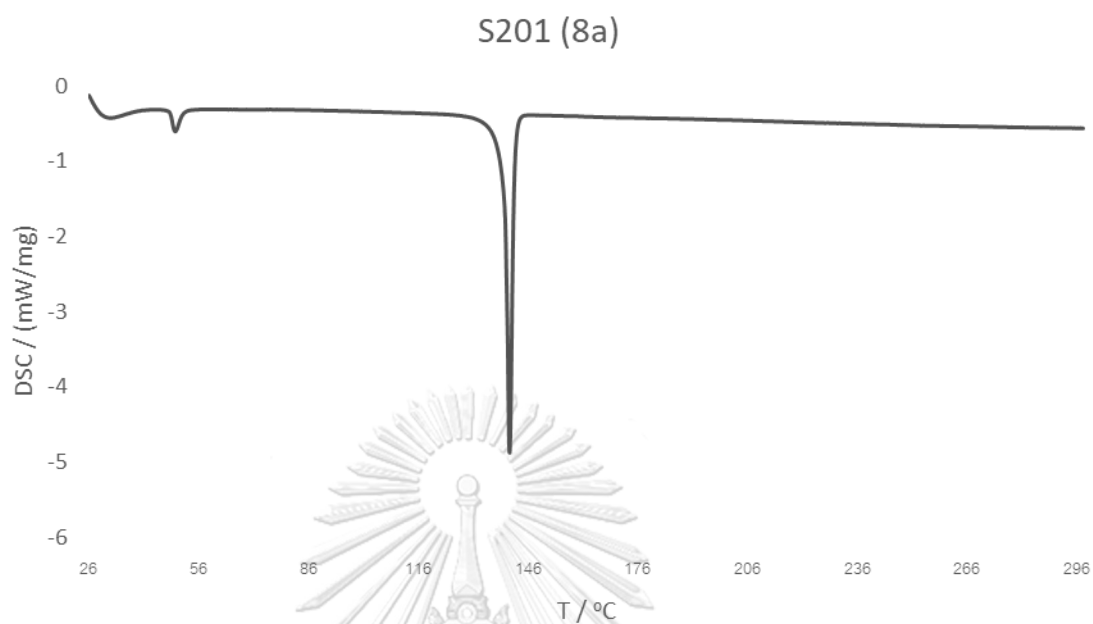
Appendix Figure S46 DSC thermogram of compound **8**a

S202 (8b)
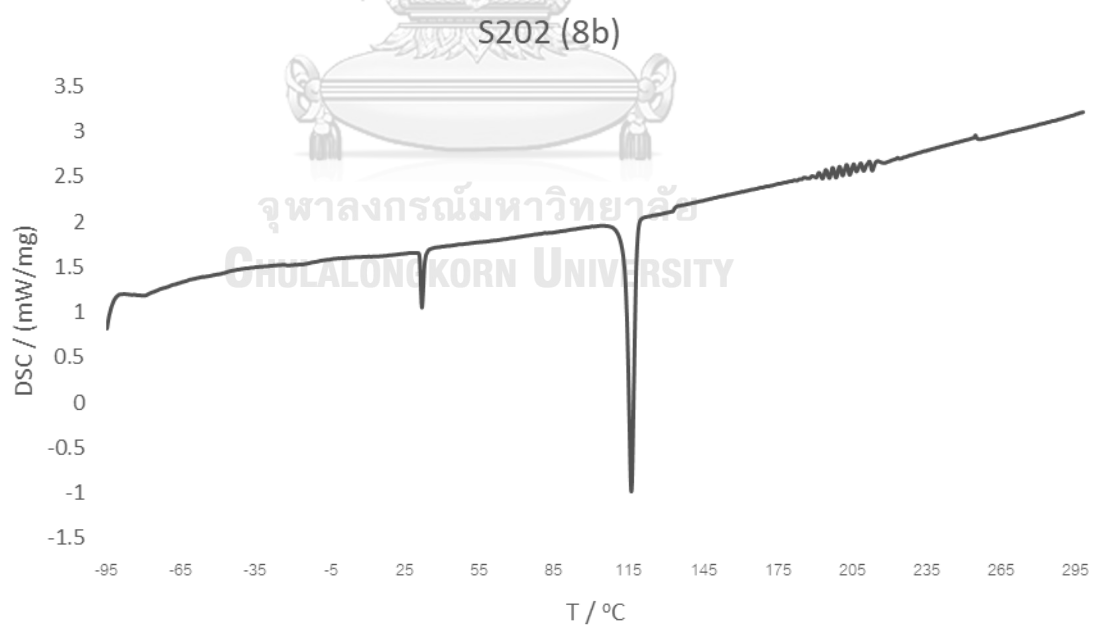
Appendix Figure S47 DSC thermogram of compound **8**b

S203 (8c)

Appendix Figure S48 DSC thermogram of compound **8**c
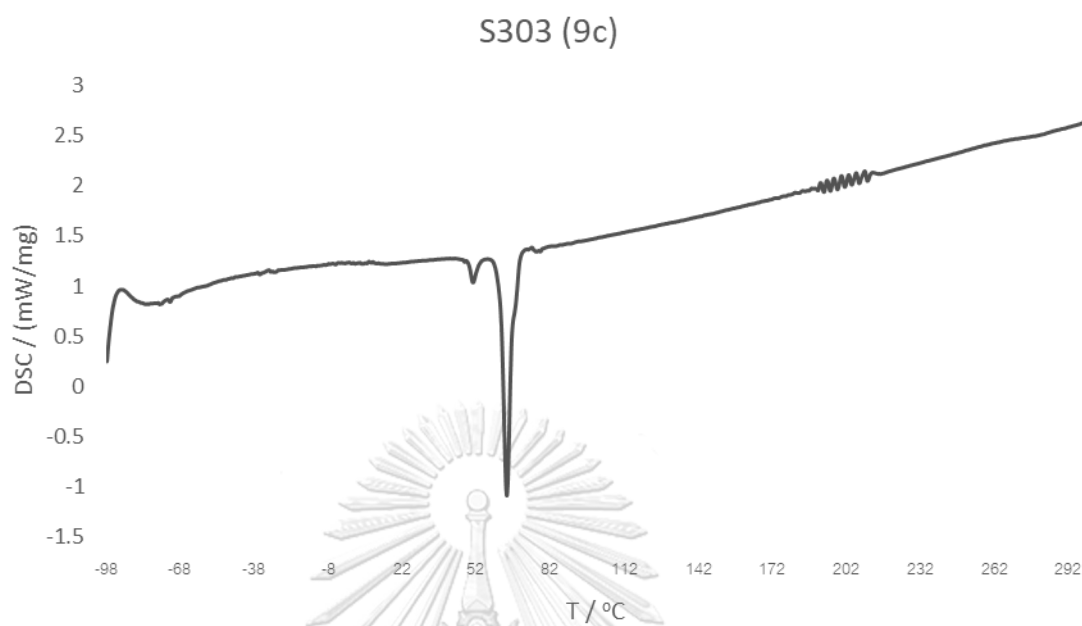
S300 (9)
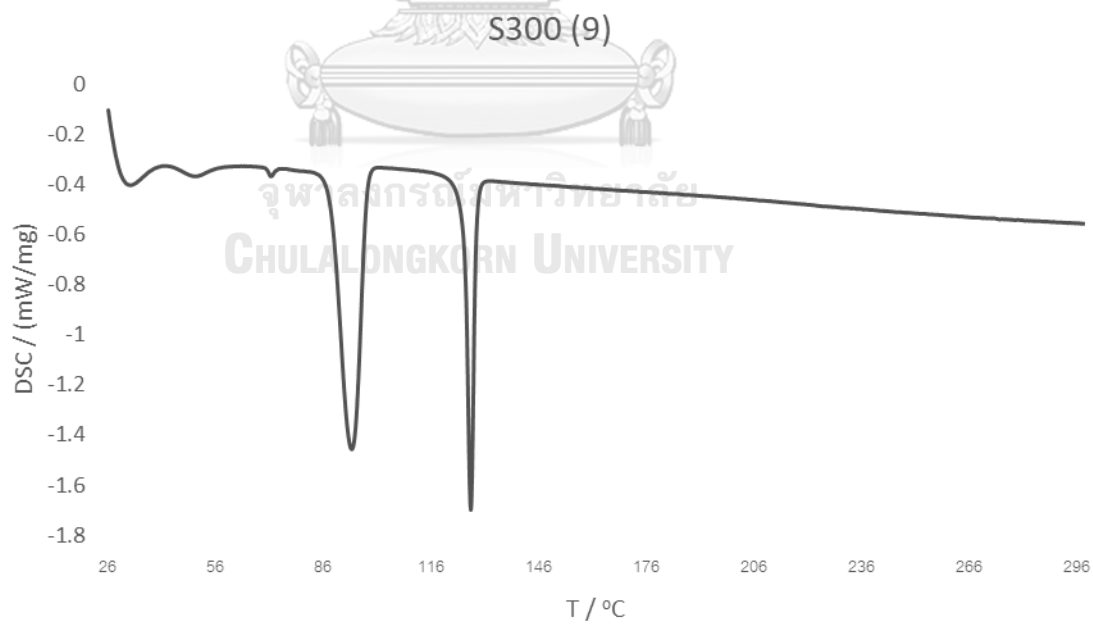
Appendix Figure S49 DSC thermogram of compound **9**
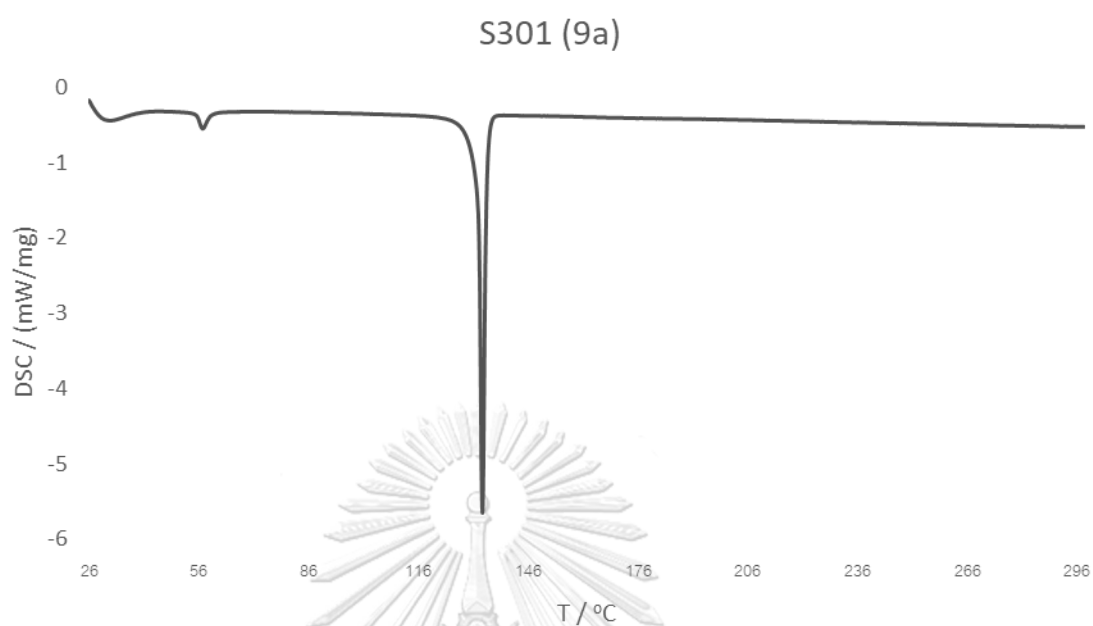
Appendix Figure S50 DSC thermogram of compound **9a**
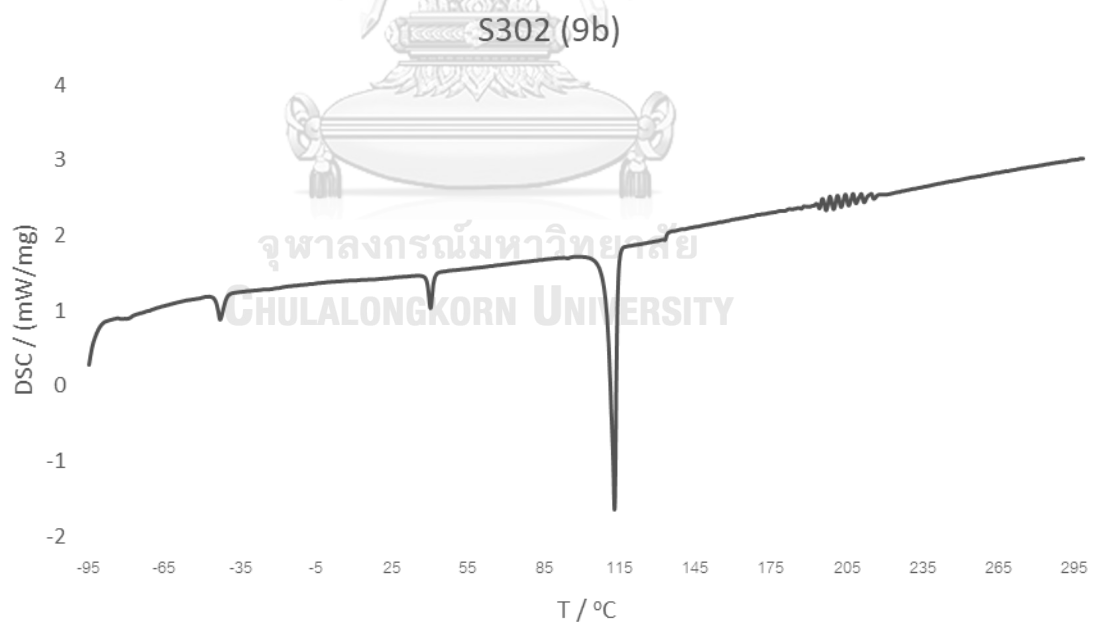
Appendix Figure S51 DSC thermogram of compound **9b**

S303 (9c)

Appendix Figure S52 DSC thermogram of compound **9c**

VITA

NAME	Dumrongsak Aryuwananon
DATE OF BIRTH	20 December 1983
PLACE OF BIRTH	Angthong
INSTITUTIONS ATTENDED	Kasetsart University
HOME ADDRESS	59/754 The Tempo Grand (Sathorn-Wutthakat), Bang Kho, Chom Thong, Bangkok 10150
PUBLICATION	S. Wirojsaengthong, D. Aryuwananon, W. Aeungmaitrepirom, B. Pulpoka and T. Tuntulani. A colorimetric paper-based optode sensor for highly sensitive and selective determination of thiocyanate in urine sample using cobalt porphyrin derivative. Talanta, 2021, 231, 122371.